DEVELOPMENTAL ALTERATIONS OF RAPHÉ NUCLEI IN AUTISTIC SUBJECTS 5-15 YEARS OF AGE- METHODS AND TECHNICAL LIMITATIONS

by

JAREK WEGIEL

A dissertation submitted to the Graduate Faculty in Biology in partial fulfillment of the

requirements for the degree of Doctor of Philosophy,

The City University of New York

2013

This manuscript has been read and accepted for the Graduate Faculty in Biology in satisfaction of the dissertation requirement for the degree of Doctor of Philosophy.

_____ _____

Date Dr. Probal Banerjee, Chair of Examining Committee

_____ _____

Date Dr. Laurel Eckhardt, Executive Officer

_____

Dr. Efrain Azmitia, New York University

_____

Dr. Abha Chauhan, NYS Institute for Basic Research

_____

Dr. Jeffrey Goodman, NYS Institute for Basic Research

_____

Dr. Abdeslem El Idrissi, College of Staten Island

_____

Dr. William L'Amoreaux, College of Staten Island

Supervisory Committee

THE CITY UNIVERSITY OF NEW YORK

Abstract

DEVELOPMENTAL ALTERATIONS OF RAPHÉ NUCLEI IN AUTISTIC SUBJECTS 5-15 YEARS OF AGE- METHODS AND TECHNICAL LIMITATIONS

by

Jarek Wegiel

Advisor: Professor Probal Banerjee

The role of the serotonergic system in autism is supported by more than 500 reports. They reveal a link between serotonergic system alterations and social deficits, repetitive behavior, hyperactivity, anxiety and obsessive compulsive behavior observed in autism. However, in spite of evidence of altered development of brain serotonergic system and contribution of these alterations to the autism phenotype, the raphé nuclei, which are the source of brain serotonin, have not been examined.

The aim of this stereological and quantitative immunofluorescence-based study of raphé nuclei in autistic subjects 5 to 15 years of age and age matched control subjects was to (a) establish methods of preparation, staining, and analysis of fixed human brainstem samples obtained from brain banks, and (b) characterize the pattern of developmental abnormalities which may contribute to the autistic phenotype.

Routine neuropathological brainstem dissection results in partial or complete loss of raphé nuclei integrity. From 9 autistic and 6 control subjects only four pairs 5 to 15 years of age were qualified for the study of raphé nuclei. Formalin-fixed brainstem was dehydrated and embedded in polyethylene glycol and cut into serial 50-μm-thick sections. They were stained to

estimate cell volume, and immunostained and examined by fluorescence microscopy to estimate the amount of tryptophan hydroxylase (TPH) which is a measure of serotonin synthesis level.

3-D reconstruction demonstrated topography and size of raphé nuclei and explained why preservation of raphé nuclei located in the midline required modification of brainstem sampling. Nucleator applied to TPH (+) sections revealed 24% smaller neuronal soma volume in the dorsal raphé nuclei of autistic subjects than in control group. Application of immunofluorescence and ImageJ software (NIH) revealed significant increase in tryptophan hydroxylase (TPH) immunofluorescence in spite of smaller size of raphé neurons.

These data indicate developmental impairment of neuron growth comparable to that observed in cortex and in subcortical structures. Enhanced TPH immunofluorescence in raphé neurons was consistent with enhanced immunoreactivity in serotonergic fibers in several brain regions of autistic subjects (Azmitia et al. 2011). Pathology detected in raphé neurons suggests that target brain areas were exposed to altered levels of serotonin, which may modify function of cerebral cortex and subcortical structures and contribute to the autistic phenotype.

Acknowledgments

I would like to express my gratitude to my advisor Professor Probal Banerjee for his guidance, suggestions and patience, and Professor Efrain Azmitia for advice on research design and interpretation of findings. This work was made possible because of the foundation in this area laid by Dr. Azmitia's research. Both Professors helped me to deal with the challenges of the first study of its kind. I wish to thank members of my dissertation committee: Dr. Abha Chauhan, Dr. William L'Amoreaux, Dr. Abdeslem El Idrissi, and Dr. Jeffrey Goodman for the helpful discussions and time.

I would like to thank Dr. George Merz from IBR for confocal microscopy help, Dr. Michael Flory for statistical analysis guidance and Sara Guariglia for advice in study design. I would like to thank all of Prof. Banerjee's lab members, especially Sreyashi Samaddar, for inspiring discussions and help with the project. I thank Dr. Robert Freedland for advice on the program.

I wish to express my deep appreciation to all the members of the Biology Doctoral Program at the Graduate Center and the CSI Center for Developmental Neuroscience for guidance and support. I would like to thank Ms. Diane Cocozza for assistance. I thank the Center of Developmental Neuroscience, the Institute for Basic Research and the College of Staten Island for providing the resources that made this work possible.

I am deeply indebted to the families of the tissue donors who made this study possible. Tissue and clinical record acquisition was made possible by the Autism Tissue Program (Princeton, NJ; Directors: Jane Pickett, Ph.D. and Daniel Lightfoot, Ph.D.) and Dup15 Alliance (Ms. Kadi Luchsinger). The tissue was obtained from the Harvard Brain Tissue Resource Center, Belmont, MA, the National Institute of Child Health and Human Development Brain and Tissue

Bank for Developmental Disorders at the University of Maryland, Baltimore, and the Brain Bank for Developmental Disabilities and Aging of the New York State Institute for Basic Research in Developmental Disabilities, Staten Island, NY.

Table of Contents

List of Tables

List of Figures

1. INTRODUCTION

Autism was identified and described in 1943 by psychologist Leo Kanner as a disturbance of affective contact. Although it was once thought of as a rare condition affecting 4 in every 10,000 children, it is now considered as one of several disorders classified as Autism Spectrum Disorders, showing a dramatic increase in prevalence reported in almost all states of the U.S. The Center for Disease Control (CDC 2000, 2007, 2009) records indicate that in 1980, the rate of ASD diagnosis was about 1/2000 subjects but after 1980 a consistent increase in diagnosis of ASD was observed to 1/150 in 2007 (6.6/1000) and 1/110 in 2009. The Report of the Centers for Disease Control and Prevention (CDC) published in 2012 and summarizing results of the study of 8.4 % of the US population of 8-year old children in 2008 revealed a 1 in 88 overall prevalence of autism spectrum disorder (ASD) with a 1 in 54 prevalence for males and a 1 in 252 prevalence for females ($p < 0.01$), with a male to female ratio of 4.7 to 1. In the past 60 years, autism evolved from an obscure and rare psychiatric disorder to one of our most challenging medical problems.

The past two decades of accelerated research resulted in improvements of autism diagnostic criteria, better understanding of autism multi-factor etiology and clinicopathological correlations. However, mechanisms contributing to the complex clinical autism phenotype are not known. One of the intensively studied hypotheses is concentrated on contribution of serotonergic system pathology to developmental alterations and clinical phenotype of autism. This hypothesis is supported by more than 500 papers published after Schain and Freedman's first report (1961) demonstrating a link between serotonin and autism (Lam et al. 2006). These papers reveal a significant role of serotonin in brain development and maturation, and the link

between alterations of the serotonergic system and all major clinical manifestations of autism, including social deficits, repetitive behavior, anxiety, hyperactivity, impulsive and aggressive behavior, and obsessive compulsive behavior (Buitelaar and Willemsen-Swinkels 2000).

Recent studies of serotonergic innervation of the brain of autistic subjects revealed significant abnormalities (Azmitia et al. 2011ab). However, the type, distribution, and severity of changes in raphé nuclei, the source of brain serotonin, are still not known. This study is concentrated on detection and reduction of technical limitations in research on raphé nuclei, standardization of methods of unbiased stereological evaluation and fluorescence-based quantitative estimates of developmental abnormalities of raphé nuclei of autistic subjects, as well as detection of changes in 5- to 15-year old autistic subjects.

1.1. Autism clinical phenotype – signs of serotonergic system contribution to autism phenotype

Autism is a lifelong developmental disorder characterized by (a) qualitative impairments in reciprocal social interactions, (b) qualitative impairments in verbal and nonverbal communication, (c) restricted repetitive and stereotyped patterns of behavior, interests and activities, and (d) onset prior to the age of 3 years. There is no specific biochemical indicator or distinct neuroanatomical abnormality or neuropathological marker that defines autism, and the diagnosis is based only on clinical and behavioral assessment (American Psychiatric Association 2000). Because of similar qualitative deficits in social behavior and communication, the autistic disorder (DSM 299.00), Asperger's syndrome (DSM 299.80) and pervasive developmental disorder – not otherwise specified (PDD-NOS) (DSM 299.80) are classified as autism spectrum disorder (Freitag 2007).

Evolution of clinical diagnostic criteria of autism from DSM-II to DSM-V. In the past decades the methods of diagnosing of autism have evolved. Evolution of diagnostic criteria affects diagnosis of subjects whose brains are examined postmortem and may affect results and conclusions of postmortem studies of brains of individuals diagnosed with ASD.

Since Leo Kanner's report (1943), autism remained a poorly characterized developmental disability undistinguished from schizophrenia childhood type (Diagnostic and Statistical Manual of Mental Disorders DSM-II; 1965-1977), or diagnosed as infantile autism (DSM-III (1977-1984), or autistic disorder (DSM-III-R; 1984-1995). DSM-IV (1996) classified autism disorder as one of five Pervasive Developmenal Disorders, including Apergers's disorder, Rett syndrome, Childhood Disintegrative Disorder, and Pervasive Developmental Disorder – Not Otherwise Specified (PDD-NOS).

According to DSM-IV, the hallmark of autism is a severe impairment in social relations. Autism is diagnosed in subjects with developmental abnormalities with 6 or more of the 12 features characterizing (a) social interactions, (b) verbal and non-verbal communication, and (c) repetitive and stereotypical behaviors. The onset of these clinical symptoms must be observed prior to three years of age. These criteria distinguish autism from other Pervasive Developmental Disorders, including childhood disintegrative disorder (CDD) and Rett syndrome.

Currently, identification of autism is based on application of (a) Autism Diagnostic Interview-Revised (ADI-R) (Lord et al. 1999), Autism Diagnostic Observation Schedule-Generic (ADOS-G), and Pervasive Developmental Disability- Behavior Inventory (PDD-BI) (Cohen et al. 2003).

According to the fifth edition of the Diagnostic and Statistical Manual of Mental Disorders (DSM-5) to be published in May 2013, Autism Spectrum Disorder includes autistic

disorder (autism), Aspergers's disorder, childhood disintegrative disorder, and pervasive developmental disorder not otherwise specified (American Psychiatric Association, DSM-5: The Future of Psychiatric Diagnosis; www.DSM5.org). According to a new standard, three diagnostic domains will be reduced to two: (1) social/communication deficits and (2) fixed interests and repetitive behaviors. This change is based on studies indicating that deficits in communication and social behaviors are inseparable. Deficits in communication and social behaviors are considered as a single set of symptoms with contextual and environmental specificity. Delays and deficits in language do not define diagnosis of autism but they influence the clinical symptoms of ASD. In a new definition of autism, unusual sensory behaviors are included within a subdomain of stereotyped motor and verbal behaviors. Moreover, it is expected that DSM-V will drop the term Asperger syndrome. Asperger syndrome is distinguished from autism by relatively normal language development including timing, grammar, and vocabulary, but diagnosis of Asperger syndrome is based on the presence of all other DSM-IV diagnostic criteria of autism (Miles 2011).

Diversity of individual presentations of autism. Autism is defined by a common set of diagnostic modalities but individual clinical presentation includes subclassification into complex or essential autism, gradual or regressive onset, and such associated features as: identified genetic disorder, epilepsy, intellectual disability, anxiety, sensory abnormalities, and self-injurious behavior.

Complex and essential autism. About 30% of children are diagnosed with complex autism, defined by the presence of dysmorphic features, microcephaly or structural brain malformation. Seventy percent of children with autism are diagnosed with essential autism, defined as autism without physical abnormalities (Miles et al., 2005).

Course of disease. Two patterns of clinical course have been identified. The most common is gradual onset of autism in early childhood. However, in about 14% (Colorado) or 32% (Utah), significant regression is observed at the age of 18 to 33 months and this form of autism is classified as regressive autism (US Department of Health and Human Services, 2007). The clinical course of autism can be modified by intensive behavioral treatment using applied behavior analysis methods (ABA). ABA produces substantial improvements in some children who had moderate to severe delays in cognitive, communication, social, and adaptive skills in most or all domains after 2 to 3 years of early intensive behavioral treatment (McEachin et al. 1993, Perry et al. 1995, Weiss 1999, Green et al. 2002).

Intellectual disability. In about 45% of children, autism is associated with mental retardation defined as intelligence quotient (IQ) scores of < 70 (Department of Health and Human Services, 2007). A comparison of autistic children diagnosed in 1987 and 1998 reveals that one of the features of a new trend in diagnosis of autism is a decrease in prevalence of autism associated with severe and profound mental retardation, and doubled prevalence of cases of autism without mental retardation.

Epilepsy. Epilepsy among children in the general population is estimated at 2-3%, whereas about 30% of autistic individuals develop epileptic seizures (Gillberg 2000, Tuchman and Rapin 2002). All seizure types are seen in autism, including tonic-clonic, complex partial, atypical absence, and myoclonic. Two peaks of high seizure frequency were reported - before the age of 5 years and after the age of 10 years (Tuchman and Rapin 2002). Dysplasia and heterotopia in the hippocampus, amygdala and neocortex are known as epileptogenic foci. They were identified in idiopathic autism and their prevalence increases in autistic subjects diagnosed with dup15 whose death was seizure-related. Serotonergic fibers show unmodified morphology

in cryptogenic epilepsy (no cortical dysplasia), but in patients with focal cortical dysplasia with giant neurons and giant astrocytes, dysplastic epileptogenic areas show serotonergic hyperinnervation with increased density of serotonergic fibers. (Trottier et al. 1996).

Anxiety. Approximately 80% of children diagnosed as high functioning ASD (De Bruin 2007) and up to 40% of ASD children with IQ below 70 have a concurrent anxiety disorder (Sukhodolsky 2008). Anxiety is defined as a state of chronic apprehension about future harm, characterized by tension, worry, negative affect, and a feeling of insecurity elicited by unpredictability and by the perception of potential, unseen, or symbolic threats (Grillon 2008). Individuals with anxiety are hyper-vigilant, constantly scanning the environment for potential threats. When such a stimulus is detected, the individuals narrow their attention and have trouble disengaging from it (Craske 2009). This negative arousal combined with difficulties controlling negative emotion leads to overreactivity (Green 2010). Cognitive/language impairments of autistic children reduce the ability of expressing fear and anxiety and enhance anxiety. Multiple genetic and environmental factors may be interacting and contributing to the condition. Anxiety has long been treated by anti-anxiety (tranquilizers, benzodiazepine) and anti-depressant medications including Selective Serotonin Reuptake Inhibitors (SSRIs) and Monoamine Oxidase Inhibitors (MAOIs). The non-pharmacological treatment of choice for anxiety is Cognitive Behavioral Therapy (CBT) (Ollendick 2006).

Sensory abnormalities and pain. Sensory abnormalities in autism had been reported in Kanner's original description of the disorder in 1943. Autistic individuals have various perceptual processing abnormalities, which are manifested by a hypersensitivity to tactile and auditory stimuli (Gomot 2002). In ASD, both sensory under-responsiveness and over-responsiveness have been observed (Baranek 2006). Baranek showed that 69% of young autistic

children had a high level of multimodal sensory processing problems. Sensory alterations include taste, smell, and tactile sensitivity, auditory filtering, underreactivity and stimulation seeking (Corbett 2009).

Sound sensitivity has been reported to vary with times and type of sound. Positive auditory experiences including interaction have been reported with music. Heightened awareness of sound and curiosity have also been reported. Autistic children show sensitivity to bright light, especially sunlight. Some have negative reactions to certain visual stimuli such as television. Others have positive experiences and enjoy controlling light sources. Tactile stimuli had positive effects when they involved interpersonal touching or certain natural phenomena such as wind. Autistic children seem to have an aversion to actions addressed towards the head and face. Negative food experiences can include taste, smell, texture and visual aspects. A common theme has been the inability to control or terminate a stimulus often being a negative experience (Dickie 2009).

Self injurious behavior (SIB). The serotonergic system has been identified to have a role in SIB (Cook, 1999). SIB may include head banging, picking, and self-biting/hitting/scratching. It is believed that self-injury is related to altered pain processing. While normally pain is a result of proper activation of sensory neurons which detect tissue damaging stimuli (nociceptors), sensitivity can increase after repetitious injury, due to a possible change in intracutaneous nerves. Response to abnormal sensory experiences such as increased pain sensitivity due to altered nerve fibers may result in self-injury. The chronic inflammatory response to chronic SIB may produce pain and the feed forward cycle can continue indefinitely. A chronic state of pain can result in sickness behavior including decreased exploration and

socializing, as well as changes in sleep patterns. Decreased pain responses result in self-injurious behavior (Symons, 2011).

Role of serotonin in affective disorders. Numerous studies indicate that a deficiency of central serotonergic signaling may predispose individuals to development of mood disorders including aggression, anxiety, impulsivity, depression, and obsessive-compulsive disorder (Lucki 1998, Mann et al. 2001, Nelson and Chiavegatto 2001, Lemberger et al. 1985, Hrdina et al. 1989). Impairment of 5-HT synthesis by tryptophan depletion worsens the clinical state of patients diagnosed with depression (Shopsin et al. 1975, Delgado et al. 1990). Altered serotonin neurotransmission has been associated with affective disorders (Risch and Nemeroff 1992) and suicidal behavior (Arango and Mann 1992). Decreased serotonin transporter (SERT) was reported in the frontal cortex and hypothalamus of suicide victims (Stanley et al. 1982, 1983, Paul et al. 1984, Arato et al. 1991).

The serotonin system is involved in modulation of impulsive aggressive behavior (Brown et al. 1982, Olivier et al. 1989, Olivier and Mos 1992, Miczek et al. 2004, Faccidomo et al. 2008). Changes of 5-HT levels regulate distinct phases of aggressive behavior. The prefrontal cortex is the most involved area in the execution and recovery from an aggressive encounter (Van Erp and Miczek 2000, Halasz et al. 2006, Miczek and Fish 2006).

Controversies regarding treatments targeted at serotonergic system. Significant improvements observed in overall functioning and in a wide range of symptoms, including anxiety, aggression, and repetitive behavior were reported in children and young adults with autism treated with selective serotonin reuptake inhibitors (SSRIs), including fluoxetine and related drugs (Mehlinger et al. 1990, Gordon et al. 1992, McDougle et al. 1996b, DeLong et al. 1998). DeLong et al. (1998) reported excellent response in 30% and good response in another

30% of autistic children. However, in 40% lack of response or negative response with aggressiveness, agitation, and hyperactivity were observed. In addition to these only at times positive results, Kolevzon et al. (2006) revealed that SSRIs do not improve social and communication deficits.

A selective response of some autism modalities to SSRIs (Brodkin et al. 1997, Kolevzon et al. 2006, King et al. 2009) suggests that the serotonergic system is affected by developmental alterations and that these changes contribute to some autistic symptoms. Moreover, detection of positive and negative response and no response suggest interindividual differences in serotonergic system alterations of autistic subjects. Studying the raphé nuclei as the source of serotonergic innervation of the brain, and target cortical and subcortical structures may identify differences which contribute to (a) heterogeneity of clinical manifestations, and (b) heterogeneity of patient response to treatment. This assumption was confirmed by Azmitia et al. (2011 a,b) postmortem studies of serotonergic innervation in 2.8 to 29-year old autistic subjects which revealed an increase in 5-HT axons in the medial and lateral forebrain bundles, and increased density of 5-HT-positive axons in the amygdala, piriform cortex, and in the temporal superior and parahippocampal gyrus. In autistic subjects 8 years of age and older, several types of dystrophic SERT-positive fibers were detected in the termination fields, including long heavily immunolabelled axons with irregularly spaced small circular or elliptical varicosities. These axons have intensively SERT immunoreactive bulbous, tapered or “cork-screw” endings. The detected increase in the number of serotonin-positive axons in the cortex and forebrain pathways may explain the negative response of autistic patients to SSRIs and suggests that in some cases application of serotonin antagonists may result in clinical improvement (Azmitia et al. 2011 a,b).

1.2. Autism etiology and links to serotonergic system

It is estimated that an earlier age of diagnosis and inclusion of milder cases account for more than two thirds of the reported increase of autism prevalence (Hertz-Picciotto and Deliche 2009). The true increase in the prevalence of autism is linked to genetic factors, environmental factors acting during pre-, peri-, and postnatal life, and concurrent diseases (Muhle et al. 2004; Newschaffer et al. 2002; Rutter et al. 1994, Landrigan, 2010). The etiology has a significant contribution to type, topography and severity of neuropathological changes and autism clinical phenotype.

Genetic factors. Autism has a strong genetic component (Bailey et al. 1995). Gene mutations, gene deletions, copy number variants and other genetic anomalies are linked to autism. Autism is highly heritable. Heritability provides an estimate of the proportion of phenotypic variation in the population that is due to genetic variation (Brown 2010). The study of 503 pairs of autistic twins born between 1992 and 2000 in California revealed concordance rates among the monozygotic males of 57% and among the monozygotic females of 67%. The heritability is estimated in range of 19-35% for males and 50-63% for females (Liu et al. 2010). Identical twin discordance might be due to epigenetic changes (Kaminsky et al. 2009).

Several potential candidate genes have been identified including the tuberous sclerosis gene on chromosomes 9 and 16; gamma-aminobutyric acid receptor-beta 3 on chromosome 15; neuroligins on the X chromosome (Vorstman et al. 2006) and *PTEN* on chromosome 10 (Butler et al. 2005). Moreover, two types of genetic defects of the serotonergic system are considered as increasing autism susceptibility: modifications of the serotonin transporter gene on chromosome 17 (Vorstman et al. 2006) and modifications detected in the tryptophan hydroxylase gene on chromosome 12 (Coon et al. 2005).

Approximately 5% to 10% of autism cases are associated with several distinct genetic conditions including fragile X syndrome, tuberous sclerosis, phenylketonuria, Rett syndrome and chromosomal anomalies such as Down syndrome (DS) and chromosome 15 duplication (Folstein and Rosen-Scheidley, 2001; Fombonne, 2003;Yonan et al. 2003). The prevalence of autism in boys with DS was estimated as at least 7% (Kent et al. 1999). The prevalance of autism in the fragile X syndrome is estimated as 15 - 28% (Hagerman 2002). Partial duplications, deletions, and inversions in the 15q11-q13-region account for 1% to 4% of autism cases (Cook, 1998; Gillberg, 1998). Application of the Gilliam Autism Rating Scale (GARS; Gilliam et al. 1995) to the idic15 group revealed that 20 of 29 children and young adults with idic15 were autistic (69%) (Rineer et al. 1998). Comparable prevalence of autism (78%) has been reported in a postmortem group of subjects diagnosed with dup15.

Genetic factors are clearly implicated in autism etiology, however they account for only 7-8% of autism cases (review by Landrigan 2010). The occurrence of sporadic cases, different clinical phenotype, discordant development in monozygotic twins, occurrence in family of autism as well as of only autistic traits suggests the contribution of a combination of genetic and environmental factors to autism etiology (Daniels 2006). Environmental factors could act together with inherited susceptibilities or through epigenetic changes (Mehler et al. 2008).

Environmental factors. The most powerful evidence is provided by studies specifically linking autism to fetus exposure in early pregnancy to thalidomide, misoprostol, valproic acid , the organophosphate insecticides, maternal rubella infection and other environmental factors (Chess, 1971, Strömland et al. 1994, Miller et al. 2005). The variation in interplay between different environmental exposures and genetic susceptibilities may result in the observed heterogeneity in the autism phenotype (Landrigan 2010). The significant contribution of

epigenetic factors to autism etiology is strongly supported by results of early screening tests that reveal signs of autism in about one-quarter of premature babies (Limperopoulos et al. 2008), and presence of autism-related behavioral profile in early infancy (Karmel et al. 2010). These data suggest that etiologic heterogeneity has a significant contribution to clinical diversity of autism and potentially to alterations detected in postmortem studies.

The role of maternal tryptophan and serotonin in fetus development. In the brain of a human fetus, first serotonergic neurons are detectable in the 5^{th} week of gestation. Maternal and placental serotonin control fetal brain development before and during development of fetal serotonergic system (Côté et al. 2007). To produce serotonin, placenta and fetal brain cells use maternal tryptophan (Bonin et al. 2011). Connors et al. (2006) postulated that maternal tryptophan and serotonin deficit may alter fetal brain and fetus raphé development with lifelong functional consequences including autism.

Serotonin in developing brain. Serotonin is one of the first brain neurotransmitters regulating cell proliferation, differentiation, and apoptosis (Whitaker-Azmitia 1991, Azmitia 2001, Verney et al.. 2002). The 35-fold increase in the level of tryptophan hydroxylase mRNA between embryonic day 18 and postnatal day 22 (Rind et al. 2000) suggest that serotonin plays a significant role in brain development. The increase of serotonin level during infancy and decrease to adult levels at age of five years appears to correspond to a high demand for serotonin during fetal and child development and reduced demand in late childhood and in adults. It also suggests that any modifications of this highly regulated process may result in defects of brain development, functional abnormalities and autism (Sodhi and Sanders-Bush, 2004).

Fetal serotonergic system exposure to maternal medication and drugs. A growing percentage of pregnant women receive SSRIs prescribed to treat depression, anxiety, and

obsessive-compulsive disorder (Wisner et al. 2000, Cohen et al. 2004). Increase of the percentage of females using antidepressants during pregnancy, from 1% in 1990 to 13% in 2010 parallels the increase in the prevalence of autism observed in these two decades. *In utero* exposure to antidepressants interacting with fetal SERT and a developing serotonergic system is considered one of several new epigenetic factors contributing to a growing risk of autism. Fetus exposure to SSRIs during the first trimester increases risk of autism by 3.8 times (Hadjikhani 2010, Croen et al. 2011). Experimental studies show that transient exposure may result in permanent alterations in the offspring's serotonergic system. SSRIs decrease the level of TPH in the dorsal raphé and serotonin transporter level in the cortex, with permanent effect observed in adult animals (Maciag et al. 2006). The second new risk factor is a growing prevalence of fetus exposure to drugs, including cocaine and such amphetamines as ecstasy, both binding to SERT. Ecstasy increases serotonin level and causes serotonin fiber degeneration (O'Hearn 1988). Cocaine (Akbari et al. 1992) as well as ethyl alcohol also increase serotonin concentration (Eriksen et al. 2002, Zhou et al. 2003) and may contribute to developmental alterations including autism (Davis et al. 1992, Nanson 1992).

1.3. Serotonergic system pathology in autism

5-hydroxytryptamine (5-HT; serotonin) serves as both a neurotransmitter and an important developmental signal in the brain. Serotonin regulates the size of neurons, the size of the dendritic tree and the number of synapses in innervated cortical and subcortical structures and cerebellum. Therefore, developmental abnormalities in the serotonergic system may contribute to structural and functional changes in target brain regions and structures. Virtually all regions of the brain receive serotonergic afferents from raphé system neurons (Azmitia 2012).

The rostral raphé nuclei form ascending pathways of axons mainly to the forebrain. The caudal raphé system innervates the lower brainstem and the spinal cord (Aitken and Törk, 1988; Lidov and Molliver, 1982). Dysregulation of the 5-HT system during development may be responsible for both developmental abnormalities and functional deficits seen in autism (Anderson et al. 1990, Chandana et al. 2005, Chugani et al. 1999, 2002, Cook et al. 1993, Janusonis et al. 2006, McNamara et al. 2008, Whitaker-Azmitia, 2005). In fact, all known chemical inducers of autism including cocaine, thalidomide, valproate and alcohol modulate 5-HT levels in the brain (Harris et al. 1995; Kramer et al. 1994; Narita et al. 2002; Rathbun and Druse 1985; Stromland et al. 1994).

A broad spectrum of studies indicate that developmental alterations of the peripheral and brain serotonergic system are involved in the autism clinical phenotype:

1. Increased prevalence of hyperserotonemia in the blood in autistic subjects (Schain and Freedman 1962, Cook and Leventhal 1996, McBride et al. 1998, Hranilovic et al. 2007, and Melke et al. 2008).
2. The association between hyperserotonemia and increased risk of recurrence of autism within families (Cook et al. 1990, Piven et al. 1991, Cross et al. 2008).
3. The correlation between blood serotonin level and severity of clinical symptoms (Hérault et al. 1996).
4. The correlation between low level of serotonin precursor (tryptophan) and severity of stereotyped behaviors in autistic subjects (McDougle et al. 1996a).
5. Impairment of the serotonergic system in the brain of autistic subjects (Chugani et al. 1997, 1999, Makkonen et al. 2008).
6. Link between brain serotonin deficit and severity of social deficits (Chugani et al. 1999)

7. Link between reduced uptake of tryptophan and severe language deficits (Chandana et al. 2005).
8. Amelioration of obsessive compulsive behavior, anxiety and aggression in some subjects treated with SSRIs (McDougle et al. 1996, de Long et al. 1998, Fatemi et al. 1998, Hollander et al. 2005, Kolevzon et al. 2006).
9. Abnormalities of serotonergic fibers in many target cortical and subcortical structures known to be involved in autism phenotype (Azmitia et al. 2011a).
10. Azmitia (2011b) review reveals links between serotonergic system alterations and epilepsy, immune dysregulation, gastrointestinal and sleep disorders, as well as anxiety, aggression, obsessive compulsive behavior and mood disorders observed in autism.

Blood hyperserotonemia. The blood hyperserotonemia observed in autism is an increase in the serotonin level in blood platelets by 25% to 50% (Anderson 2002). Blood platelets themselves do not synthesize 5-HT, but they take up serotonin from plasma using serotonin transporter (SERT). Since the first report published by Schain and Freedman in 1961, hyperserotonemia was confirmed in many reports (Hanley et al. 1977, Anderson et al. 1990, Cook 1996, McBride et al. 1998, Mulder et al. 2004, Hranilovic et al. 2007, Melke et al. 2008). Therefore, hyperserotonemia is considered the most consistent serotonin-related finding in autism. However, the cause of hyperserotonemia in autistic subjects is not clear. The relationship between peripheral hyperserotonemia and central nervous system dysfunction remains unknown. SERT polymorphic variants affect platelets' serotonin uptake rates (Anderson et al. 2002) and platelet serotonin levels (Coutinho et al. 2004). SERT polymorphism is unlikely the cause of hyperserotonemia in autism (Anderson et al. 2002, Persico et al. 2002). Mice lacking the 5-HT_{1A}

receptor expressed in the gut (Kirchgessner et al. 1996), develop autistic-like blood hyperserotonemia (Janusonis et al. 2006), which may be caused by altered regulation of the gut 5-HT release rate. Janusonis' (2008) model predicts that platelet serotonin level should be sensitive to changes in the platelet serotonin uptake rate constant, the proportion of free serotonin cleared in the liver and lungs, the gut 5-HT production rate and its regulation. Spivack et al. (2004) reported a negative correlation between plasma-free 5-HT concentration and the level of aggressiveness in autistic adults.

Platelet serotonin level in autism. Hranilovic et al. (2007) revealed that the mean platelet serotonin level in 53 autistic subjects aged 16 to 45 years was 75.7+-37.4 ng/μL whereas in 45 control subjects aged 20 to 55 years the mean level was 59.2+-16.2 ng/μL. 32% of autistic subjects revealed hyperserotonemia. A negative correlation was observed between platelet serotonin level and speech development, but there is no correlation with severity of symptoms as measured by total CARS score and degree of mental retardation (Hranilovic 2007). A significant negative correlation between whole blood 5-HT levels and verbal abilities of autistic subjects and their first degree relatives was found by Cook et al. 1990 and Cuccaro et al. 1993.

Origin of blood serotonin and serotonin degradation. Plasma serotonin is the product of enterochromaffin cells of the gut mucosa (Gershon 2004). Human gut serotonin production was estimated at 3,000 ng/min (Anderson et al. 1987). In the GI tract, serotonin is also produced by myenteric neurons (Wardell et al. 1994, Furness et al. 1982, Erde et al. 1985). Extracellular serotonin is taken up by SERT- expressing gut cells (Gershon and Tack 2007). Serotonin diffused in blood plasma is used by SERT-positive blood platelets. However, the majority of plasma serotonin is rapidly cleared by the liver and lungs (Thomas and Vane 1967, Anderson et al. 1987).

Brain - dynamic changes in serotonin level during development and maturation.

Severity of hyperserotonemia is correlated with severity of autistic behaviors (Chandana et al. 2005; Chugani et al. 1999, 2002; Kuperman et al. 1987). Chugani et al. (1999) and Chandana et al. (2005) reported significant differences in early postnatal serotonin level in the frontal, temporal, parietal and occipital cortex between children with autism and control subjects. Serotonin level in a normal human cortex, as in rodents, is highest shortly after birth and decreases with age up to sexual maturity. However, young children with autism have a significantly attenuated peak in serotonin synthesis compared to age- matched controls (Chugani et al. 1999; Chandana et al. 2005). Their capacity for serotonin synthesis increases gradually from 2 to 15 years.

A causal role for serotonergic abnormalities in the etiology of autism is also suggested by studies indicating autism-specific genetic polymorphisms in 5-HT metabolizing enzyme, transporter or receptor genes (Sutcliffe et al. 2005).

Cellular consequences of increased serotonergic activity during brain development.

The first serotonergic neurons are detected by the 5^{th} week of gestation (Sundstrom et al. 1993). Their number increases dramatically by the 10^{th} week (Kontur et al. 1993, Levallois et al. 1997) and at the age of 15 weeks of gestation raphé nuclei are formed (Takahashi et al. 1986). Serotonin levels increase throughout the first two to five years, but in adulthood serotonin level is only 50% of the concentration observed in infancy (Toth and Fekete 1986, Chugani et al. 1999). This suggests that high levels of serotonin are necessary during brain development and suggests the contribution of serotonin to normal brain development. Whitaker-Azmitia (2005) hypothesized that serotonin neuron development is associated with an increase of the serotonin to a level at which serotonin innervation reaches a level higher than that required for normal

brain structure/function. A negative feedback mechanism, most likely mediated by the 5-HT_{1A} receptor, curtails neuron growth to adult brain level.

Cellular consequences of peripheral hyperserotonemia in autism. According to the second Whitaker-Azmitia (2005) hypothesis, peripheral hyperserotonemia observed in some autistic children may affect development of the brain serotonergic system with structural and functional consequences contributing to a behavioral autism phenotype. Hyperserotonemia at early stages of brain development, when the blood brain barrier is immature, results in an excessive amount of serotonin that can enter the brain of the developing fetus, and down-regulate development of the raphé nuclei through negative feedback. The 5-HT_{1A} receptor present both on the body of the serotonergic neurons in the raphé nuclei and in brain target neurons, plays an inhibitory role in autoregulation of serotonergic neuron development, and acts as an inhibitory autoreceptor in the mature brain (Whitaker-Azmitia and Azmitia 1986, Lauder et al. 2000, Gaspar et al. 2003).

1.4. Serotonin, serotonin transporter, and receptors

5-HT synthesis. Over 95% of the body 5-HT is present in the gastrointestinal tract (Erspamer 1966), mostly in enterochromaffin cells of the mucosal epithelium (Gershon et al. 1994) and in serotonergic neurons of the enteric nervous system (Gershon et al. 1994, Erde et al. 1985). Serotonin action is regulated temporally and spatially by cells possessing enzymes catabolyzing 5-HT (Martel 2006). Enzymes catabolyzing 5-HT, including monoamine oxidase (MAO) and glucuronyl transferase are located in the cell cytoplasm. Therefore, inactivation of 5-HT of extracellular origin requires 5-HT internalization by cell plasmalemma. In the central and

peripheral nervous system, 5-HT is inactivated primarily by reuptake into the serotonergic neurons.

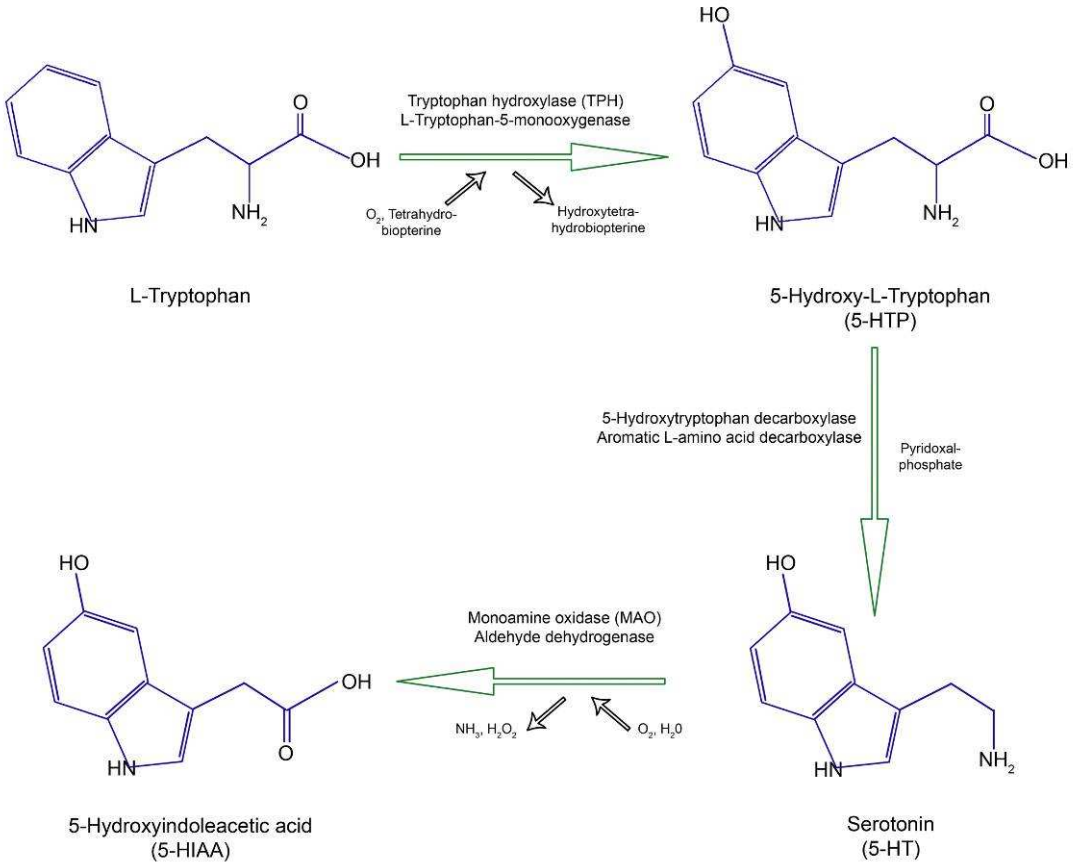

Fig. 1. 5-HT synthesis. The rate of 5HT synthesis is limited by the intracellular level of L-tryptophan, the essential amino acid provided with food, and tryptophan hydroxylase (TPH).

In humans and animals, serotonin is synthesized in a two- step process from the amino acid L-tryptophan. The first step requires tryptophan hydroxylase (TPH). The TPH- mediated reaction is the rate limiting step in this pathway. TPH exists in two forms: TPH1 present in various tissues and TPH2 which is a brain-specific isoform. Genetic polymorphisms in both TPH1 and TPH2 influence susceptibility to anxiety and depression. Addition of a hydroxyl group to L-tryptophan results in 5-hydroxy-L-tryptophan (5-HTP). The product of action of 5-Hydroxytryptophan decarboxylase on 5-hydroxy-L-tryptophan is serotonin (5-HT). Monoamine

oxidase and aldehyde dehydrogenase break down serotonin to 5-hydroxyindoleacetic acid (5-HIAA) which is excreted**.**

5-HT distribution. Experimental studies of the rat brain revealed that 5-HT immunolabeling in axons is distributed diffusely throughout the portion of axonal cytoplasm or is observed in large (80 to 150 nm in diameter) dense core vesicles (DCV). However, application of different protocols of tissue preservation suggests that 5-HT distribution is in part modified by fixation techniques. In glutaraldehyde- fixed tissue more diffuse labeling is observed in axons and in axon terminals whereas in acrolein-fixed tissue immunolabeling of 5-HT was found mainly in dense core vesicles (DCV) in axons and axon terminals (Pickel and Chan 1999).

Synaptic and non-synaptic transmission of 5-HT. Serotonin transmission might be restricted to the synaptic cleft (hard-wired neurotransmission) or neurotransmitter diffusion to remote sites (volume or paracrine transmission). Knowledge of synaptic transmission in the brain is based in part on studies of acetylcholine action at the neuromuscular junction, where ACh released into the synaptic cleft diffuses and interacts with intrasynaptic receptors. Rapid binding to receptors restricts ACh diffusion and increases probability of degradation of ACh by acetylcholinesterase (Magleby and Terrar 1975, Bartol et al. 1991). This process is known as “buffered diffusion” (Katz and Miledi 1973) and is restricted spatially to the synaptic cleft.

In contrast, 5-HT can participate in what has been termed “volume” (Fuxe and Agnati 1991) or paracrine transmission in the dorsal raphé and in the substantia nigra pars reticulata (Bunin and Wightman 1998). In the DRN, 5-HT neurons exhibit little synaptic specialization and the majority of 5-HT uptake sites is extrasynaptic. In the DRN serotonergic neurons accumulate 5-HT in the cell body and dendrites in vesicles in a releasable form (Hery and Ternaux 1981, Iravani and Kruk 1997, Bunin and Wightman 1998) as well as in axon collaterals and terminals

(Mosko et al. 1977, Liposits et al. 1985). Ultrastructural studies suggest junctional and non-junctional release of 5-HT but non-junctional predominates. For the serotonergic system which communicates mainly by extrasynaptic means, synapses may exist simply as a point of anatomical connectivity, but transmission is based on extrasynaptic mechanisms (Bunin and Wightman 1998).

Dopamine also diffuses from the synaptic cleft and interacts with receptors and transporters at remote sites (Smiley et al. 1994, Nirenberg et al. 1997). The dopamine (DA) transporter regulates the lifetime of DA in the extracellular space and the distance DA can travel from its release site (Garris and Wightman 1995, Giros et al. 1996). Interactions of 5-HT and dopamine in extrasynaptic space allow for longer range of activity and less specific interactions than neurotransmission restricted to the synaptic cleft (Clements 1996). The computed excess of both receptor and transporter sites relative to the number of 5-HT molecules suggests that innervated brain structures (such as substantia nigra) may optimally use the large amount of 5-HT released by rapid bursts that can originate in the cell bodies of the raphé neurons (Hajos et al. 1996). In contrast to glutamate and GABA using synaptic transmission and not activating second messenger systems but directly activating ion channels, most DA and 5-HT receptors are coupled to second messengers (Kandel et al. 1991).

Serotonin transporter (SERT)

SERT, a 630 residue hydrophobic phosphoglycoprotein with the molecular weight of 59kD (Blakely et al. 1991, Hoffman et al. 1991, Mayser et al. 1991, Baker et al. 1994) is a member of the Na+/Cl- dependent plasma membrane transporter family. It is expressed in perisynaptic areas of afferent fibers from median and dorsal raphé nuclei. The prefrontal cortex as well as hippocampal sectors CA1 and CA3, have the highest densities of this transporter. The

serotonin transporter takes up released serotonin from the synapse to replenish neuron stores. Dysfunction of the receptor and the subsequent abnormal levels of serotonin in the synapse are characteristic of anxiety, depression, alcoholism and drug addiction. Some medications that treat these conditions work by blocking this transporter (Wersinger 2006). Antidepressants increase serotonin levels by blocking SERT. Serotonin re-uptake depends on the level of active transporter on the cell surface.

SERT is a marker of serotonergic axons. Immunostaining for SERT allows one to follow projections of serotonergic fibers from the raphé nuclei to brain target areas (Verney 2002). Serotonin transporters appear evenly distributed throughout the dorsal raphé nucleus. Repeated application of certain antidepressants changes expression of the serotonin transporter in the dorsal raphé (Stockmeier 1996). Removal of extracellular serotonin by SERT proteins is a major pathway for 5-HT inactivation. Serotonin that is not bound to receptors is removed from the synapse by transporters and transported back into the neuron where it is metabolized.

Molecular cloning of SERT from human placenta (Ramamoorthy et al. 1993), rat brain (Blakely et al. 1991), basophilic leukemia cell cDNA libraries (Hoffman et al. 1991) and from human raphé (Lesch et al. 1993) revealed the 5-HT transporter's primary structure. SERT contains 12 putative transmembrane domains, cytoplasmic N- and C-termini and N-glycosylation sites within the large extracellular loop between transmembrane segments 3 and 4 (Blakely et al. 1993).

Serotonergic raphé neurons reveal high levels of SERT mRNA (Austin et al. 1994, Charnay et al. 1996). In situ hybridization studies in the rat (Fujita et al. 1993) and human (Austin et al. 1994) brain revealed that SERT mRNA is predominantly expressed in raphé neurons but failed to demonstrate SERT mRNA in glial cells.

SERT catalyzes the co-transport of Na^+, Cl^- and 5-HT and removes 5-HT from the extracellular space. The uptake mechanism is activated within less than a millisecond after transmitter release. Therefore SERT shapes the time course of the postsynaptic response (Bruns et al. 1993). 5-HT release is a near instantaneous process that accompanies impulse flow, whereas uptake is time-dependent (Bunin and Wightman 1998).

Relationships between 5-HT release, SERT, and 5-HT extracellular levels.

Ultrastructural immunolabeling demonstrates 5-HT in large dense core vesicles (Pickel and Chan 1999). Vesicular release of 5-HT by serotonergic neurons (Gobbi et al. 1998) is accompanied by reuptake into these neurons through the serotonin transporter (SERT) (Qian et al. 1995). The extracellular 5-HT levels reflect vesicular release and plasmalemmal reuptake through SERT. Experimental studies of the nucleus accumbens in the rat suggest that increased 5-HT release without concomitant increase in SERT expression in individual axons may contribute to higher extracellular levels of serotonin (Pickel and Chan 1999). Similar relationships are observed between extracellular levels of dopamine and plasmalemmal dopamine transporter (Nirenberg et al. 1997, Jones et al. 1996).

The studies of Down syndrome and an experimental model of DS (Ts65Dn mice) indicate that alterations in the serotonergic system are involved in abnormal neurogenesis and developmental neuronal deficits (Bianchi et al. 2010). This concept is supported by reports documenting reduced 5-HT level in DS (Risser et al. 1997) and the causative link between 5-HT depletion and permanent reduction in neuron number in the adult brain (Whitaker-Azmitia 2001). Antidepressants increase neurogenesis in the dentate gyrus and subventricular zone of the lateral ventricle (Malberg et al. 2000, Shankaran et al. 2006). Treatment of neonate Ts65Dn mice (animal model of DS) from postnatal day P3 to P15 with fluoxetine, an antidepressant that

inhibits serotonin reuptake increases neuronal proliferation in the adult Ts65Dn mice (Clark et al. 2006). P15 Ts65Dn mice had defective proliferation in the hippocampal dentate gyrus, subventricular zone, striatum and neocortex, but defects of proliferation were completely rescued by fluoxetine. Moreover, behavioral tests revealed complete recovery of memory performance in fluoxetine treated Ts65Dn mice (Bianchi et al. 2010).

SERT distribution. SERT immunogold labeling is detected in ultrastructural studies in axons, axonal terminals, dendrites and glial processes. SERT immunolabeling prevails at nonsynaptic sites of axons (Zhou et al. 1998, Pickel and Chan 1999). In dendrites, SERT immunogold particles are observed (a) along plasma membrane of one dendrite apposed to other dendrite, (b) along plasma membrane of dendrite far from synapses or (c) along plasma membrane apposed to synaptic terminals.

In unmyelinated axons, SERT is observed along plasma membrane (a) apposed to other unmyelinated axon, (b) unmyelinated axon apposed to the dendrite, or (c) synaptic terminals. Reaction is observed along plasma membranes or associated with membranes of small synaptic vesicles (SSVs) of axons.

Double immunolabeling for 5-HT and SERT shows that small unmyelinated axons express both SERT and 5-HT. Labeling for 5-HT is seen as diffuse labeling within the axon, whereas immunogold SERT labeling is localized along the plasma membrane.

In the rat nucleus accumbens, SERT was detected in 60-61% of unmyelinated axons. Immunolabeling appeared denser in small axons than in axon terminals. Immunolabeling for SERT was detected also in 2 to 4% of dendritic profiles or dendritic spines as well as in glial processes (Pickel and Chan 1999). These observations suggest a role for SERT in synaptic and nonsynaptic communication. The extrasynaptic distribution of SERT (Pickel and Chan 1999) and

dopamine transporter DAT (Nirenberg et al. 1997) suggests that monoamines diffuse from sites of release into the synaptic cleft to distant receptors in a paracrine mode of transmission (Bunin and Wightman 1998). This hypothesis is consistent with the presence of receptors for 5-HT and dopamine located at pre- and post-synaptic sites, as well as nonsynaptic sites on plasma membranes (Pickel and Sesack 1995, Hirst et al. 1998ab, Jakab and Goldman-Rakic, 1998).

SERT expression and 5-HT uptake by glial cells. The results of studies of SERT expression in glial cells are inconsistent. A study of SERT distribution in rat brain revealed that there is no evidence for the presence of SERT activity in glial cell bodies and processes (Sur et al. 1996). However, it was shown that cultured astroglial cells take up 5-HT (Whitaker et al. 1983). Moreover, the Na^+-dependent, fluoxetine sensitive serotonin uptake by astrocytes from rat cerebral cortex suggests SERT involvement (Dave and Kimelberg 1994).

Drugs binding to SERT. Enhancement of extracellular concentration of 5-HT is a fundamental mechanism for the success of application of antidepressants. SERT is considered a primary target for antidepressant drugs. It was documented that antidepressants, such as fluoxetine, bind to SERT and increase extracellular level of 5-HT (Schloss and Williams 1998, Staley et al. 1998).

The role of monoamine oxidase in 5-HT pathways. It has been proposed that after reuptake mediated by SERT, the 5-HT is deaminated by mitochondrial monoamine oxidase (MAO) and that this process produces 5-hydroxyindolacetic acid (5-HIAA). MAO-A is known as having a high affinity for 5-HT. However, serotonergic neurons do not appear to have MAO-A. Therefore reuptake into the nerve terminals may lead to reutilization of 5-HT rather than degradation, whereas uptake of 5-HT by MAO-A-positive astrocytes results in 5-HT inactivation (Bel et al. 1997).

Serotonin receptors. In the nervous system the function of serotonin is mediated by 14 subtypes of 5-HT receptors (Hoyer et al., 1994; Martin and Humphrey, 1994; Saudou and Hen, 1994). The 5-HT_{1A} receptor appears the earliest of the serotonin receptors and reveals a prenatal peak. In the human cortex, density of 5-HT_{1A} receptors decreases with age (Stockmeier 1996). It is found on bodies of raphé nuclei serotonergic neurons, on target neurons, and enterochromaffin cells in the gut (Janusonis 2006). In the brain, somatodendritic autoreceptors regulate serotonin release from raphé neurons. Lack of these receptors in a critical period of brain development results in anxiety in adult mice (Janusonis 2006).

The 5-HT_{1A} receptor is involved in activation of hyperpolarizing K^+ channels, which leads to a decrease in firing of neurotransmitters. Initially after treatment with the receptor's agonist, the agonist binds to autoreceptors on raphé neurons. Serotonin release at the presynaptic terminal is decreased due to the hyperpolarizing effect of 5-HT_{1A} autoreceptors. Any excess agonist is free to act on postsynaptic 5-HT_{1A} receptors, inhibiting postsynaptic neurons. However, prolonged treatment with agonists leads to internalization and desensitization of the autoreceptors on the raphé neurons while the postsynaptic receptors are unaffected. Inhibition of autoreceptors results in an increased 5-HT release. Released 5-HT binds to postsynaptic 5-HT_{1A} receptors causing elevated signaling (Banerjee 2007).

The serotonin$_{2A}$ (5-HT_{2A}) receptor is one of the most common serotonin receptors involved in facilitating the formation and maintenance of synapses (Niitsu et al., 1995) and associated with psychological and mental events (Roth, 1994). Immunostaining shows that the entire soma and dendritic tree of Purkinje cells is covered with 5-HT_{2A} receptors (Maeshima et al. 1998). In vitro studies have shown that 5-HT inhibits the growth and arborization of Purkinje

cell dendrites through 5-HT_{2a} receptors and stimulates them through the 5-HT_{1A} receptor (Kondoh et al., 2004). 5-HT promotes the formation of synapses in a developing and mature brain and spinal cord (Chen et al., 1997; Niitsu et al., 1995; Okado et al., 1993), and this process is mediated by the 5-HT_{2a} receptor (Niitsu et al.., 1995).

SERT in astrocytes. Bel et al. 1997 suggest that a low concentration of SERT mRNA or protein in a single astrocyte may not give a detectable signal but higher numerical density of astrocytes than neurons makes astrocyte SERT a significant factor in regulation of extracellular 5-HT level. The level of extracellular 5-HT is regulated by neuronal 5-HT synthesis and release into the extracellular space, uptake by 5-HT receptors and autoreceptors and reuptake mediated by SERT on neurons and astrocytes.

The uptake of 5-HT by rat brain astrocytes has been documented (Katz and Kimelberg 1985, Kimelberg and Katz 1985, Dave and Kimelberg 1994). mRNA for the 5-HT transporter is detected in cultured rat astrocytes and in adult rat brain both in areas with serotonergic cell bodies (in midbrain and brainstem), and in areas without serotonergic cell bodies (frontal cortex). Primary cultures of cortical rat and mouse astrocytes reveal that astrocytes take up and deaminate 5-HT (Fitzgerald et al. 1990, Bel et al. 1997). In vivo studies also demonstrate that rat astrocytes uptake 5-HT and that this process is mediated by the astrocyte's serotonin transporter. Antidepressants, including citalopram, clomipramine, fluoxetine, fluvoxamine, paroxetine and sertaline inhibit serotonin uptake by astrocytes (Bel et al. 1997). Astrocytes may play a significant role in control of serotonergic activity by inactivating 5-HT in sites distant from serotonergic terminals. Therefore astrocytes are another cellular target for antidepressant drugs that inhibit 5-HT uptake. Uptake of 5-HT into astrocytes (containing MAO-A) may result in inactivation of 5-HT and regulation of extracellular serotonin level (Bel et al. 1997). The

presence of MAO-A has been shown in astrocytes by immunohistochemistry (Westlund et al. 1988).

1.5. Anatomy and connectivity of the human raphé serotonergic system

Detection of serotonergic neurons in human postmortem brain tissue samples. The raphé nuclei in the brainstem are the source of serotonin in the human brain. The term "raphé" describes a midline seam where the left and right halves of the brainstem appear to be fused (Törk and Hornung 1990). Cresyl violet staining shows that medium to large neurons with strongly stained Nissl substance form several distinct nuclei of the raphé. Heavily stained neurons corresponding to the dorsal raphé nucleus were described first by Kölliker in 1893. A detailed cytoarchitecture of the human raphé system was based on application of the aldehyde-fuchsin technique applied to thick sections by Braak in 1970. The first histological localization of monoamines was based on application of the histofluorescence technique demonstrating distribution of serotonergic neurons near the brainstem midline (Dahlström and Fuxe 1964). Characteristics of serotonergic neurons were refined by application of immunohistochemical methods demonstrating distribution of tryptophan hydroxylase involved in serotonin synthesis (Joh et al., 1975), serotonin (Steinbusch 1981) and serotonin transporter (Sur et al. 1996, Zhou et al. 1996). Cytoarchitecture and chemoarchitecture of human raphé nuclei has been described by Halliday et al. 1988a, 1990, Törk and Hornung 1990, Baker et al. 1991ab, and reviewed by Hornung (2003).

Serotonergic neurons in the human brain can be seen at 5 weeks of gestation (Sundstrom 1993). Formation of raphé nuclei can be seen at 15 weeks. Serotonin fibers grow into the cortex prenatally. Serotonin levels continue rising but after 2-5 years of life decline to adult levels.

Technology available for detection of serotonergic neurons in human postmortem material is limited. Methods of detection of serotonin in animal material cannot be used in postmortem material because serotonin rapidly dissipates from the cells after death.

Fetal brain. Brain of fetuses rapidly frozen or fixed immediately after an abortion was used by Nobin and Bjorklund (1973), Olson et al. (1973), and Takahashi et al. (1986) to demonstrate serotonergic neurons in the human fetal brainstem.

Aldehyde-fuchsin method. Braak et al. 1970 employed the aldehyde-fuchsin technique for thick sections to study the cytoarchitecture of the human raphé system. Braak's report has provided the most detailed analysis of the human raphé nuclei to date although the technique is not specific to serotonergic neurons.

Tryptophan hydroxylase. Törk and Hornung (1990) delineated serotonergic nuclei in formalin fixed human brain using mAb PH8 which recognizes tryptophan hydroxylase, the biosynthetic enzyme of serotonin (Haan et al. 1987). Törk and Hornung's (1990) protocol appears to be the best one for preservation of human brainstem for research. Törk fixed the brainstem in 4% buffered formaldehyde solution for several months, washed in phosphate-buffered solution (PBS), then immersed in a 30% sucrose solution and sectioned 50-μm-thick serial sections on a freezing microtome. Four sets of serial sections were stained with: (a) PH8 antibody (1:2000) for demonstration of tryptophan hydroxylase-like immunoreactivity, (b) antibody against tyrosine hydroxylase (TH; 1:1500) (Van den Pol et al. 1984) for tyrosine hydroxylase-like immunoreactivity, (c) Cresyl violet, and (d) Weigert staining. Every eighth section of one complete brainstem (left and right) was immunohistochemically stained and used for 3D reconstruction of TPH-immunopositive neurons, presumed to be serotonergic neurons (Hornung and Kraftsik 1988).

Anatomical divisions of the human raphé nuclei

Based on cyto- and chemoarchitecture, spatial distribution and projections (Halliday et al. 1988a, 1990, Törk and Hornung 1990, Baker et al. 1991a and b), and properties of neuronal precursor populations (Ding et al. 2003) six clusters of serotonergic neurons in the human brainstem are divided into a rostral and a caudal group.

Rostral group. The rostral group accounts for 85% of all serotonergic neurons in the brain (Hornung 2003), is confined to the mesencephalon and rostral pons, and consists of the Caudal Linear Nucleus (CLN), Dorsal Raphé Nucleus (DRN), and Median Raphé Nucleus (MRN)(also called Nucleus Centralis Superior Pars Medialis). Serotonergic neurons of a rostral group project mainly to the forebrain.

Caudal group. The caudal group consists of the Nucleus Raphé Magnus (NRM), Nucleus Raphé Obscurus (NRO), and Nucleus Raphé Pallidus (NRP). The caudal group extends from the caudal pons to the caudal portion of the medulla oblongata. Neurons of the caudal group project to the caudal brainstem and to the spinal cord (Hornung 2003).

Caudal Linear Nucleus (CLN). The CLN is located dorsal and caudal to the interpeduncular nucleus and occupies a region on the midline between the two red nuclei (Halliday and Törk, 1986). The CLN contains a heterogenous population of neurons including large serotonergic and dopaminergic neurons pigmented like neurons in the substantia nigra or locus coeruleus, and neurons positive for substance P (Halliday et al. 1990). The majority of serotonergic neurons have a few dendrites oriented in the dorsoventral and rostrocaudal direction (parallel with the midline) (Törk and Hornung 1990). Due to the large population of serotonergic neurons, the CLN is considered the most rostral portion of the serotonergic raphé system.

According to Hornung (2003) estimates, serotonergic neurons in CLN are ten times less numerous than in the dorsal or in the median raphé nuclei.

Dorsal Raphé Nucleus (DRN). The DRN is located on the border of the mesencephalon and pons. The most rostral DRN cells appear at the level of the caudal part of the oculomotor nucleus. The largest portion of this nucleus is present caudally to the oculomotor complex and is the largest at the level of the trochlear nucleus. At this level serotonergic neurons extend laterally into the ventral periaqueductal gray and partially surround the medial longitudinal fasciculus. The DRN is subdivided into four subdivisions: dorsal (DRD), ventral (DRV), interfascicular (DRIF)(also called Nucleus Centralis Superior Pars Dorsalis) and ventro-lateral (DRVL) (Baker et al. 1990). The caudal subdivision of the dorsal raphé nucleus (DRc) becomes slender and extends to the midpontine level. DRN neurons are large multipolar cells extending their dendrites for about 100 μm from the cell body (Törk and Hornung 1990, Baker et al. 1990). In about 40% of neurons in the rostral half of DRN serotonin is colocalized with substance P (Baker et al. 1991a) but some neurons also synthesize several neuropeptides including dynorphin, angiotensin, neurotensin or enkephalin (Jennes et al. 1982, Björklund and Hökfelt 1985).

The ventrolateral group located just dorsal to the trochlear nuclei is characterized with the highest numerical density of serotonergic neurons. The small multipolar neurons in this subnucleus extend caudally from the midbrain (anterior pole of DRN) into the rostral pons (Törk and Hornung 1990).

The lateral group of cells, which cannot be recognized in Nissl stainings, includes the largest TPH positive neurons in the dorsal raphé, which are loosely arranged. They have a characteristic morphology- they are multipolar, have 3-4 straight, aspiny dendrites that have

dichotomous divisions. The dendrites end approximately 100 μm from the cell soma. (Törk and Hornung 1990)

The dorsal subnucleus is located dorsomedial to the ventrolateral group and ventral to the aqueduct floor. Medium-seized neurons are loosely arranged (Underwood 1999). The two wings of the dorsal subnucleus are joined at the midline.

The interfascicular subnucleus located between left and right medial longitudinal fasciculi stretches from the rostral end of the dorsal raphé to the caudal end of the median nucleus. The densely arranged neurons are oriented parallel to midline. The caudal portion of the dorsal nucleus is made up of two strips of neurons on either side of midline. The cells are densely arranged, and small to medium sized with short dendrites. The caudal group continues well into the rostral pons (Törk and Hornung 1990).

Median Raphé Nucleus (MRN) (also called Nucleus Centralis Superior Pars Medialis). In the human brainstem, the volume of the MRN is the largest of all the raphé nuclei. The MRN extends from the caudal limit of the decussation of the superior cerebellar peduncle to the level of the trigeminal motor nucleus. The MRN is divided into a rostral half and caudal half. The rostral half is located in the midline and called the median region or median raphé proper. In this subdivision more than 80% of neurons synthesize serotonin. The caudal half consists of a paramedian region and two lateral extensions in the reticular formation. The dorsal extension consists of serotonergic neurons in the nucleus pontis oralis (PnO). The ventral extension consists of serotonergic neurons dispersed in the supralemniscal nucleus (SuL) (Baker et al. 1991a). The percentage of serotonin producing neurons is significantly less in lateral divisions of the MRN (Baker et al. 1991b). Few neurons in the MRN contain substance P, cholecystokin, dynorphin, enkephalin, or neurotensin (Björklund and Hökfelt 1985).

TPH-immunoreactive neurons have round cell soma and thin short dendrites. They are densely packed in the rostral portion of the MRN and loosely arranged in the caudal part. The caudal portion is rich in TPH-negative cells.

Caudal group of raphé nuclei. The three nuclei of the caudal group account for only 15% of serotonergic neurons in the human brain (Hornung 2003).

Nucleus Raphé Magnus (NRM). The NRM is the largest nucleus of the caudal group made up of about 30,000 neurons (Hornung et al. 2003). It's located above the medial lemniscus at the level of the facial nucleus, adjacent to the midline. The NRM extends from the rostral superior olive back to cranial nerve XII. It consists of medium sized to large multipolar neurons. There is continuity between the NRM and the cluster located in the neighboring gigantocellular reticular nucleus (pars α)

Nucleus Raphé Obscurus (NRO). The NRO is located caudally to the NRM in the dorsal half of the medulla close to the midline. The NRO is divided into the paired subnucleus extraraphalis and an unpaired subnucleus intraraphalis. The **subnucleus extraraphalis** is made up of elongated and multipolar neurons with long dendrites. The **subnucleus intraraphalis** consists of medium to large, spindle-shaped neurons with large dark Nissl bodies (Azmitia 1999). Neurons of the NRO express substance P (Del Fiacco et al. 1984, Halliday et al. 1988b, Rikard-Bell et al. 1990) and galanin (Blessing and Gai 1997).

Nucleus Raphé Pallidus (NRP). The NRP is an unpaired median nucleus with medium and large cells. These contain few peripheral Nissl bodies and have irregular ragged edges. The NRP is located adjacent to the midline between the pyramids and the overlying medial lemniscus. NRP is the smallest group in the raphé system with only approximately 1,000 serotonergic neurons (Hornung 2003). The nucleus has its maximal development at the level of

the rostral pole of the inferior olive. At the caudal end of the nucleus only a few cells can be seen between the fibers of the medial lemniscus.

Reticular formation - chemical and functional differentiation of serotonergic neurons. The pontine reticular formation includes the rostral and caudal pontine reticular nucleus composed mainly of small to medium-sized neurons, except in the gigantocellular reticular nucleus. They project to the thalamus, hypothalamus, septum, and medial frontal cortex (Jones and Yang 1985, Robertson and Feiner, 1982). Rostral and caudal reticular nuclei are involved in sleep (Morrison and Reiner 1985), coma (Katayama et al. 1986), horizontal gaze control (Fuchs et al. 1985), pain perception (caudal paralemniscus) (Mehler et al. 1960). The gigantocellular reticular nucleus (Olszewski and Baxter 1954) contains the largest multipolar neurons which are probably involved in general arousal. Several clusters of large multipolar TPH-IR neurons with long aspiny dendrites are present in the reticular formation, especially in the rostral portion of the pons laterally to the median nucleus (Törk and Hornung 1990). One of the most prominent gatherings of serotonergic neurons in the reticular formation is located in the human (Törk and Hornung 1990), cat (Jacobs et al. 1984) and monkey (Azmitia and Gannon 1986) oral pontine nucleus. The second large cluster of TPH-IR neurons located dorsally to the medial lemniscus is the human homolog to the B9 cell group identified by Dahlström and Fuxe (1964). Westlund's (1988) observation that in contrast to raphé MAO B-positive neurons, serotonergic neurons in the reticular formation are MAO B-negative, suggests that reticular formation serotonergic neurons represent chemically and functionally different populations of serotonergic neurons with different connections.

Serotonergic neurons in the central gray. Rostrally to the dorsal raphé nucleus are serotonergic neurons dispersed in three nuclei of the central gray (Nobin and Bjorklund 1973).

Three major subdivisions: median, dorsal and lateral central gray nuclei were identified by Olszewski and Baxter (1954). Golgi studies distinguished loosely dispersed fusiform, stellate and pyramidal neurons (Mantyh 1982). Central gray neurons are innervated by serotonergic neurons. While the role of serotonergic innervation of the central gray neurons has not be determined, Soubrie's (1986) review suggests their role in human behavior. They may modulate numerous connections of the central gray with amygdala, hypothalamus, hippocampus and several cortical regions (Beitz 1991).

Morphometric studies of human raphé nuclei. Only a few immunocytochemistry-based morphometric studies of human raphé nuclei are published. Several characterize the DRN in alcoholism and depression (Underwood et al. 2007, Halliday et al. 1993, Baker et al. 1996). While Underwood et al. did not demonstrate a difference in the number of PH8-immunoreactive neurons in DRN in the alcoholic group, Halliday et al. (1993) observed fewer serotonergic neurons in alcoholic individuals with Wernicke encephalopathy and Wernicke-Korsakoff syndrome compared to controls. Baker et al. (1996) reported lower TPH immunoreactivity but no difference in the total number of neurons.

The number of DRN serotonergic PH8-immunoreactive neurons in 6 control subjects 17 to 74 years of age was determined as 80,386 ±10,238 and was similar to estimates in alcoholic individuals (85,884±12,478; n = 9, aged 16 to 66 years).

The volume of the DRN was 88±9 mm^3 in controls and 55±5 mm^3 in alcoholics. The length of the DRN was 15±2 mm in controls and 18±1 mm in alcoholic individuals. The average size of DRN neurons was 352±12μm^2 in the control group vs 360±15 μm^2 in alcoholic subjects. However, alcoholic individuals had optical density TPH-IR 42% greater than the control subjects dorsal raphé nucleus ($p = 0.028$). There was no effect of age or severity of disease. However, the

density of neuron processes (area of immunoreactive processes/DRN crossection area) was 2.2-fold greater in the DRN of alcoholics than in control subjects (p=0.03) and increase correlated with duration of alcoholism.

Autoradiographic and immunohistochemical studies have shown that in the rat the DRN contains about 35,500 neurons among which 11,500 contain 5-HT (Descarries et al. 1982). The cat DRN is reported to have 24,300 5-HT neurons, which constitute about 70% of the total (Wiklund et al. 1981). In human the DRN contains about 165,000 5-HT- immunoreactive neurons (Baker et al. 1991a).

The study suggests increased content of TPH which may reflect an increase in the overall synthesis of 5-HT. Lower CSF 5-HIAA in alcoholic subjects (Fils-Aime et al. 1996) and higher TPH-IR optical density may indicate abnormal enhanced intracellular accumulation of 5-HT but reduced release. These data suggest that lower serotonin function in alcoholic individuals is not due to deficit of 5-HT-synthesizing neurons or reduced level of TPH. Reduced serotonin transporter binding in the brainstem of alcoholic subjects demonstrated in SPECT imaging (Heinz et al. 1998) but an unmodified number of neurons suggests less transporter binding per serotonergic neuron.

Connections of the raphé nuclei. Virtually all regions of the brain receive serotonergic afferents from raphé system neurons (Azmitia 2012). Studies on rat indicate that the serotonergic system can be divided into two developmentally distinct subsystems (Aitken and Törk 1988, Lidov and Molliver 1982). The rostral raphé nuclei form ascending pathways of axons sent mainly to the forebrain. The caudal raphé system mainly innervates the lower brainstem and the spinal cord. The superior group of raphé nuclei projects to the forebrain. Limbic areas, primary sensory association areas, suprachiasmatic nucleus in the hypothalamus and substantia nigra are

abundant in serotonin fibers. All cortical layers receive serotonergic projections with higher branching in granule cell layers (IV).

The dorsal raphé nucleus innervates the occipital lobe and most of lateral thalamus via the dorsal raphé cortical tract. The interfascicular subdivision of the DRN (also called nucleus centralis superior pars dorsalis) innervates the frontal cortex, lateral regions of hypothalamus, amygdala, corpus striatum, and lower hippocampus via the lateral forebrain bundle. The median raphé nucleus (also called nucleus centralis superior pars medialis) innervates the medial cortex, medial regions of the thalamus, septum, and upper hippocampus via the medial forebrain bundle. (Azmitia 2012)

The caudal raphé system innervates the lower brainstem and spinal cord. The ventral horn of the spinal cord is innervated by the nucleus raphé obscurus. This entry is made through the posterior fasciculus. Serotonin fibers follow the MLF and tectospinal tract. The dorsal horn is innervated by the nucleus raphé magnus. Ventral lateral medullary neuron fibers use the lateral fasciculus to innervate the lateral horn (Azmitia 1999).

Various synaptically connected target regions may be innervated by fibers from a single serotonergic neuron or group of neurons. It is estimated that one serotonergic neuron can influence approximately 10,000 target neurons. The diversity of cellular targets of raphé serotonergic neurons including neurons, glia, ependymal cells, and brain neuroendocrine centers, suggests that serotonin is involved in homeostatic regulation of the entire brain (Azmitia 1999, 2012).

Raphé nuclei function (respiration, blood pressure, arousal). The serotonergic system of the medulla oblongata consists of 5-HT neurons located in the midline raphé, lateral extra raphé and helps regulate autonomic and respiratory function (Kinney and Paterson 2004). These

medullary nuclei are interconnected (Kinney et al. 2001) and project to nuclei in the brainstem and spinal cord and influence respiratory drive (Bou-Flores et al. 2000), blood pressure regulation (Henderson 2000), thermoregulation (Berner et al. 1999), upper airway reflexes and arousal (Krammer et al. 1979). Medullary 5-HT neurons have also been proposed to be central respiratory chemosensors (Richerson 2004) critical in generation of respiratory rhythm (Pena and Ramirez 2002, Tryba et al. 2006).

Dorsal Raphé role in pain modulation. DRN is a powerful pain modulator. Electrical stimulation of DRN can cause powerful antinociception (Fardin 1984). Oliveras et al. (1979) reported that DRN is the most effective nucleus for stimulation- produced analgesia. Moreover, stimulation of DRN increases the analgesic effect of morphine (Samanin and Valzelli 1971) whereas DRN lesions partly abolish morphine induced analgesia (Yaksh 1977)**.**

Difference between axons of DRN and MRN. Experimental studies with anterograde tracer (*Phaseolus vulgaris* leukoagglutinin) administered by iontophoresis indicate that rat dorsal and median raphé nuclei give rise to axons that are morphologically different. Axons which arise from neurons in the DRN are fine and typically have small, pleomorphic varicosities that range from extremely fine granular dilatations to spindle-shaped, fusiform varicosities from 1 to 3 μm diameter) (type D axons). Axons of neurons of the MRN are characterized by large (3 to 5 μm diameter) spherical varicosities (type M axons). DR and MR projections overlap in many cortical areas. However, large varicose type M fibers appear to preferentially innervate the hippocampus and other limbic areas. In the frontal cortex there is an extremely high density of fusiform and granular (Type D) fibers (Kosofsky and Molliver 1987). Larger size and greater varicosity of 5-HT axons has been reported in the nucleus accumbens shell (Sequela et al. 1989). A relatively homogenous distribution of fine, sparingly varicose 5-HT immunoreactive axons was observed

in the core of the NAc (Van Bockstaele and Pickel 1993) and in the dorsal striatum (Azmitia and Segal 1978, Steinbusch et al. 1978, Soghomonian et al. 1989). These data indicate that the structure of axon terminals of serotonergic neurons is determined by the cells of origin and not by local factors at the site of termination.

Differential vulnerability of 5-HT immunoreactive fibers. Projections of raphé nuclei differ both structurally and pharmacologically. They exhibit striking differences in vulnerability to the amphetamine derivative 3,4-methylendioxymethamphetamine (MDMA, Mamounas et al. 1991). Thin, slightly beaded fibers originating from dorsal raphé are selectively ablated following administration of MDMA. Thicker, beaded fibers originating from median raphé are more resistant to MDMA (Mamounas et al. 1991).

5-HT-positive varicosities. The density of 5-HT varicosities in the SNr was determined as $9x10^6$ sites/mm^3 (Moukhles et al. 1997). Varicosities are positive for both 5-HT and SERT (Sur et al. 1996).

1.6. Neuropathology in Autism

Macrocephaly and microcephaly in autism. Macrocephaly was detected in 37% of autistic children under the age of 4 years (Courchesne et al. 2001), whereas microcephaly was detected in 15.1% of 126 autistic subjects from 2 to 16 years of age (Fombone et al. 1999). The study of 107 dup(15) cases revealed macrocephaly in 2.8% and microcephaly in 16.8% (Schroer et al. 1998). The postmortem dup(15) group is characterized by a high prevalence of microcephaly, intellectual deficits, epilepsy and epilepsy related death.

Accelerated brain growth. The abnormal trajectory of brain growth appears to be a global marker of developmental changes. By 3-5 years old, 12-20% of autistic subjects are

macrocephalic (Lainhart et al. 2006). Reduction in brain growth by the age of 5 years results in partial normalization of brain size and head circumference (Courchesne et al. 1987, Redcay and Courchesne 2005). Post childhood, brain volume has been shown to decrease at a higher rate than in normal individuals (Courchesne et al. 2010).

Courchesne (2003) has identified 4 phases of brain growth characteristic to autism: (a) small or normal brain volume at birth; (b) rapid overgrowth in first year of life; (c) age 2-4, decline of growth; and (d) close to normal brain size in late childhood and adulthood. Brain enlargement is not present at birth. The outgrowth has been shown to occur in a gradient, with most happening in the frontal and temporal cortex and least in the occipital. These changes occur in regions responsible for development of high order social, emotional, and language functions (Courchesne et al. 2007). The increased brain size is mostly due to increased white matter volume in cerebrum and cerebellum as well as increased gray matter volume in cerebrum (Carper et al. 2002). Theories for the overgrowth have included failure of apoptosis and excess neurons due to alterations of cell cycle regulation. Courchesne et al. has shown excess in neuron number in autistic males (Courchesne et al. 2010). The list of possible causes includes excessive numbers of neurons, excessive rate of growth for either neurons or glia, increased density of minicolumns, early expansion of dendritic arbors, increased number of connections, and premature myelination (Courchesne et al. 2003).

The cerebellum of autistic individuals also shows age-specific changes. The hemispheres are about normal size in childhood while in adulthood become reduced in size. Lobules VI to VII of the vermis display hypoplasia at 10 months of age, through infancy, childhood and into adulthood (Courchesne 2010). The studies of the brainstem revealed various striking abnormalities, including abnormal inferior olives (Bauman 1985), reduced neurons in facial

nucleus, a shortening of the brainstem and a non- existent superior olive (Rodier 1996). Jou et al. has shown a decrease in gray matter volume in the brainstem (Jou 2009).

Neuron number in autism. Several reports suggest brain region–specific alterations in the number of neurons ranging from a striking increase to a decrease below control level. Neocortical studies have revealed a 67 % increase in the number of neurons in the prefrontal cortex (Courchesne et al. 2011) and a 53 % increase in the ratio between von Economo neurons and pyramidal neurons in the fronto-insular cortex (Santos et al. 2011). However, in the fusiform gyrus a reduced number of neurons was found (van Kooten et al. 2008). Both qualitative (Kemper and Bauman 1993) and quantitative studies (Bailey et al. 1998, Fatemi et al. 2002) revealed a regional decrease of the number of Purkinje cells and prenatal loss of Purkinje cells (Whitney et al. 2008, 2009). Increased cell packing density reported in several nuclei in the amygdala of 9-29 year old autistic subjects (Bauman and Kemper 1985, 1994) suggested arrested amygdala development (Kemper and Bauman 1993). However, estimates of packing density do not take into account the volume of an anatomical region. Unbiased stereological methods revealed reduced number of neurons in the amygdala overall and in the lateral nucleus in nine autistic subjects from 10 to 44 years of age. The cause of the lower number is not known. Authors assumed that in autistic subjects few neurons were generated during development or that excessive degeneration/loss reduced the number of neurons to one lower than in control level (Schumann and Amaral 2006). Kulesza et al. (2011) reported a significant decrease in the number of neurons in the superior olivary complex of autistic subjects 2 to 36 years of age suggesting a link between these developmental defects and auditory deficiency commonly reported in autistic subjects. It has been suggested that Purkinje cells disappear between the 32nd gestational week and birth (Whitney et al. 2009) whereas defects of the brainstem tegmentum,

including superior olive complex, are a result of alterations around the fourth gestational week, coinciding with neural tube closure (Rodier et al. 1996). The number of neurons in the raphé nuclei was not examined in autistic subjects.

Neuron volume in autism. The first neuropathological studies of brains from autistic subjects showed that autism is associated with neuropathological changes (Bauman and Kemper, 1985; Courchesne et al., 1987; Damasio et al., 1980; Hashimoto et al., 1989, 1993; Murakami et al., 1989; Ritvo et al., 1986). Curtailed development of neurons seen as a feature of an immature brain (Friede 1975) was one of the first findings in autism reported by Bauman and Kemper (1985, 2005). Reduced size of neurons is the most consistent pathology reported in brains of people with autism (Courchesne et al. 2005 a,b, Casanova et al. 2006, Van Kooten et al. 2008, (Jacot-Descombes et al. 2012).

Casanova's 2006 study of the superior and middle frontal gyrus in 6 autistic subjects 4-24 years of age compared to 6 age-matched control subjects showed reduced minicolumnar width, increased neuron density (by 23%) and reduced neuron size. Van Kooten's 2008 study of the fusiform gyrus of 7 autistic subjects 4 to 23 years of age and 10 control subjects 4 to 65 years of age revealed a reduced total number of neurons and reduced mean perikaryal volume of neurons in layers V (21%), and VI (-13.4%). The authors considered these developmental alterations as a sign of pathology contributing to impaired face processing in autism. The study of the inferior frontal cortex BA 44 and 45 involved in language processing, imitative functioning and social processing networks revealed smaller pyramidal neuron volume in layers III (-18%), V (-18.5%) and VI (-22%) in autistic subjects 4 to 52 years old compared to age- matched control subjects (Jacot-Descombes et al. 2012). Significantly smaller neurons in layers I-III and V-VI in the anterior cingulate cortex in autistic males 15 to 54 years of age suggests a contribution to

abnormal affective and cognitive behaviors, defects of emotional attachments and emotional self control, poor adaptive responses to changing conditions, and deficits of attention (Simms et al. 2009).

The reduction by 24% in Purkinje cell size in autistic subjects 20-30 years of age compared to age- matched controls was considered by Fatemi et al. (2002) as a marker of Purkinje cells atrophy.

Minicolumns are the basic functional units of the neocortex. Reduced minicolumn width observed in autistic subjects is associated with an increased number of minicolumns per cortical unit volume and reduced neuron soma and neuron nucleus size (Casanova et al. 2002, 2003). Such closely packed minicolumns could result in a more complex cortex where each functional unit is more interdependent (Williams and Casanova 2010; Baron-Cohen 2004).

2. AIMS AND HYPOTHESES

Raphé nuclei in autism. Imaging studies reveal signs of impairment of the serotonergic system in autism (Chugani et al. 1997, 1999, Makkonen et al. 2008). These data support clinical applications of serotonin- enhancing drugs such as serotonin reuptake inhibitors (Mehlinger et al. 1990, Fatemi et al. 1998, Kolevzon et al. 2006). However, lack of improvement or worsening of clinical status (Brodkin et al. 1997, King et al. 2009, Williams et al. 2010) is in conflict with the assumption that serotonin level is reduced in the brain of autistic patients. To address this Azmitia at al (2011ab) performed the first postmortem study of both serotonergic pathways and serotonergic innervation in brain target structures of young autistic subjects. The authors found increased number of serotonin axons immunoreactive to 5-HT transporter in forebrain pathways (medial forebrain pathway, stria terminalis and ansa lenticularis) and in target areas (amygdala, temporal cortex and globus pallidus). The detected signs of over-activity of the serotonergic system may explain adverse effects of SSRI application additionally enhancing serotonin utilization in the brain of autistic patients (Azmitia et al. 2011ab). Presence of developmental alterations within serotonergic pathways and serotonergic innervation in all examined target structures suggests that these changes are a reflection of developmental alterations in neurons in raphé nuclei which synthesize serotonin and produce serotonergic pathways and axonal projections within target brain structures. Characterization of serotonin producing neurons and level of TPH reflecting serotonin synthesis in neurons in the raphé of autistic subjects may fill the gap between imaging studies showing reduction in brain serotonin (Chugani et al. 1997, 1999) and studies demonstrating an increase in serotonin transporter-positive axons (Azmitia et

al. 2011ab). Therefore, the overall aim of this study is to characterize the pattern of developmental alterations in raphé nuclei of autistic subjects.

Technical limitations and risk factors. In contrast to the genetic uniformity, age and gender sampling, and identical protocols of tissue fixation without a postmortem delay in experiments on serotonergic system in animals, the postmortem human material is strikingly different due to a combination of genetic and epigenetic factors, a broad spectrum of differences in postmortem cell structural and chemical degradation, and different methods of brain dissection and tissue preservation for postmortem studies. However, only human tissue is a carrier of autistic developmental and age associated changes that define the autism clinical phenotype, and only human brain studies can specifically address conflicting observations. In contrast to the highly standardized quantitative stereological methods, immunofluorescence-based methods of quantitative human tissue evaluation do not have universally accepted standards and have limited software support. Therefore this first stereological and immunofluorescence-based quantitative study of raphé in autistic subjects is focused both on standardization of methods of tissue preservation for quantitative evaluation and detection of markers of developmental alterations in raphé nuclei of autistic subjects. The review of literature and the amount and quality of material suitable for postmortem study of the brainstem revealed a conflict between methods of tissue preservation for routine pathology and quantitative studies of the raphé nuclei complex in the human brainstem. Therefore, a significant effort was focused on standardization of methods facilitating studies of the serotonergic system in autism.

Specific Aims

Aim 1: To detect the type and topography of developmental changes in raphé nuclei of autistic children.

Hypothesis 1: A study of raphé nuclei of 5-15 year old autistic subjects can identify early developmental changes in the serotonergic system. Genetic and epigenetic factors determine both clinical differences among autistic subjects and interindividual differences in type and topography of morphological changes. It is hypothesized that in spite of interindividual differences, delayed neuronal growth and alterations in TPH cellular expression are dominant features of autistic subjects' raphé nuclei which may contribute to the autistic phenotype.

Aim 2: To establish standards for brainstem tissue preservation, immunostaining, and quantitative evaluation.

Hypothesis 2: One may assume that establishment of standards of tissue preservation and evaluation will help demonstrate that:

- Developmental morphological changes are mainly quantitative and are detectable with unbiased morphometric methods.
- Developmental abnormalities result in measurable changes of expression and distribution of tryptophan hydroxylase, the key marker of neuron serotonin synthesis.

The brain of autistic subjects is a unique registry of the organism's response to genetic and/or epigenetic factors including pre- and postnatal exposure to noxious factors and changes related to multiple and diverse treatments. This complexity and diversity corresponds to

complexity and diversity of clinical autism manifestations. One may expect that this study will help in designing standards for large group studies, and in developing methods to identify developmental alterations in the raphé and their contribution to autistic phenotype.

3. MATERIAL AND METHODS

3.1. Material

The autistic group consisted of 4 subjects ranging from 5 to 15 years of age including 2 females and 2 males, whereas the control group consisted of 4 subjects 6 to 15 years of age, including 3 males and 1 female (Table 1). These cases were selected from 9 autistic subjects and 6 control subjects. Selection was based on clinical diagnosis of autism and existence of complete raphé nuclei for qualitative and quantitative studies.

Clinical characteristics of autistic subjects. Medical records of autistic subjects consisted of psychological, behavioral, neurological and psychiatric evaluation reports. In those records, the Autism Diagnostic Interview-Revised (ADI-R) or ADOS-G7 was applied by a licensed psychologist as a standard tool for characterizing behavioral alterations related to autism. For postmortem cases, ADI-R was based on clinical records and interview of parent or caregiver. These were obtained from ATP portal as they are available for researchers using donated tissue.

Table 1. Control and autistic subjects qualified for study

Group	Brain Bank #	Histol #	Cause of death	Hemi; BS only	Age (y)	Sex	PMI (h)	Fix (m)
Autism	B7002	M1-08	Drowning	R	5	F	33.0	6
Autism	B5569	M2-08	Drowning	R	5	M	25.5	98
Autism	B7079	M13-10	Asphyxiation due to hanging	R	15	M	23.2	3
Autism	B7619	M3-10	Acute aspiration pneumonitis	LR	15	F	-	15
							Mean	31 m
Control	CNL1567	M9-10	Asphyxiation due to hanging	L (BS)	6	F	-	59
Control	CNL 1388P	M4-06	Drowning	L	4	M	72	9
Control	CNL1548	M1-10	Carbon monoxide intoxication	L	10	M	-	48
Control	CNL1566	M8-10	Carbon monoxide intoxication	L (BS)	15	M	32.0	52
							Mean	42 m

Inclusion criteria. Inclusion of a subject in this study was based on a summary of scores of four domains:

(A) qualitative abnormalities in reciprocal social interaction;

(B) qualitative abnormalities in verbal and nonverbal communication;

(C) restricted, repetitive, and stereotyped patterns of behavior, and

(D) abnormality of development evident at or before 36 months (Lord et al. 2000).

In three cases (M2-08, M13-10, and M3-10) autism was confirmed using ADI-R, whereas in M1-08 autism diagnosis was confirmed with ADOS-G7.

Table 2. Neurological evaluation of autistic subjects

Case #	Seizures	Anxiety	Sleep	Sensory alterations	Other
M1-08	No seizures		Sleep onset difficulties	Sensitive to smells, light, sounds.	Developmental delay
M2-08	No seizures	Freq. agitation, screaming and crying. Treatment: Prozac for 3 years, 2.5 mg on daily basis; Valium-occasionally.	Significant sleep disorder with sleep walking. Night: 3-4 h of sleep; afternoon: 3 h of sleep. Treatment: melatonin	Significantly reduced sensitivity	Regression at age of 6 m. Often laughed for no apparent reason
M13-10	No seizures				
M3-10	No seizures	Anxiety, hyperactive, attention disorder			

Table 2 summarizes neurological records including some related to serotonergic function. Numerous data indicate that a deficiency of central serotonergic signaling may predispose individuals to development of mood disorders including aggression, anxiety, impulsivity, depression and obsessive-compulsive disorder (Lucki 1998, Mann et al. 2001, Nelson and Chiavegatto 2001). These symptoms are also observed in subjects diagnosed with autism. Due to clinical diagnosis of mood disorders patients are treated, among others, with selective serotonin reuptake inhibitors (fluoxetine, paraxetin, citalaprom and others) which may modify expression of tryptophan hydroxylase and/or serotonin transporter. An uncontrolled pattern of laughing is associated with function or dysfunction of the raphé magnus and rostral nucleus obscurus (Assal et al. 2000). Insomnia and abnormal sleep patterns are reported in approximately 60% of children with autism (Souders et al. 2009).

Allergies and treatments of autistic subjects. The 5-year old boy (M2-08) had

records of severe allergic symptoms including frequent swelling and rashes in response to milk, soy and various other food products. He was treated with Benadryl, as needed, and epinephrine to reduce swelling.

Pregnancy, perinatal and postnatal period - potential risk of exposure to epigenetic factors. Records for the same subject (M2-08) reveal significant exposure to pregnancy-related risk factors. The mother suffered from cluster headaches in the first trimester and was treated with Imitrex. In the third trimester she was also diagnosed with hypoglycemia, decreased blood pressure, and fainting. During early childhood, the examined subject was diagnosed with chronic otitis media and required multiple treatments with antibiotics and bilateral ear tube installation. Significant behavioral regression was reported at the age of 6 months.

Genetic component in two autistic subjects. Family medical records of M2-08 reveal pervasive developmental disorder, bipolar disorder, dyslexia and learning disabilities in the maternal extended family. The 15 year old female (M3-10) was diagnosed with dup(15) and autism. Dup(15), known also as supernumerary isodicentric chromosome 15q11.2-q13 or inverted duplication 15, is a relatively common genetic anomaly observed as tetrasomy or mixed trisomy/tetrasomy of a segment of the proximal long arm of ch15. In 69% of maternal origin duplications of 15q11.2-q13, copy number alterations are associated with autism, as well as with intellectual deficits, epilepsy, seizures, hyperactivity and hypotonia commonly observed in idiopathic autism groups (Cook et al. 1997, Dawson et al. 2002, Bolton et al. 2001 and 2004).

Tissue acquisition. Brain tissue samples, usually one entire brain hemisphere, were assigned to a project funded by the U.S. Department of Defense Autism Spectrum Disorders Research Program. The PI of Neuropathological Subproject in this Program Project approved application of brainstem tissue for this study of the serotonergic system. Beginning in 2010, I

prepared (processed, embedded, cut and immunostained) 5 brainstems for this project and used 3 brainstems already removed, embedded and cut in 2006 and 2008. In 2010, the brainstem dissection protocol was modified to improve preservation of raphé nuclei. The modifications were done under consultation of Prof. Efrain C. Azmitia from NYU.

Due to sudden unexpected death of all autistic and control subjects, the autopsy was performed by medical examiners. After tissue recovery by forensic pathologists and partial brain dissection to preserve samples for routine toxicology and pathological evaluation and diagnosis, remains of the brain or one intact brain hemisphere cut midsaggitally were sent to brain banks, consistently with next of kin donation. Brain tissue for this project was obtained from the Harvard Brain Tissue Resource Center and the Brain Bank for Developmental Disabilities and Aging of the NYS Institute for Basic Research in Developmental Disabilities. Brain banks are authorized to request medical records and caregiver's additional data, but the scope of records provided ranges from very detailed to a few demographic records.

Brainstem sampling. Brain dissection by medical examiners is performed consistently with pathology standards. A midsaggital cut is used to divide the entire brain including brain hemispheres and the brainstem into left and right hemisphere. This cut may result in partial loss of raphé nuclei located in the brainstem midline. The next cut on the level of the midbrain exposes the substantia nigra for routine pathology evaluation, but this cut results in a loss of caudal linear nucleus and portion of dorsal raphé nucleus.

Anonymity of the donor and coding of the tissue. Each brain hemisphere number given by the institution that received the donation was used as the only identifier of clinical records and tissue samples. The methods applied in this study were approved by the Institutional Review Board at the New York State Institute for Basic Research in Developmental Disabilities.

3.2. Methods

Fixation. The brain hemispheres with cerebellum and brainstem had previously been fixed with 10% buffered formalin for an average of 42 months in the control group (from 9 to 59 m). Average fixation time of brain hemispheres of autistic subjects was 31 m (range 3 to 98 m).

Dehydration. Formalin was washed from tissue using overnight rinses with filtered water. The brainstems were then dehydrated in a series of ethyl alcohols on shaker (50% ethanol for 3 days; 70% ethanol for 4 days; 80% ethanol for 3 days; 95% for 4 days, 100% for 2 days).

Embedding and sectioning. The brainstem was embedded in polyethylene glycol (PEG, Iqbal et al. 1993). Serial 50 μm-thick sections were cut, washed 3x in EtOH to remove residues of PEG and stored in 70% ethanol. Due to faster penetration of EtOH and PEG into a smaller brainstem, sample processing was shorter than processing of the brain hemisphere.

Human brainstem processing and embedding protocol

Washing overnight in tap water

Dehydration: EtOH 50% 3 days
EtOH 70% 4 days
EtOH 80% 3 days
EtOH 95% 4 days
EtOH 100% 2 days

Infiltration: PEG 400 (I) 2 days (room temp)
PEG 400 (II) 2 days (room temp)
PEG 1000 (I) 2 days (42 ^{o}C)
PEG 1000 (II) 2 days (42 ^{o}C)
Embedding PEG 1000 (fresh; 42 ^{o}C)

PEG block storage: 4°C

Cutting: 50μm-thick serial sections.

Storage of sections: 70% EtOH

Colorimetric staining

Detection of serotonin synthesizing neurons. Neuron morphometry (cell volume measurement) was done using sections immunostained with PH8 mouse monoclonal antibody anti- human tryptophan hydroxylase (Millipore Catalogue No. MAB5278, Millipore, Temecula, CA). Serotonin is rapidly metabolized and the level of serotonin decreases several hours after death to an undetectable level (Joyce 1962). Serotonin synthesizing neurons are detected with mAb PH8 that binds a common epitope of tryptophan hydroxylase, tyrosine hydroxylase, and phenylalanine hydroxylase (Cotton et al. 1988). Tryptophan hydroxylase converts tryptophan to 5-hydroxytryptophan, therefore the cellular level of this serotonin synthesis-limiting enzyme is a measure of serotonin synthesis. In formalin fixed brain tissue, at lower PH8 concentrations (1:5,000 – 1:10,000) only serotonergic neurons are stained, whereas in increased concentrations all brainstem monoaminergic neurons, including noradrenergic neurons of the locus coeruleus and dopaminergic neurons in the substantia nigra are stained. However, in contrast to light brown staining of noradrenergic and dopaminergic neurons, tryptophan hydroxylase positive neurons synthesizing serotonin are brown/black.

After wash in fresh 70% ethanol, tissue was washed for 15 min in ascending concentrations of EtOH (70%, 80%, 95%). Blocking of endogenous peroxidase was done with 0.5% hydrogen peroxide in absolute methanol. After a PBS wash, the sections were then treated with 10% FBS in phosphate buffer solution (PBS) for 30 minutes to block nonspecific binding. The antibody PH8 was diluted in 10% FBS serum in PBS (1:4000), and sections were treated overnight at 4°C. The sections were washed and treated for 30 minutes with biotinylated sheep anti-mouse IgG antibody diluted 1:300. The sections were treated with an extravidin peroxidase conjugate (1:200) for 1 hour, and the product of reaction was visualized with diaminobenzidine

(0.5 mg/mL with 1.5% hydrogen peroxide in PBS). After immunostaining, sections were lightly counterstained with hematoxylin.

Immunofluorescence staining

TPH. Immunofluorescence was applied to detect and measure cellular content of tryptophan hydroxylase. This method of estimation of TPH signal was selected due to less dependence on multi-step immunocytochemistry such as that finalized with DAB as a chromogen and variability with incubation times. Mouse monoclonal Ab PH8 (1:5000) was used as primary antibody and affinity-purified donkey antisera against mouse IgG labeled with Alexa Fluor 555 (1:500) were used for immunodetection of reaction product. Alexa Fluor 555 was chosen over previously tested Alexa Fluor 488 due to bleed-through with 488. Sections were mounted with Prolong Gold Antifade reagent (P36930, Molecular Probes).

SERT. Serotonin transporter was detected with monoclonal Ab ST51 (1:600) and antisera against mouse IgG labeled with Alexa Fluor 555 (1:500)(MAB Technologies).

Neuronal nuclear marker. Antibodies that recognize the DNA-binding, neuron specific protein NeuN are used for immunodetection of neurons in human surgical and autopsy brain tissue (Andres et al. 2005). NeuN protein is restricted to neuronal nuclei, perikarya and some proximal neuronal processes. Anti NeuN antibodies react with most neuronal cell types. However, several types of neurons, including Purkinje cells, most neurons in the retina and in sympathetic chain ganglia are not immunolabeled (Wolf et al. 1996). Tests with mouse monoclonal anti-NeuN antibody MAB377 (Millipore, catalog no. MAB377, 1:2000 dilution) also revealed lack of reaction with neuron nucleus and soma in human raphé nuclei. This was confirmed in another lab.

TOPRO-3 from Invitrogen (1:1000) was used as a nuclear marker. DAPI (non-neuron specific) was considered. However, it is not viewable under all confocal setups due to optimal excitation wavelength of DAPI, which is in the near UV range. Nuclear staining was done only for visualization of cells when combined with immunostaining for TPH as TOPRO also stains non-serotonergic neuron nuclei and non-neuron nuclei. TOPRO3 was used because of its long wavelength fluorescence far from green and red fluorophores. Various TOPRO concentrations and incubation times were tested and optimal conditions were selected.

Long PMIs, autolytic changes, and variable time of tissue fixation affected structure and biochemical properties of tissue, including immunostaining, immunofluorescence and nuclear staining. TOPRO nuclear staining with soma staining or lack of nuclear staining in presence of cytoplasmic staining was often observed in neurons. These staining artifacts could be due to degradation of the nuclear envelope. A long postmortem interval such as reported in examined cases is the cause of growing permeability of the lysosomal membrane, and leaking of lysosomal enzymes that break down organelles, membranes and proteins. Damage of nuclear membranes results in DNA and histone leak into the cytoplasm and observed distortion of nuclear markers in human material. Immediate fixation of animal material prevents this type of artifact.

Axonal marker. Axons of raphé nuclei neurons were detected with mouse monoclonal pan-axonal neurofilament marker SMI-312 (1:1000)(COVANCE, Princeton, NJ).

Imaging. Images were generated using a Nikon C1 confocal microscope system with EZC1 image analysis software.

Immunofluorescent staining standardization

The original immunofluorescent staining revealed strong background and numerical data did not show the significant differences seen visually between examined control and autistic subjects. The staining protocol was revised. Standardization of staining protocol involved: (1) antigen retrieval, (2) incubation time and antibody dilutions, (3) nuclear staining, (4) application of detergents, (5) use of proper controls (Table 3-4).

In formalin- fixed tissue with protein cross-links which mask the antigenic sites, antigen retrieval increases immunolabeling. Heat induced epitope retrieval using a buffer was applied, however, when temperature exceeds 80-85º C and time exceeds 15 min the risk of tissue damage increases. The standard used in preservation of tissue for immunofluorescence-based quantitative analysis was 2x saline sodium citrate buffer (SSC) for 2 hours at 65ºC. The SSC buffer was used at a neutral pH because depending on epitope, retrieval at a lower or high pH may lead to decreased immunolabeling.

Triton X-100, a popular detergent for improving penetration for immunohistochemistry was used in low concentrations. Reducing Triton-X concentration to 0.1% improves immunofluorescence with PH8 and ST51 in comparison to 0.4% Triton.

Washing of serial sections in ethanol was expanded to include 70%, 50%, and 30% before immersing in PBS to make the transition from alcohol less destructive for free floating sections.

Serum blocking times from 3 hours to overnight were tested and 3 hour long blocking was chosen to reduce unspecific binding. Due to a short time, the concentration of sera was increased to 10%. These conditions prevented both unspecific binding and excessive blocking that may cause masking of antigenic sites.

The indirect staining method was used with primary and secondary antibodies. Monoclonal antibodies were used where possible to reduce cross-reactivity. Various primary antibody concentrations were tested to determine optimal concentration where staining was strong but the least background was seen. Tests were performed with various concentrations of secondary antibody to set optimum conditions. Concentration of secondary antibodies was decreased from 1:300 to 1:500 to reduce background staining. Incubation time was decreased from overnight to 3 hours to preserve specific staining but reduce background and unspecific precipitations.

Positive controls utilized were pathology- free dorsal raphé sections. Elimination of primary antibody was applied for negative controls.

Summary of sample procedure (TPH). EtOH washes were extended to include 70%, 50%, and 30%. These were followed by 3x wash in cold PBS totaling 30 min. Antigen retrieval at 65C in 2x SSC buffer was followed by room temperature wash in same buffer. Nonspecific staining was blocked at room temperature using 10% serum of the host of the secondary antibody. Samples were left overnight at 4^{o} Celsius in primary antibody diluted in PBS/10% serum of host of secondary antibody. After 30 min total wash in cold PBS, sections were treated in the dark with secondary antibody linked to fluorochrome in 10% serum/PBS/0.1% Triton-X for 3 hours in room temp. Another wash with cold PBS was followed by labeling with 1:1000 TOPRO3 in PBS/Triton for 10 minutes in the dark. Another wash in cold PBS totaling 30 min was followed by mounting with antifade mounting medium in the dark.

Table 3. TPH protocol

Procedure for TPH stack measurements	Case Section Staining with PH8, and TOPRO	Case Section Negative control for staining with PH8
Wash in descending EtOH concentrations	70%, 50%, 30% EtOH (x 5min)	70%, 50%, 30% EtOH (x 5 min)
Cold PBS	3x10 min	3x10 min
Antigen retrieval	2x SSC buffer/ 2 h 65 ^{o}C	2x SSC buffer/ 2 h 65 ^{o}C
Wash	5 min in SSC 2x	5 min in SSC 2x
Block unspecific binding using serum of the host of secondary ab	10% donkey serum/PBS, 0.1% TritonX 3 h (room temp)	10% donkey serum/PBS, 0.1% TritonX 3 h (room temp)
Wash.	No	No
Primary ab diluted in PBS/serum of the host of the secondary Ab	PH8 Mouse 1:5,000 (in PBS/Donkey Serum) OVERNIGHT (4 ^{o}C)	10% Donkey Serum /PBS, 0.1% Triton X OVERNIGHT (4 ^{o}C)
Cold PBS	3x10 min	3x10 min
Secondary Ab diluted in PBS (in dark)	Donkey Alexa Fluor 555-tagged anti-mouse (red) 1:500 (in 10% donkey serum /PBS/0.1% TritonX), 3 h room	Donkey Alexa Fluor 555-tagged anti-mouse (red) 1:500 (in 10% donkey serum /PBS/0.1% TritonX), 3 h room
Cold PBS (in dark)	3x10 min	3x10 min
Label with TOPRO3 in PBS, 0.1% Triton X-100 (in dark)	10 min. TOPRO 1:1000 in PBS, 0.1% Triton X-100	10 min. TOPRO 1:1000 in PBS, 0.1% Triton X-100
PBS (in dark)	3x10 min	3x10 min
Mounting	Keep in dark	Keep in dark

Table 4. SERT Protocol

Staining with ST51	Case#	Case#
	Section#	Section#
	Staining with ST51, and TOPRO	Negative control for staining with ST51
Wash in 70%, 50%, 30% EtOH	5 min	5 min
Cold PBS	3x10 min	3x10 min
Antigen retrieval	2x SSC buffer/2 h 65 ^{o}C	2x SSC buffer/2 h 65 ^{o}C
Wash	5 min in SSC 2x	5 min in SSC 2x
Block unspecific binding using serum of the host of secondary Ab	10% donkey serum/PBS, 0.1% Triton X100; 3 h room temp.	10% donkey serum/PBS, 0.1% Triton-X100 3 h (room temp)
Wash.	No	No
Primary ab diluted in PBS/serum of the host of the sec Ab	Abcam Mouse ST51. 1:600 (in 10% Donkey Serum/PBS, 0.1% Triton X100) (overnight, 4 ^{o}C)	10% Donkey Serum /PBS, 0.1% Triton X100 (overnight, 4 ^{o}C)
Cold PBS	3x10 min	3x10 min
Secondary Ab diluted in PBS (DARK)	Donkey Alexa Fluor 555-tagged anti-mouse (red) 1:500 (in 10% donkey serum /PBS/0.1% Triton X100), 3 h room temp.	Donkey Alexa Fluor 555-tagged anti-mouse (red) 1:500 (in 10% donkey serum /PBS/0.1% Triton X100), 3 h room
Cold PBS (DARK)	3x10 min	3x10 min
Label with TOPRO3 in PBS, 0.1% Triton X-100 (DARK)	10 min TOPRO 1:1000 in PBS, 0.1% Triton X-100	10 min TOPRO 1:1000 in PBS, 0.1% Triton X100
PBS (DARK)	3x10 min	3x10 min
Mounting (DARK)	Keep in dark	Keep in dark

Intraneuronal distribution of TPH. Double immunofluorescence (Table 5) was applied to determine the pattern of distribution of TPH in neuronal soma and processes. TPH was used as a marker of sites of serotonin synthesis. Pan-axonal neurofilament marker SMI-312 was used as selective marker of cytoskeleton in axons. TPH-positive but SMI-312-negative processes correspond to dendrites of serotonergic neurons.

SERT distribution in serotonergic neurons. Double immunofluorescence with ST51 detecting SERT and with SMI-312 was applied to differentiate SERT in serotonergic neuron soma and dendrites versus SERT distribution in SMI-312-positive axons.

Table 5. Double immunostaining protocol sample

Double staining with PH8 and SMI	Case#	Case#	Case#
	Section#	Section#	Section#
	Staining with PH8, SMI and TOPRO	Negative control for staining with PH8	Negative control for staining with SMI
70%, 50%, 30% EtOH	x5 min	x5 min	x5 min
Cold PBS	3x10 min	3x10 min	3x10 min
Antigen retrieval (65°C)	2x SSC buffer 2 h	2x SSC buffer 2 h	2x SSC buffer 2 h
Wash	5 min in SSC 2x	5 min in SSC 2x	5min in SSC 2x
Block unspecific binding using serum of the host of secondary ab	10% donkey serum/PBS, 0.1% TritonX 3hrs, RT	10% donkey serum/PBS, 0.1% TritonX 3 h, RT	10% donkey serum/PBS, 0.1% TritonX 3 h, RT
Wash.	No wash	No wash	No wash
Primary ab diluted in PBS/serum of the host of the sec ab	PH8 Mouse 1:5,000 (in PBS/Donkey Serum), overnight, 4 ^{o}C	10% Donkey Serum /PBS, 0.1% Triton X, overnight, 4 ^{o}C	PH8 Mouse 1:5,000 (in PBS/Donkey Serum), overnight 4^{o}C
Cold PBS	3x10 min	3x10 min	3x10 min
Secondary Ab diluted in PBS (DARK)	Donkey Alexa Fluor 555-tagged anti-mouse (red) 1:500 (in 10% donkey serum /PBS/0.1% TritonX), 3 h RT	Donkey Alexa Fluor 555-tagged anti-mouse (red) 1:500 (in 10% donkey serum /PBS/0.1% TritonX), 3 h RT	Donkey Alexa Fluor 555-tagged anti-mouse (red) 1:500 (in 10% donkey serum /PBS/ 0.1% Triton), 3 h RT
Cold PBS (DARK)	3x10 min (DARK)	3x10 min (DARK)	3x10 min (DARK)
Block using serum of host of second secondary ab	10% goat serum/PBS, 0.1% TritonX 3 h, RT (DARK)	10% goat serum/PBS, 0.1% TritonX 3 h, RT (DARK)	10% goat serum/PBS, 0.1% TritonX 3 h, RT (DARK)
2nd Primary ab diluted in PBS/serum of the host of the sec ab (DARK,overnight)	anti-axonal SMI-312R antibody mouse monoclonal 1:1000 (in 10% goat serum/PBS, 0.1% TritonX	anti-axonal SMI-312R antibody mouse monoclonal 1:1000 (in 10% goat serum/PBS, 0.1% TritonX	10% goat serum/PBS, 0.1% TritonX
Cold PBS	3x10 min (DARK)	3x10 min (DARK)	3x10 min (DARK)
2nd Secondary Ab (DARK)	Goat Alexa Fluor 488-tagged anti-mouse (green); 1:500 in PBS 3 hrs, 10% goat serum 0.1% TritonX	Goat Alexa Fluor 488-tagged anti-mouse (green); 1:500 in PBS 3 hrs, 10% goat serum 0.1% TritonX	Goat Alexa Fluor 488-tagged anti-mouse (green); 1:500 in PBS 3 hrs, 10% goat serum 0.1% TritonX
PBS	3x10 min (DARK)	3x10 min (DARK)	3x10 min (DARK)
Label with TOPRO3 in PBS, 0.1% Triton X-100	10 min. TOPRO 1:1000 in PBS, 0.1% Triton X-100 (DARK)	10 min. TOPRO 1:1000 in PBS, 0.1% Triton X-100 (DARK)	10 min. TOPRO 1:1000 in PBS, 0.1% Triton X-100 (DARK)
PBS	3x10 min (DARK)	3x10 min (DARK)	3x10 min (DARK)
Mounting	Keep in dark	Keep in dark	Keep in dark

Anatomical parcellation of the raphé nuclei. Large, heavily stained neurons clustered dorsally to the trochlear nucleus and corresponding to the dorsal raphé nucleus were described in the human brain by Kölliker in 1893 (Kölliker, 1893). Dahlström and Fuxe distinguished nine nuclei of serotonin-containing neurons in the midline of the brainstem of animals and labeled them in caudo-rostral order from B1 to B9 (Dahlström and Fuxe 1964). Serotonergic neurons not related to raphé nuclei were found also in the reticular formation lateral to the raphé nuclei in several species of animals (Jacobovitz and MacLean 1978, Poitras and Parent 1978, Steinbusch 1981, Steinbusch and Nieuvenhuys 1983) and much more numerous in primates (Azmitia and Gannon, 1986) and in human fetus brain (Nobin and Björklund 1973, Olson et al. 1973, Takahashi et al. 1986).

The basic histological characteristics of the human raphé system were reported by Braak in 1970 who applied staining with aldehyde-fuchsin. Immunohistochemical detection of serotonin in postmortem human material is limited because serotonin dissipates rapidly after death. The application of mouse monoclonal antibody PH8 which recognizes in formalin- fixed tissue tryptophan hydroxylase, the biosynthetic enzyme of serotonin (Haan et al., 1987), resulted in Törk and Hornung's (1990) detailed delineation of human raphé nuclei and computer supported reconstruction of the serotonergic system in the human brainstem (Hornung and Kraftsik, 1988).

3D Reconstruction. For mapping, PH8 immunostained serial sections were photographed using objective lens 1.25x. Prints at final magnification were combined into panels. 852 images were used to build 71 panels. Contours of 6 raphé nuclei and several other subregions rich in tryptophan hydroxylase positive neurons were delineated. Among these structures were the B9 area, lateral paragigantocellular nucleus, pontis oralis nucleus, and

paramedian raphé nucleus. The 3D reconstruction starts with a loose cloud of PH8 positive neurons in the central gray and few neurons belonging to the beginning of the caudal linear nucleus and continues to the end of the nucleus obscurus in the medulla oblongata.

Mercury Systems Amira 4.1.2 was used to reconstruct the brainstem from digital microscope photographs. Manual segmentation was performed on serial sections. In a single case, the entire brainstem including both hemispheres was available for examination (15 yr old female; M3-10). This sample was used for 3d reconstruction. Raphé nuclei in this subject were present in 710 sections, each 50 μm thick. Total length of raphé nuclei complex was 35mm. Segmentation produced 3 dimensional polygon surfaces for each structure which were rendered to 2d for final editing and layout in Adobe Photoshop CS2.

3d reconstruction was also performed on 20x magnification of PH8 positive neurons. Confocal series of immunofluorescent digital images were transferred to Amira (Mercury Systems). 3D surfaces were created using Amira's realtime threshold- based isosurface function. The series consisted of 175 512x512 pixel images.

Morphometry. All morphometric measurements were performed without knowledge of the subject's age, severity of mental retardation, gender, clinical diagnosis, or neuropathological status for the material being analyzed. Neuronal morphometry was performed at a workstation consisting of Axiophot II (Carl Zeiss) light microscope with Plan Apo objectives 1.25x (numerical aperture, N.A., 0.15); 2.5x (0.075), and 40x (N.A. 0.75), specimen stage with 3-axis computer-controlled stepping motor system (Ludl Electronics; Hawthorne, NY, USA), CCD color video camera (CX9000 mbf Bioscience) and stereology software (Stereo Investigator, MicroBrightField Bioscience, Inc., Williston, VT, USA).

Numerical density of TPH-positive neurons. Evaluation of the total number of neurons for the entire raphé nuclei complex and per individual nuclei was impossible because in majority of cases only half of the brainstem was available. One half and a portion of the second half was preserved in 8 cases included in this analysis. Therefore the study was limited to unbiased numerical density of TPH-positive neurons in the available half of the brainstem.

The numerical density of neurons was evaluated using the optical disector method (Stereo Investigator, MicroBrightField). The optical disector is used to count objects without any assumptions about neuron size, shape or orientation in equal distance serial sections. The region of interest (individual raphé nucleus) was delinated using Stereo Investigator. Grid size and the virtual counting space were designed for each brain structure individually to adapt to the size and shape of the region of interest, and to reduce SD and the coefficient of error (CE). Using a 40x objective lens the focal plane (optical section) was moved a known distance (depth of dissector = 30 μm) and the number of number nuclei of TPH-positive neurons was determined per dissector. The motion through the focal plane axis was determined using a position encoder mounted on the microscope. A 5-μm top guard zone was applied to eliminate an area of mechanical damage by knife. Consistently with Stereo Investigator instructions, neurons that fall inside of the counting frame and those on the top and right line of the counting frame were included, whereas those on the left and bottom line were excluded. The number of neurons per cubic mm was calculated for the individual raphé nucleus. Numerical density of TPH-positive neurons immunodetected with PH8 antibody in DAB protocol was determined.

Volume of TPH-positive neuron soma. The volume of the neuron soma was estimated with the nucleator method (Gundersen, 1988) using MicroBrightfield software. The software defined a systematic random sampling sequence of counting frames within the boundaries of the

ROI. Guard zones were set on top and bottom of every section to prevent bias related to sectioning artifacts. Grid size and the virtual counting space were designed for each brain structure individually to adapt to the size and shape of the region of interest, and to reduce SD and the coefficient of error (CE). More than 100 neuronal measurements per case resulted in CE <0.01. The software provided volume per cell which was then used to calculate mean TPH positive neuron soma volume per section and structure.

Fluorescence intensity measurements. ImageJ software was used to measure neuron mean gray value of signal for each cell (PH8). All photographs with a specific staining were taken at same gain level preset in confocal microscope control software.

Sampling standardization. Application of automated estimation of TPH immunofluorescence in raphé neurons to detect difference between autistic and control subjects required standardization of:

(a) Image acquisition, sampling of size, number and distribution of test units (stacks),

(b) Image analysis, and

(c) Background.

Selection of interfascicular nucleus for quantitative immunofluorescence.

The dorsal raphé nucleus was chosen based on DRN's high neuron density, large size and widespread projections, including areas linked with autism phenotype: frontal cortex (executive function), hypothalamus (social interactions, aggression), striatum (rituals, stereotypes, planning movement, cognition), nucleus accumbens (social attachment, reward), amygdala (social activity, anxiety, aggression, fear, cognition), and substantia nigra (reward, addiction, movement).

It was not possible to work on the Dorsal Raphé Nucleus as a whole as it consists of several known subdivisions and the test area would give different results based on placement, as different DRN subdivisions have characteristic neuron distribution, density, orientation, etc.

The interfascicular subdivision was chosen because it has a characteristic neuron distribution including a parallel orientation and is bordered on 3 sides by non-dorsal raphé structures, making for easier delineation in fluorescence. More importantly, fibers from the interfascicular subdivision of the DRN travel in the lateral forebrain bundle and innervate the frontal cortex, hypothalamus, amygdala, and striatum involved in functional changes observed in autism.

Image acquisition - stack number, size, distribution

Stack number. Tests were done to determine what number of stacks would provide a representative sample of serotonergic neurons. Results from 4 stacks systematically distributed within a DRN subdivision per case were compared to results from a single stack. Differences within stacks of the same DRN subdivision were large (mean intensity ranging more than 2-fold in IF subdivision), therefore it was concluded that using a single stack to represent a DRN subdivision was inadequate. A test for placement of stacks randomly over the DRN without taking into account subdivision boundaries, showed 4-fold variation making this approach unusable as well.

Stack distribution and size. At 40x, four sets of images (four image stacks) were able to fit in the IF structure. The total thickness of the stack was 25µm with 25 images in each stack. To reduce cutting- and mounting –related distortions of the specimen and corresponding images, the top and bottom 5 images were removed as guard zones. This correction reduced the stack thickness to 15µm and 15 images. The single image area was 512 x 512 pixels (318 x 318µm).

The volume of the stack was 318 x 318 x 15µm = 1.52 million μm^3. This volume was almost 170 times larger than the average volume of neuron (approximately 9,000 μm^3).

Fluorescence image analysis

Selection of neuron soma TPH immunofluorescence as most representative measure of neuron 5-HT synthesis. Tests of intensity measurements of an entire field of view showed significant differences in intensity within an individual. Intensity measurements of entire field resulted in 4 datapoints per brain, whereas individual soma intensity measurements resulted in 60+ datapoints per brain.

Due to the fact that stacks and therefore stack projection images contain variable numbers of neurons, the total fluorescence per image is biased by differences in number of neuronal bodies. To reduce bias associated with variable number of neurons, technical artifacts and vessels, fluorescence intensity was measured per neuron soma after outlining the soma of each neuron with cell nucleus exclusion. However, significant differences in individual neuron soma PH8 immunoreactivity observed in both control and autistic subjects are most likely a measure of individual neuron involvement in 5-HT synthesis at the time of death and this variability is reflected in case's standard deviation.

Application of average or maximum projection. Average projections were created from stacks in order to perform intensity measurements. They were more representative of stacks than maximum projections. Maximum projections create an image where each pixel contains the maximum value over all the images in the stack at that particular location whereas average intensity projections store in each pixel the average intensity over all images in stack at corresponding pixel location.

Background subtraction.

The eight brains were stained (concurrently) under the same conditions, stored in same conditions after staining (4°C), and photographed in one session under the same confocal settings including pinhole size, laser intensity, filter settings and gain. Samples were exposed to laser for the same amount of time.

Numerous standardization steps mentioned previously resulted in background reduction but not elimination. Intensity of background may be specific for each case and related to postmortem chemical cell degradation, formalin fixation, PEG exposure, nuances in section immunolabeling and other poorly characterized factors.

To compare tryptophan hydroxylase immunofluorescence in the raphé of control and autistic subjects, four approaches were tested to correct for background, including:

(a) equal background correction across all 8 cases,

(b) pair wise background correction (modification by same value in single pair),

(c) individual brain background correction (each brain corrected separately),

(d) mean cell backround correction using adjacent section without primary and secondary antibody to define cytoplasmic backround

Equal background subtraction. For across the board background subtraction method, the method consisted of starting with the highest background case, choosing 10 brightest pixels in areas with no soma/fibers and taking average of their intensities, outlining the neuron soma on image, using Math/Subtract in ImageJ software to subtract the previously mentioned value from each pixel of image for all images of all cases, and measuring average intensity per cell soma.

Pairwise background subtraction. This method differed in that the correction value was chosen from the image with stronger background in each pair of cases.

Individual background subtraction. The individual subtraction method differed in that the correction value was established for each individual brain.

External cell background correction. For each control and autistic subject the section adjacent to TPH- immunolabeled section was treated with an identical protocol but both primary and secondary antibody conjugated with fluorochrome were omitted. The aim of this external control was to define and subtract unspecific signal, including lipofuscin autofluorescence in the cytoplasm of raphé neurons. Subtraction of neuron cytoplasmic background was case specific and eliminated distortion of cellular measurements by subtraction of neuropil background.

Statistical analysis. Descriptive statistics were applied for each case including mean and standard error. T-tests were done on mean signal intensity for each case to test for equality of means. Two-tailed p values were calculated without any assumption regarding direction. Statistical analysis was performed using Excel and Stata. Tests for TPH intensity equality of means on Control vs Autism groups were carried out with the help of Dr.Flory utilizing cluster sampling . They treated individual neurons as the unit of analysis with autism as a fixed factor, while adjusting variance estimates to account for effects on sample variances of sampling a limited number of cases. Thus the precision achieved by the measurement of many neurons was taken into account while using the methods of cluster sampling to account for the fact that sampling had been done in a limited number of clusters which here are the individual cases (Cochran 1977, Scheaffer et al. 2011, Sukhatme et al. 1984). Data were poststratified to adjust for the differing numbers of neurons sampled per individual so as to weight each individual equally. Analyses were conducted using version 11.1 of the Stata statistical package (StataCorp 2009).

Spearman's rank correlation coefficient was calculated between age and TPH intensity as a nonparametric measure of statitistical dependence. This test allowed analysis of correlations without the need for a linear relationship between variables.

4. RESULTS

4.1. Clinical, pathological and technical criteria of brainstem sample selection

Application of clinical diagnostic criteria based on ADI-R and ADOS, and neuropathological criteria which eliminated cases with severe pathology related to mechanisms of death and technical criteria, resulted in reduction of the number of autistic subjects from 9 to 4 and control subjects from 6 to 4. These data indicate that 50% or more of samples cannot be used for study of raphé nuclei even in a limited scope of research, that is one half (left or right half) of the raphé and only rostral group of raphé nuclei. Evaluation of this material revealed that the method of brainstem dissection is critical for quality of brainstem sample and research design. Examination of brainstem samples provided by brain banks indicates that pathologists employ two protocols of brain dissection and that neither one is optimal for preservation of raphé nuclei for research.

Mid-saggital brain dissection. A mid-saggital cut divides the brain into a left and right hemisphere (Fig 1.5). 3D reconstruction of raphé nuclei indicates that raphé nuclei are located in the midline and extend 2-3 mm from the midline (Fig. 2). Therefore, application of this protocol results in loss of anatomical integrity of raphé nuclei and random preservation of only portions of raphé nuclei. A mid-saggital dissection is in conflict with basic needs of raphé nuclei preservation.

The assumption that each brainstem can be cut exactly in the midline is usually not true because the cut is almost always off the midline due to postmortem deformation of a 60-70 mm long brainstem sample during fixation. When a sample is bent to the left or right side, the distortion affects symmetry of raphé nuclei. When a brainstem is bent in the vertical plane, (Fig.

1), the anterior nuclei are cut and visualized in a correct transverse plane, whereas caudal nuclei (mainly magnus, pallidus and obscurus) are cut and visualized in different planes reflecting curvature of bend, and distorting spatial relationships between anterior and posterior nuclei.

Recommendations for studying half of the brainstem are based on the assumption that half of the raphé is representative of the entire raphé. However, delineation of the midline of nuclei is possible only when about 2 mm of the other half are present in the sample assigned to study. Therefore, dissection requires a 2-3 mm shift from the midline on the entire length of raphé nuclei (Fig. 3). In only a few autopsy samples, the brainstem's left or right part was preserved with extra tissue from the second half and in only these cases can half of the raphé nuclei be examined on the entire rostro-caudal extent.

However, this protocol does not provide a perfect sample for morphology as well as biochemistry or molecular biology (undetermined portions of brainstem nuclei missing, including raphé nuclei).

Transverse brainstem dissection. The second routine protocol of brainstem dissection starts with cutting off the brainstem on the level of the substantia nigra and transverse slicing of the brainstem into several (usually 4-5) slabs and alternative selection of slices for morphological and biochemical studies (Fig. 3). It results in preservation of random brainstem slices or slices with specific diagnostic or research targets, such as the substantia nigra, locus coeruleus, inferior olive, or other. Because raphé nuclei occupy approximately 45 mm in rostro-caudal direction of the brainstem, application of this protocol results in a loss of anatomical integrity and random preservation of parts of raphé nuclei for morphological and biochemical studies.

Distortion of tissue sample volume during dehydration with EtOH. Dehydration in ascending EtOH concentrations, including absolute EtOH, significantly reduces the volume of

tissue sample. Fig. 4 shows that the length of brainstem from colliculus superior (the most anterior portion of raphé) to the end of the inferior olive (the level of the most caudal portion the nucleus obscurus) is 60 mm, whereas the length of reconstructed raphé nuclei is 42% less (35 mm). Dehydration- related shrinkage affects such morphometric parameters as cell volume and length of neuronal processes. However, a comparable rate of shrinkage in all examined samples, including brainstem of control and autistic subjects, allows for detection of disease- related changes.

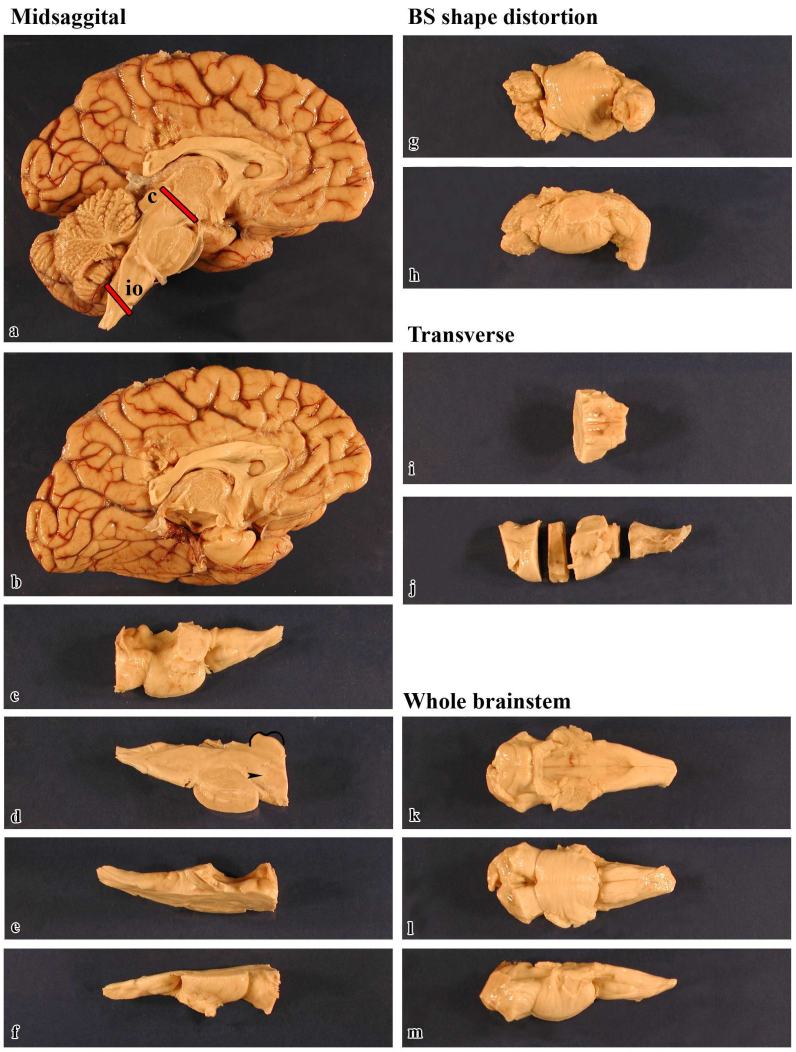

Fig. 1.5. Brainstem sampling. Hemispheric sampling based on dissection of the brain approximately in the midline provides cerebral and cerebellar hemispheric samples and usually a close to midline dissection of brainstem with loss of a portion or entire raphé nuclei located on midline. Fig (a) and (b) show left brain hemisphere before and after dissection. Lateral (c), midsaggital (d), dorsal (e), and ventral (f) view of brainstem hemisample. Cutting off the brainstem in front of colliculus "c" means that the most anterior nuclei (CLN, DRN) are preserved. A caudal cut several mm behind the inferior olive means that the most caudal portion of the raphé (RNO) is also preserved (Fig c). However, a view of the nucleus colliculus and nucleus ruber (arrowhead) crossection (Fig d) indicates that the midsaggital cut was at least 1-1.5mm too far to the left side and about 60% of raphé nuclei are missing. Figure (i) and (j) illustrate results of transverse dissection (perpendicular to long axis of brainstem) and absence of the majority (g) or large portion of the raphé nuclei, and loss of integrity of the serotonergic complex. Fig (g) (ventral view) and (h) (lateral view) show post autopsy distortion of the shape of the brainstem. This results in a distortion of topographic relationships of raphé nuclei on serial transverse sections. Dorsal (k), ventral (l) and lateral (m) view illustrates a well-preserved brainstem sample suitable for cutting serial sections and for unlimited applications in morphometric studies and 3D reconstruction.

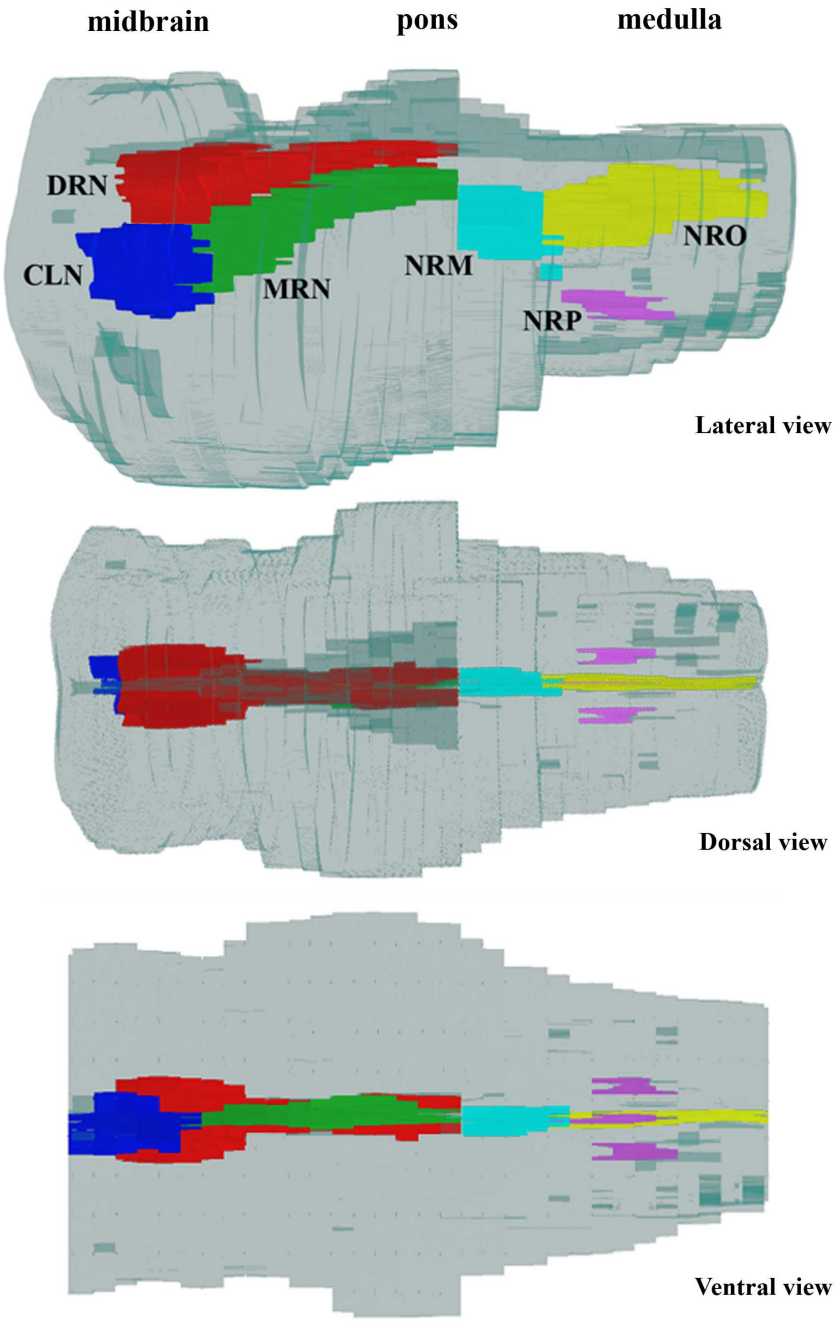

Fig. 2. 3D reconstruction of raphé nuclei. Lateral view of 3D model based on reconstruction of images of serial TPH- immunostained sections illustrates spatial distribution of raphé nuclei, their size and shape. The anterior complex of raphé nuclei consists of the three largest nuclei: caudal linear nucleus (CLN), dorsal raphé nucleus (DRN) including caudal portion of dorsal raphé nucleus (DRNc), and median raphé nucleus (MRN). The caudal complex of raphé nuclei consists of the nucleus raphé magnus (NRM), nucleus raphé obscurus (NRO), and a much smaller/poorly delineated nucleus raphé pallidus (NRP).

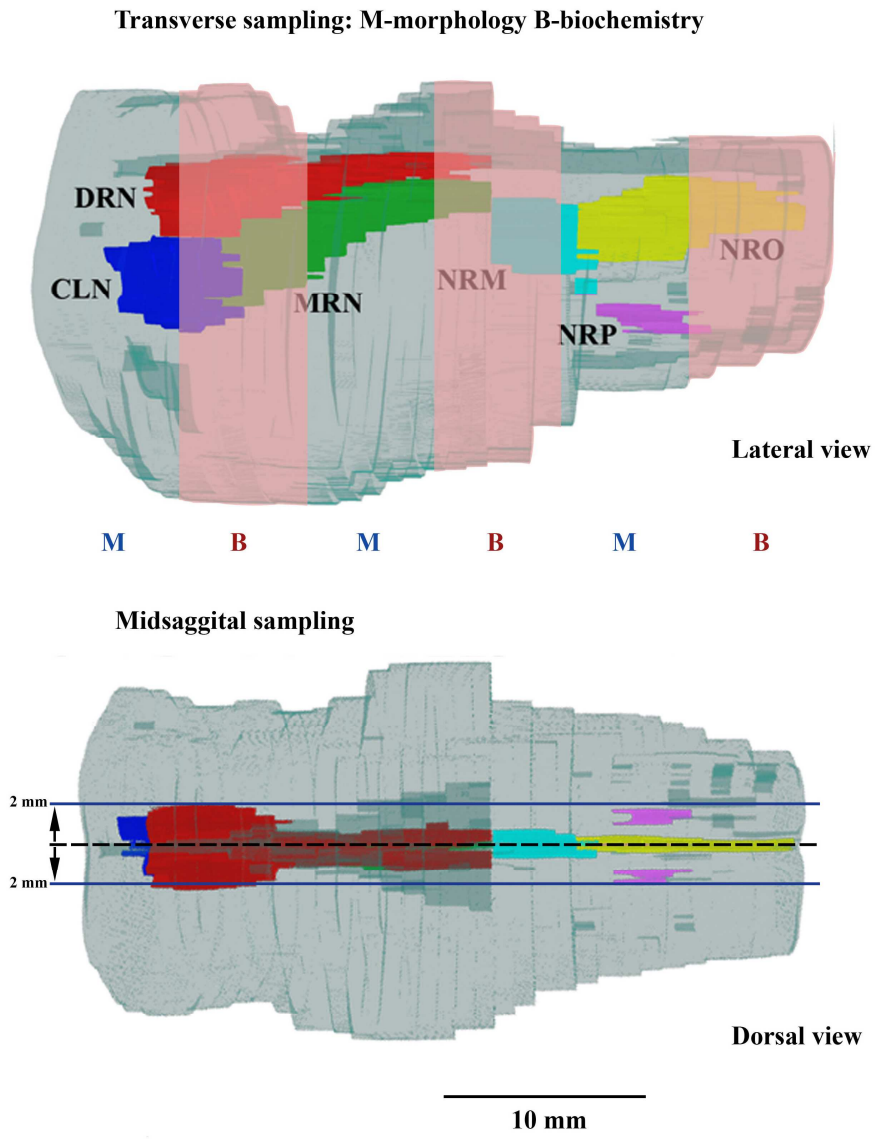

Fig. 3. Transverse and midsaggital brainstem dissection. A 3D model of raphé nuclei was used to illustrate consequences of application of two routinely used protocols of brain dissection. The lateral view demonstrates loss of integrity of raphé nuclei in transversely cut slices designated for (a) morphological studies "M" including diagnostic neuropathology and qualitative/ quantitative immunocytochemistry based evaluation, and (b) biochemical or molecular studies "B" with random preservation of brainstem nuclei known for their extremely diversified chemical and molecular properties.

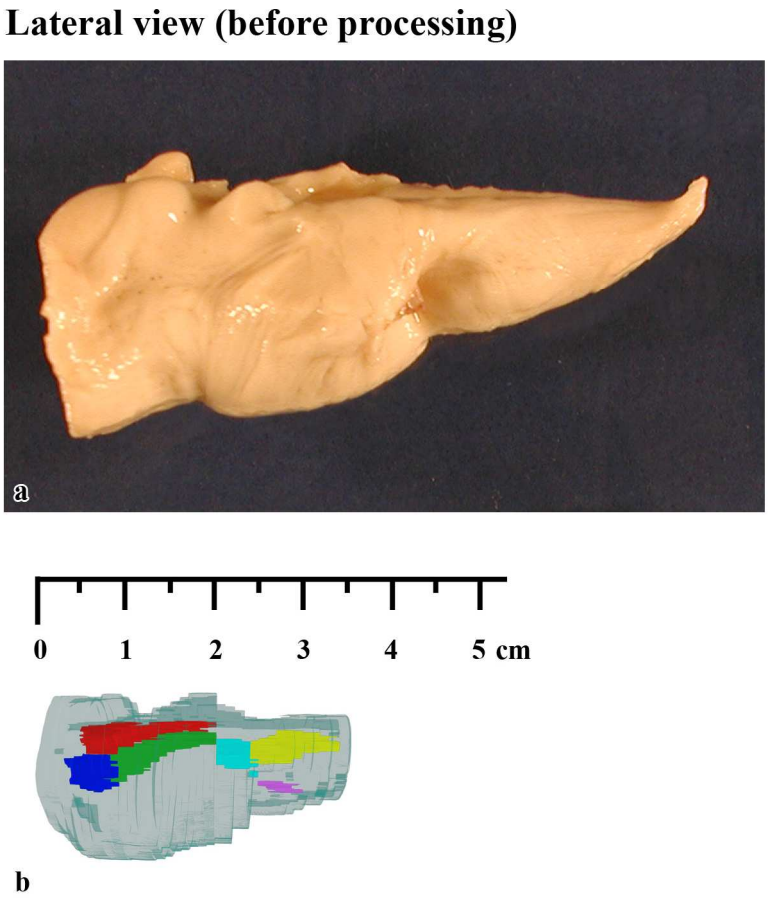

Fig. 4. Brainstem shrinkage during dehydration. Figure (a) shows size of formalin fixed brainstem sample before dehydration, embedding and cutting, whereas figure (b) shows size of reconstructed brainstem sample reduced from 60 mm to 35 mm. It corresponds to 42% shrinkage caused by dehydration in ETOH.

4.2. Clinical and pathological markers of heterogeneity within autistic group

Review of clinical records and neuropathological reports revealed striking differences between four autistic subjects qualified for this study suggesting a strong contribution of genetic factors in two cases (M2-08 and M3-10) and a combination of epigenetic factors resulting in involvement of the serotonergic system.

5-year old female (M1-08): The records of this individual demonstrate a relatively moderate pattern of clinical manifestations of autism combined with moderate sleep disorder and enhanced response to sensory stimuli. The unique feature of this subject's brain were numerous developmental defects, limited only to the cerebral cortex, and resulting in two types of cortical changes: multifocal dysplasia and multifocal bottom of sulcus microdysgenesis. Defects of cortical folding may have a genetic background but the history of this subject, including family medical history and mother's status during gestation, is not available because she was adopted at the age of 1 year. There is no record of genetic studies.

5-year old male (M2-08): All available data suggest that brain pathology might be linked to both genetic factors reflected in a complex medical history on mother's side with learning disabilities, PDD, bipolar disorder, and dyslexia, and epigenetic factors suggested by severe complications of pregnancy with cluster headaches and aggressive treatment, hypoglycemia, decreased blood pressure, fainting, premature birth, and postpartum depression. Results of application of ADI-R indicate that patient was affected by severe autism. Frequent episodes of agitation which required chronic treatment with selective serotonin reuptake inhibitors, chronic and severe sleep disorder, laugh for no apparent reason (linked to caudal raphé alterations; Assal 2000) and multifocal cortical dysplasia and cerebellar flocculo-nodular dysplasia (associated with local alterations of serotonergic system) suggest multiple links to functional and potentially structural serotonergic system changes.

15 year old male (M13-10). He was diagnosed as high functioning autism. A gap in clinical records and lack of a neuropathological report does not allow clinical and neuropathological correlations. However, suicidal death by hanging may suggest suicidal tendencies with contribution of an altered serotonergic system.

15 year old female (M3-10). She was diagnosed with autism, dup(15), attention disorder and hyperactivity. Postmortem evaluation revealed microcephaly with a brain weight of 1125g. The patient died suddenly without an apparent reason. All forms of pathology including abnormal brain growth, behavioral changes, as well as sudden unexpected death without known cause may indicate alterations of the serotonergic system.

Clinical and genetic diversity of these four subjects suggest a high risk of significant interindividual differences in morphological and immunocytochemical characteristics of raphé nuclei, and heterogeneity of results of morphometric and immunocytochemical studies. Therefore, this study is concentrated both on interindividual differences between 4 autistic subjects and differences between age- matched autistic and control subjects.

4.3. Immunocytochemistry- based anatomical subdivisions of raphé nuclei in autism

Serial sections 500 μm apart demonstrate the number and distribution of mAb PH8-positive neurons in raphé nuclei of the 4 year old control male (Fig. 5-10). The most rostral PH8-positive neurons were dispersed within the central gray matter below aqueductus (Fig 5; ss. 187 and 197) and in the midline between left and right nucleus ruber (CLN). Increases in the number of immunoreactive neurons within the central gray marked the most rostral portion of the DRN (S 237). Increases in the number of neurons in DRN were paralleled by an increase in the number of neurons in CLN. However, the CLN was small and extended only for 4.5 mm (from s 187 to 277).

The dorsal raphé nucleus is largest at the level of the trochlear nucleus (tn) with long neuronal processes traversing the trochlear nucleus, mediolateral fasciculus (mlf), and running

ventro-laterally toward the substantia nigra. Dense bundles of processes of DRN merge with the main body of the CLN (s 237). In a more caudal region the number of neurons in DRN decreases and disappearance of the neuron body rich dorsal, ventral, and ventrolateral sub-nuclei (s 297) marks the caudal end of the main part of the DRN. The main body of DRN usually examined in morphometric studies extends for 4.5 mm (between sections 207 and 297). However, the caudal portion of the DRN (DRNc) made up of only two relatively small subnuclei, dorsal and interfascicular, extends 12 mm (from s 297 to 537). The total rostro-caudal length of the main body of DRN and DRNc is approximately 16.5 mm.

The caudal portion of the CLN becomes almost invisible but in the same area the number of PH8-positive neurons increases again and these cells form the densely populated median raphé nucleus (MRN) located in the midline with numerous processes and few neurons in the paramedian nucleus. The median raphé extends for 4 mm (from s287 to 367).

Change in the shape of MRN and expansion of serotonergic neurons from the midline laterally mark the caudal end of the MRN and the beginning of rostral portion of nucleus raphé magnus (NRM). The shape of NRM is more irregular with lateral extensions merging with two large complexes of serotonergic neurons dispersed within the oral pontine nucleus (PON) located more dorsally and B9 nucleus located above the median lemniscus (ml). The caudal end of all major complexes: DRNc, NRM, and B9 nucleus marks the border between these 3 subnuclei and two of the most caudal nuclei: nucleus raphé pallidus (NRP) and nucleus raphé obscurus (NRO). The B9 nucleus is the analog of the rat B9 nucleus and in human brain is also labeled as B9 (Törk and Hornung 1990).

The nucleus raphé pallidus is small and poorly defined morphologically. In contrast to NRO, neurons of NRP are located in the midline and extend laterally a short distance above the

medial lemniscus (ml). In the rostro-caudal direction, the NRP extends a distance of 6.5 mm (between sections 577 and 707).

Neurons of the NRO form two symmetric lines separated by the distinct neuron-free bundle of fibers of the raphé, present for 6.5 mm (between sections 637 and 767) (Fig. 9-10). However, a small number of serotonergic neurons which belong to the NRO is detected in the medulla oblongata over a much longer distance including the entire length of the inferior olive (IO). Another cluster of serotonergic neurons is present in the lateral paragigantocellular nucleus located dorso-laterally to the inferior olive (sections from 647 to 767).

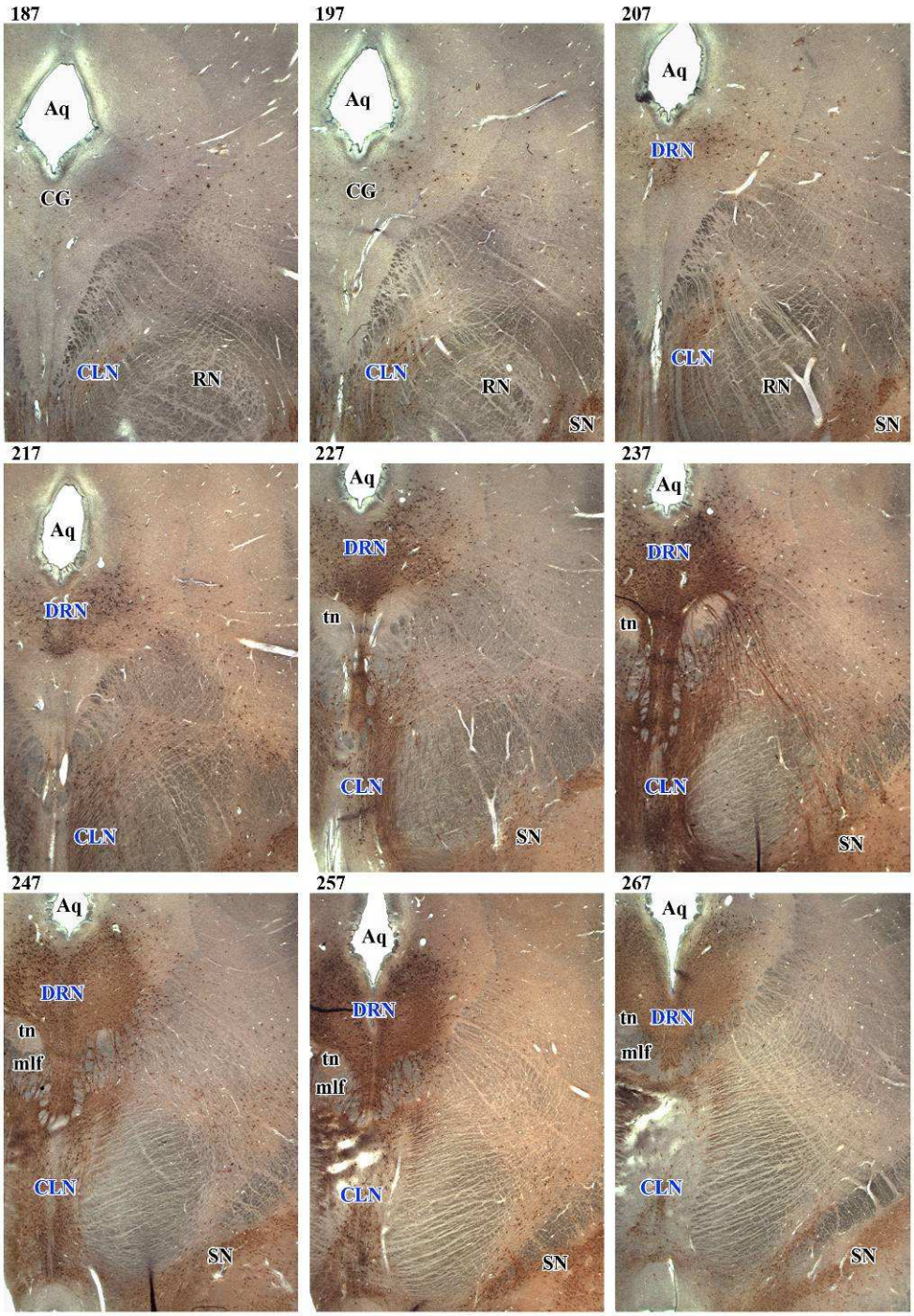

Fig. 5. Caudal Linear and Dorsal Raphé Nucleus. The most anterior part of the raphé nuclei is represented by TPH positive neurons of the Caudal Linear Nucleus (CLN), located in the midline between the red nuclei (RN). TPH positive neurons in the central gray matter (CG) represent the anterior part of the Dorsal Raphé Nucleus (DRN). The main body of the DRN is developed dorsally to the trochlear nucleus (tn). (C M4-06 4y, PH8, 1.5x)

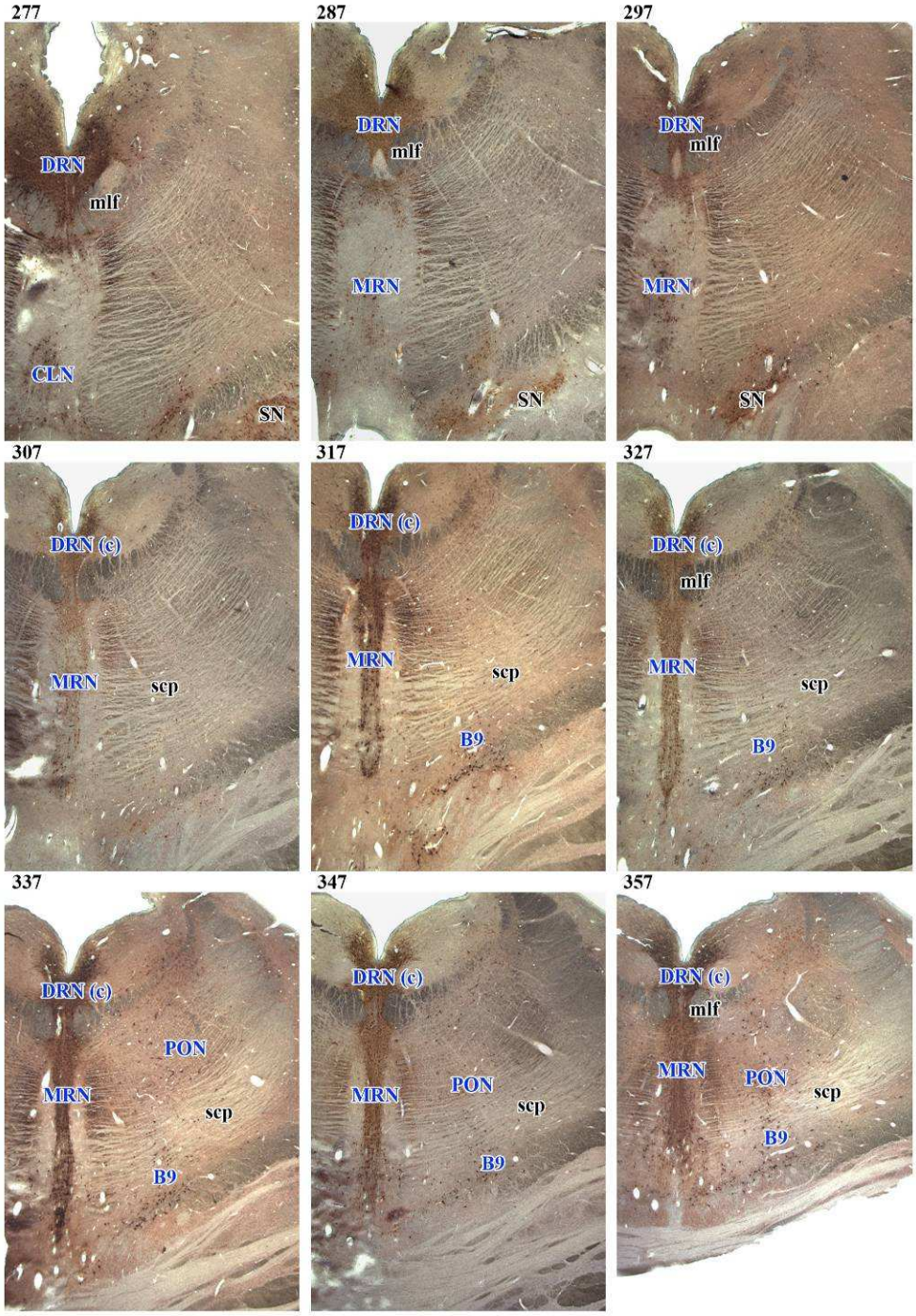

Fig. 6. Median Raphé Nucleus. The main body of the DRN becomes a long caudal DRN (DRNc). The ventrally located CLN disappears and in the same midline, densely packed neurons form the Median Raphé Nucleus (MRN). Lateral to the MRN, TPH positive neurons emerge in the oral pontine nucleus (PON) and form the B9 cell group. (C M4-06 4y, PH8, 1.5x)

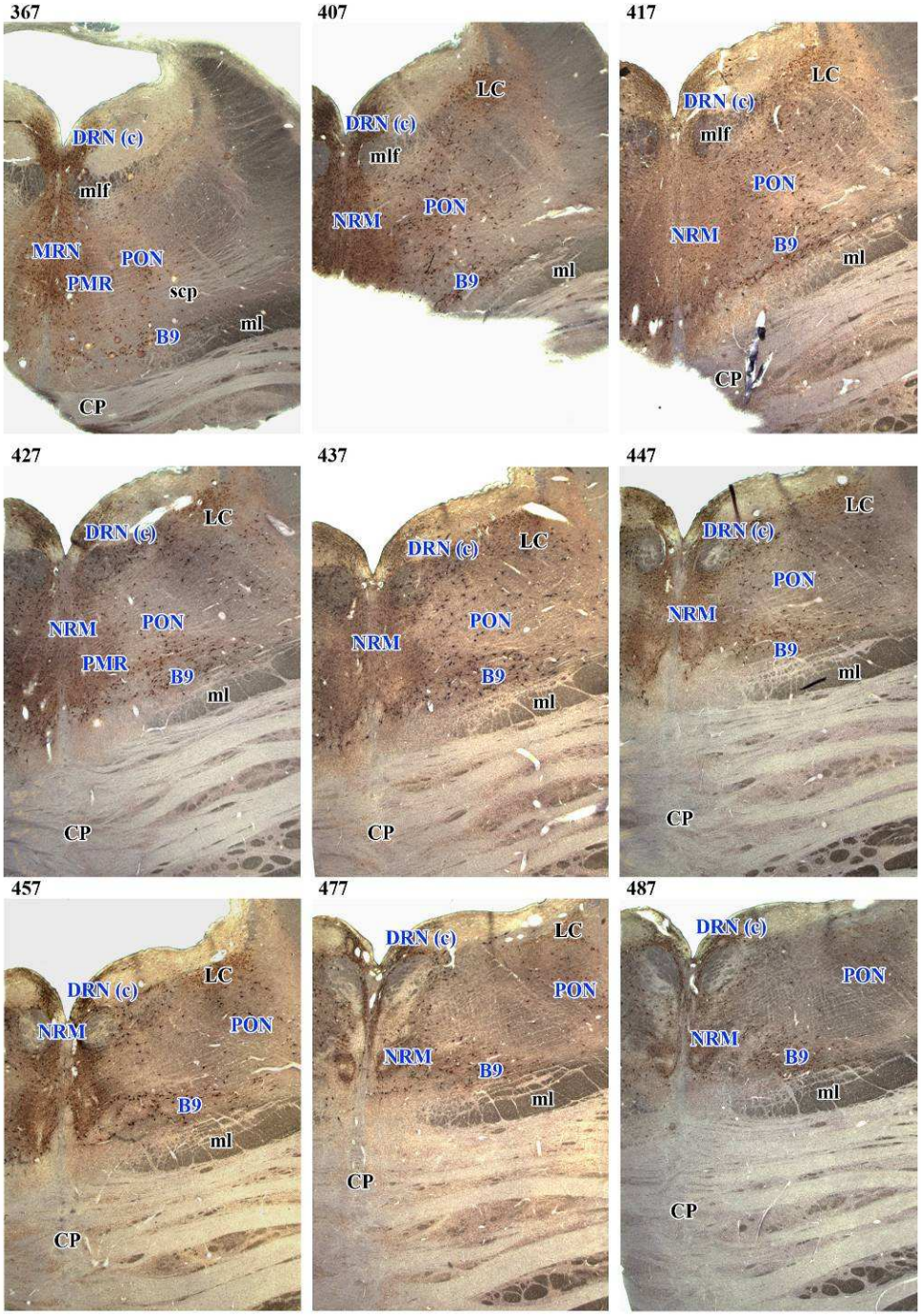

Fig. 7. Nucleus Raphé Magnus and B9. The MRN is replaced by laterally extending neurons of the Nucleus Raphé Magnus (NRM). At the level of the NRM, large populations of serotonergic neurons occupy PON and form the caudal part of the B9 cell group. Adrenergic neurons form the locus coeruleus (LC). (C M4-06 4y, PH8, 1.5x)

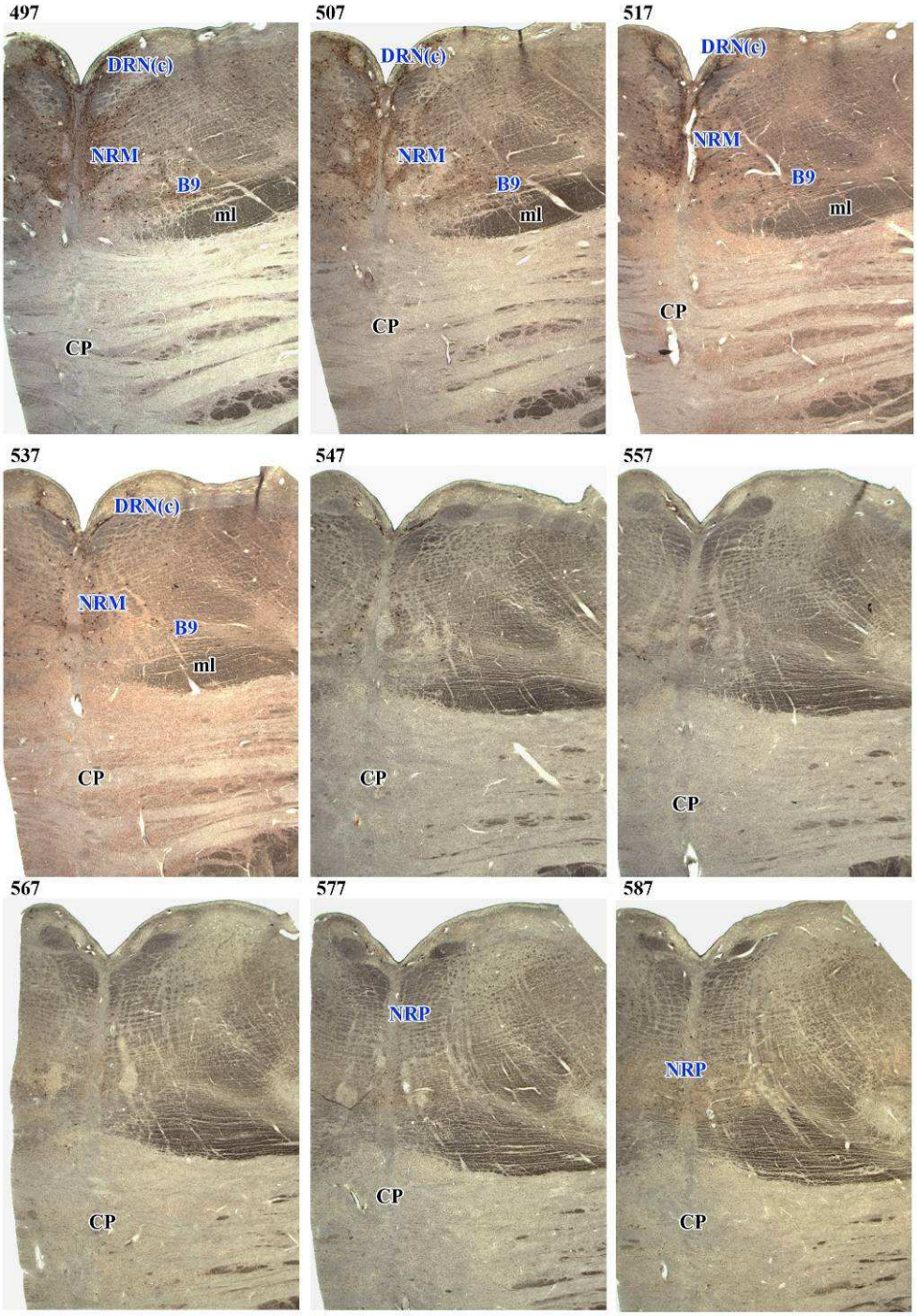

Fig. 8. Nucleus Raphé Magnus and Pallidus. The caudal portion of the DRNc and NRM is separated from the more anterior portion of the Nucleus Pallidus (NRP) and Nucleus Obscurus (NRO) by a zone almost free of serotonergic neurons (section 547-567) (C M4-06 4y, PH8, 1.5x)

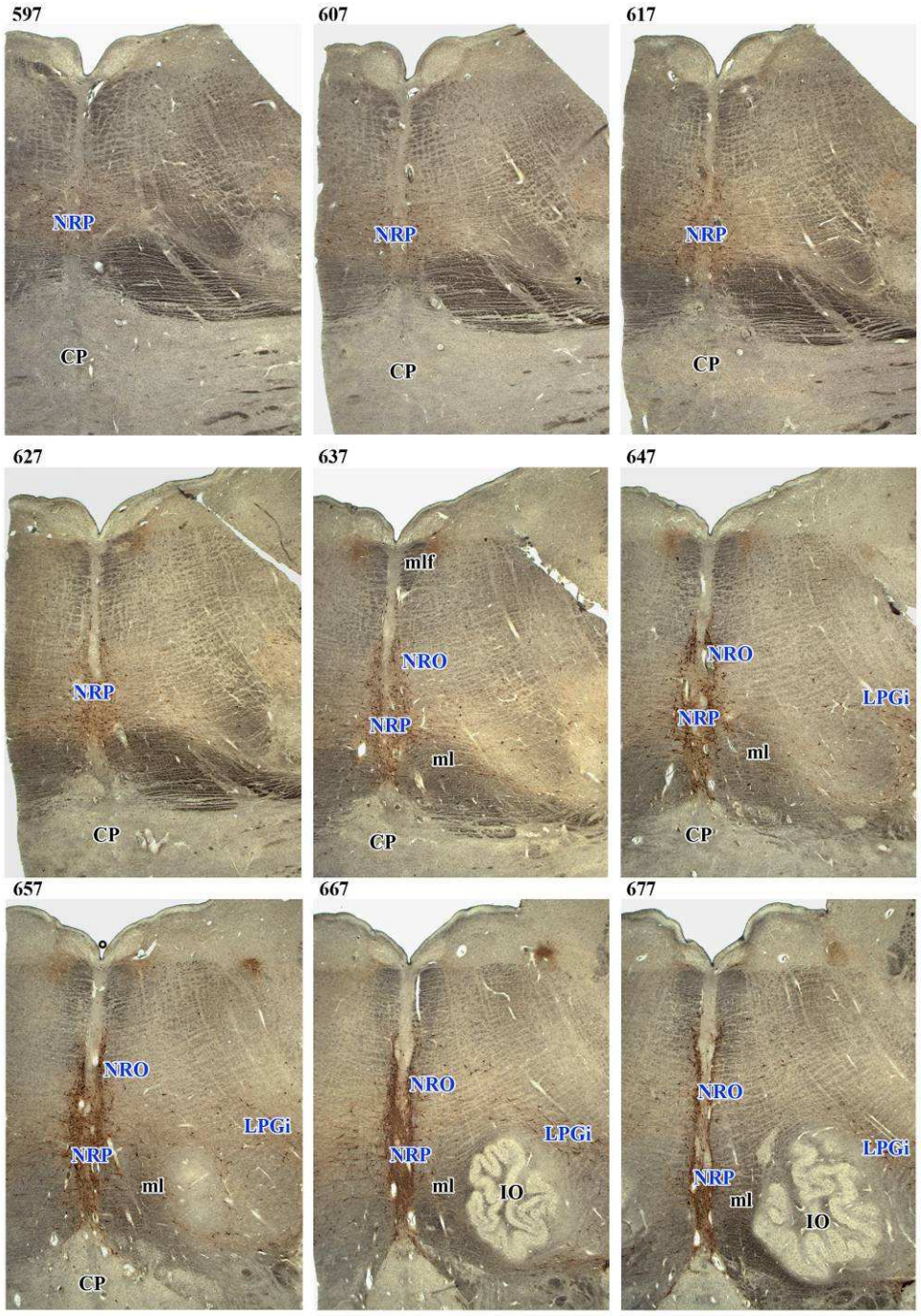

Fig. 9. Nucleus Raphé Pallidus and Obscurus. Neurons of the Nucleus Raphé Pallidus (NRP) are located in the midline ventrally to the anterior part of the Nucleus Obscurus (NRO). The two paramedian lines of neurons of the NRO are separated by the fibrous septum of the medulla, whereas NRP neurons are aggregated in the midline. Dendrites of the NRO neurons project laterally to the reticular formation and another large cluster of serotonergic neurons in the lateral Paragigantocellular Nucleus (LPGi). (C M4-06 4y, PH8, 1.5x)

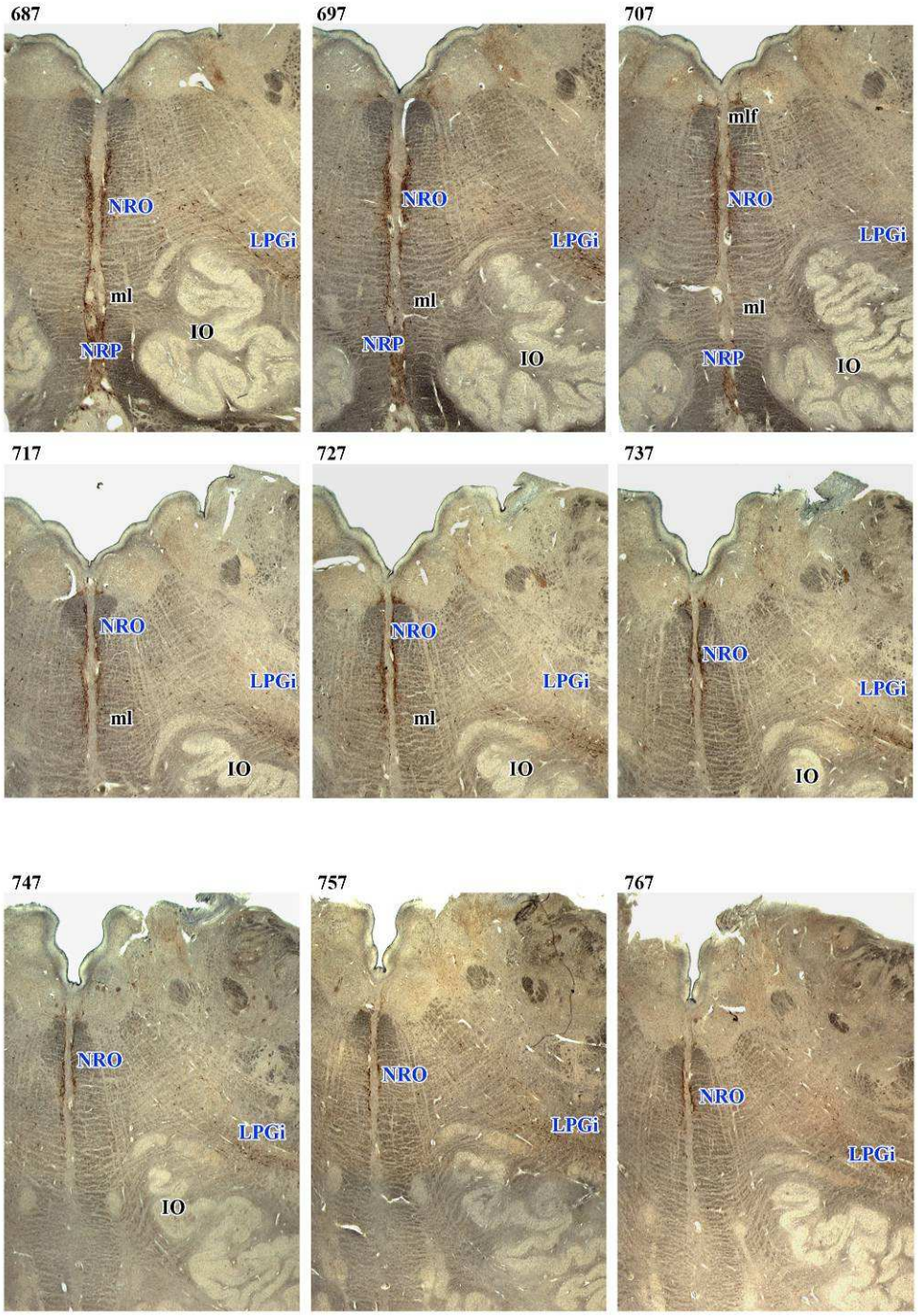

Fig. 10. Caudal portion of Nucleus Raphé Obscurus. Two paramedian clusters of NRO neurons form the long caudal portion of the raphé nuclei. At the level of the anterior part of the inferior olive (IO), the midline is occupied by the caudal part of the NRP. (C M4-06 4y, PH8, 1.5x)

4.4. Neuronal TPH distribution in 3D reconstruction.

Immunocytochemistry revealed strong PH8 immunoreactivity in raphé neurons. The aim of the 3D reconstruction was to visualize the distribution of TPH in the soma of neurons and in the dendritic tree. The 3D reconstruction shows several thick dendrites and a dense network of thin dendrites, all filled with PH8-positive material (Fig. 11). These images suggest that the amount of TPH might be a major marker of neuron involvement in serotonin production and function. Therefore the next sections are focused on detection and measurements of intracellular TPH in young autistic subjects compared to control subjects.

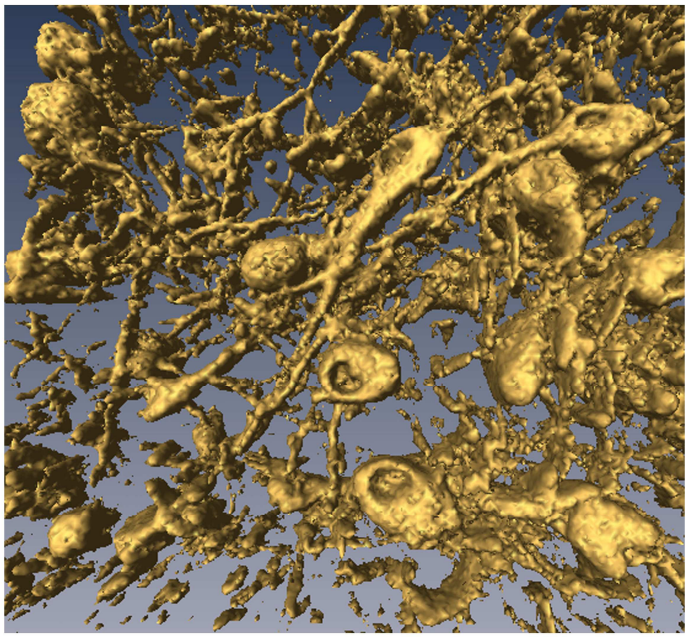

Fig. 11. 3D reconstruction of TPH (+) neurons. The most noticeable feature of 3D-reconstructed PH8 immunolabeled neurons are numerous thick branches of dendrites and dense tryptophan hydroxylase- positive dendritic network within dorsal raphé (Amira) (Autism, M3-10; 15y, PH8).

4.5. Intraneuronal TPH and SERT distribution by confocal microscopy.

TPH distribution in raphé neuron soma and dendrites. The aim of double immunolabeling was to visually examine the pattern of distribution of TPH as a marker of sites of serotonin synthesis. SMI312 was applied to identify axons. Immunolabeling of TPH with mAb PH8 revealed intense but non-uniform immunofluorescence (red) in neuron soma and less prominent fluorescence in neuronal processes in the dorsal raphé. Immunolabeling with SMI312 (green) showed a selective reaction with neurofilaments in axons of serotonergic and nonserotonergic neurons. Fig. 12 depicts TPH distribution (immunolabeling with mAb PH8) in neuronal soma and in some neuronal processes in control subject M8-10.

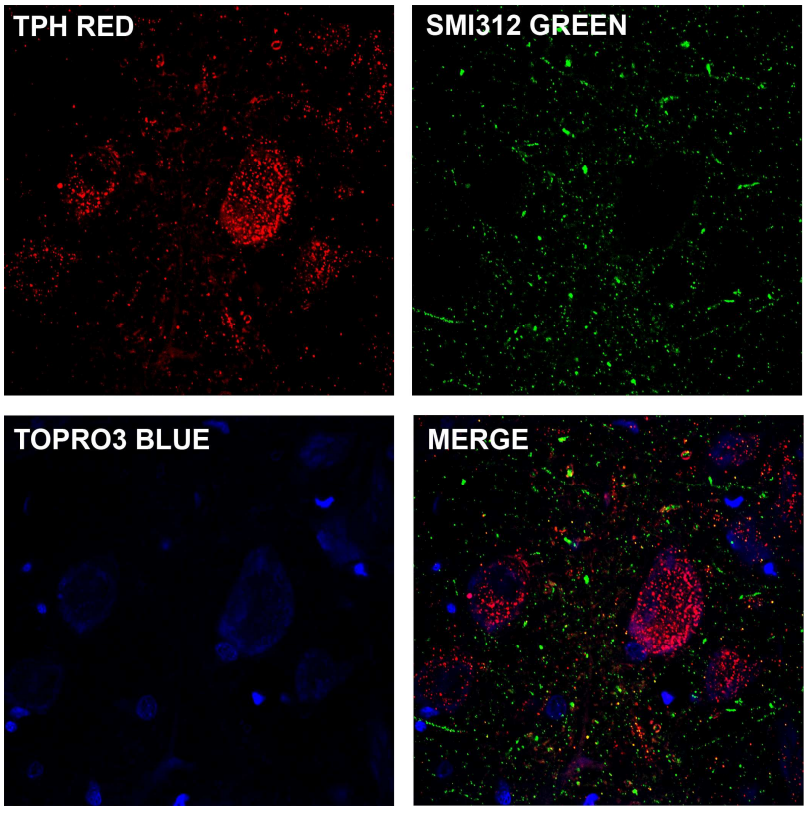

Fig. 12. TPH distribution in raphé neuron soma and dendrites. TPH (red) immunoreactivity reflects 5-HT synthesis in the neuron soma and dendrites. Green staining corresponds to SMI312 immunoreactivity with axonal neurofilaments. TOPRO (blue) shows nuclei (Obj. 100x) (15-year old control subject, M8-10).

Figure 13 illustrates TPH (shown with mAb PH8) in neuronal soma and dendrites identified as SMI312 negative in an autistic subject. PH8 identifies sites of serotonin synthesis in neuronal soma and fibers. SMI312 identifies axonal cytoskeleton and axons.

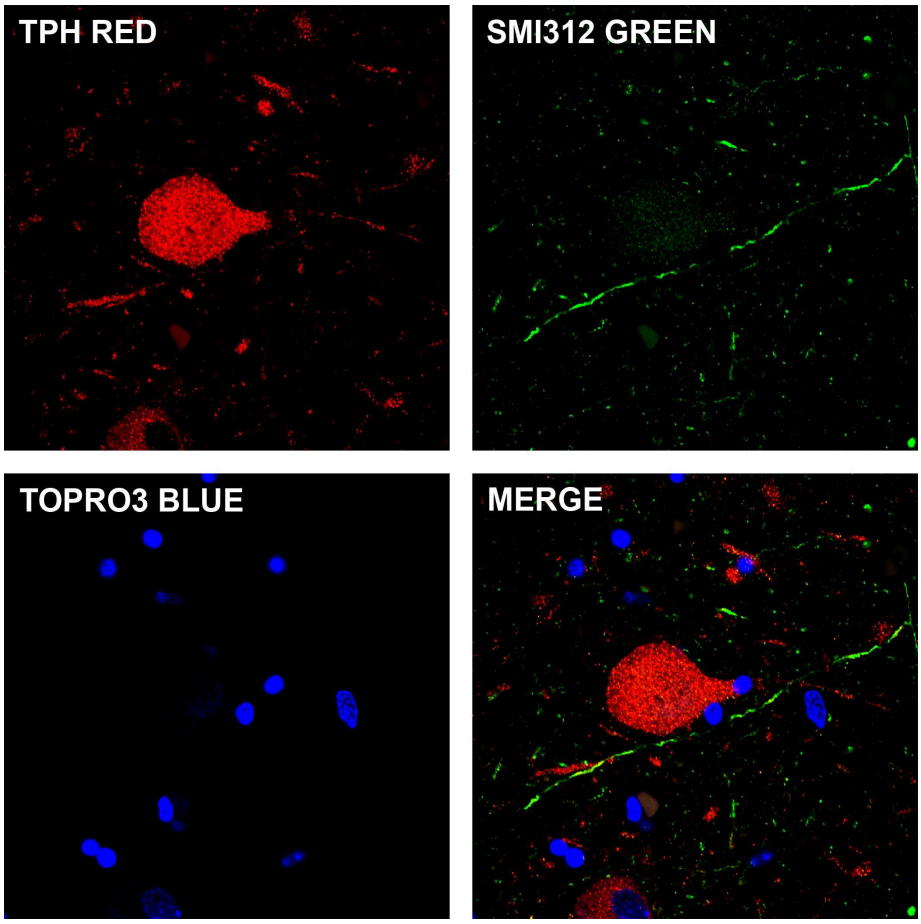

Fig. 13. Double immunolabeling for TPH and axons in raphé of autistic subject. Granular staining corresponds to TPH (red) in neuron soma and dendrites. Green immunofluorescence reflects SMI312 positive neurofilaments in axons. Nuclei shown with TOPRO (blue) (100x) (15-yr old autistic subject, M3-10).

Immunostaining of bundles of fibers adjacent to raphé nuclei shows SMI312-positive axons outside of the DRN (Fig. 14). PH8-negative (red) but SMI312-positive axons (green) confirmed the absence of TPH in these particular axons.

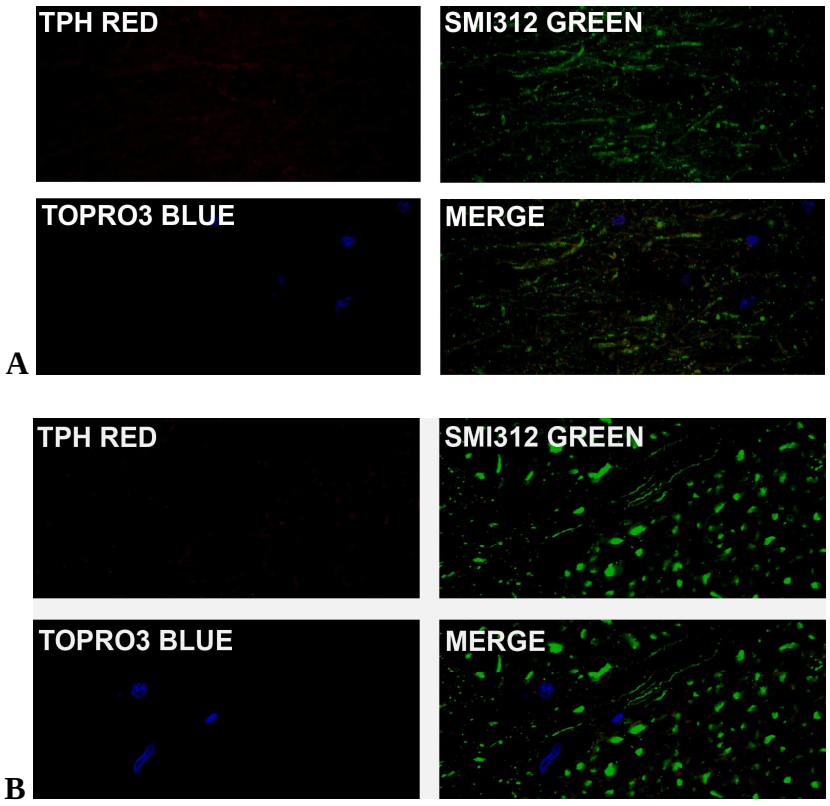

Fig. 14. Axons in vicinity of Dorsal Raphé Nucleus. SMI312 positive neurofilaments (green) in axons that are negative for TPH (red). Control case (M8-10; panel A) and autism case (M3-10; panel B). Neurons stained with TOPRO (blue)(100x).

SERT distribution in neuronal soma, dendrites and axons. The goal of double immunolabeling of SERT and SMI312 was to visualize SERT on axons of serotonergic neurons in the dorsal raphé. SERT immunofluorescence illustrates neuron serotonin reuptake and reutilization potential. Immunolabeling of SERT reveals sparse immunoreactivity within serotonergic neuron cytoplasm, cell body membrane, and processes with a strong overlap with SMI312 immunolabeling of axons. This photograph (Fig. 15) demonstrates strong immunofluorescence of SERT (red) in neuronal processes and in a portion of serotonergic neuron cytoplasm. Green fluorescence of SMI312 positive axons and yellow fluorescence in

merged images shows SERT in numerous axons. Non-overlaping red fluorescence in neuronal processes may correspond to SERT distribution in SMI312 negative dendrites.

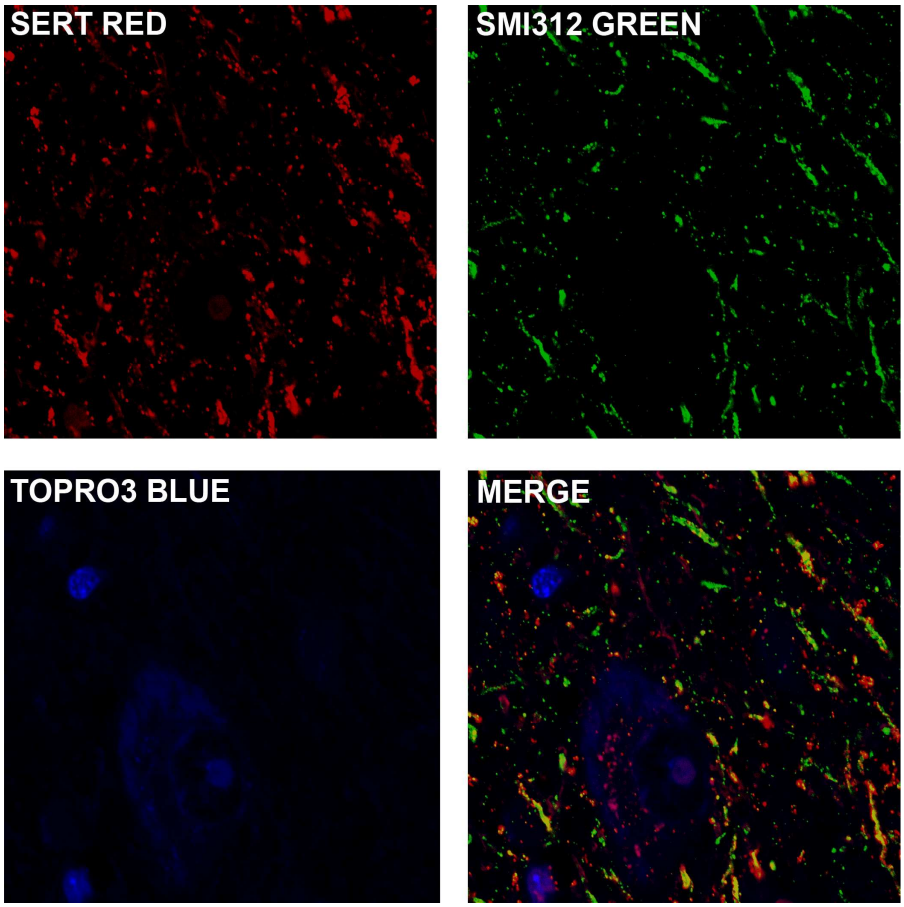

Fig. 15. SERT distribution in neuron soma, dendrites and axons in DRN of control subject. A few intracellular SERT-positive deposits (red) within neuron cytoplasm reflect SERT synthesis and intracellular transport. SERT staining in many processes corresponds to SERT distribution in cell membrane in dendrites and axons in DRN. Merged image (bottom right micrograph) illustrates distribution of SERT in SMI312 positive axons (yellow). Control 15 yr old subject (M8-10). SMI312 axons (green). Nuclear staining with TOPRO (blue). 100x.

The photographs in Fig.16 from dorsal raphé of 15-year old subject with autism show strong immunofluorescence of SERT (red) in a dense network of neuronal processes. Green fluorescence in a few longitudinally cut and transverse profiles of SMI312 positive axons

indicated that the majority of fibers in selected area are SERT-positive and SMI312-negative dendrites.

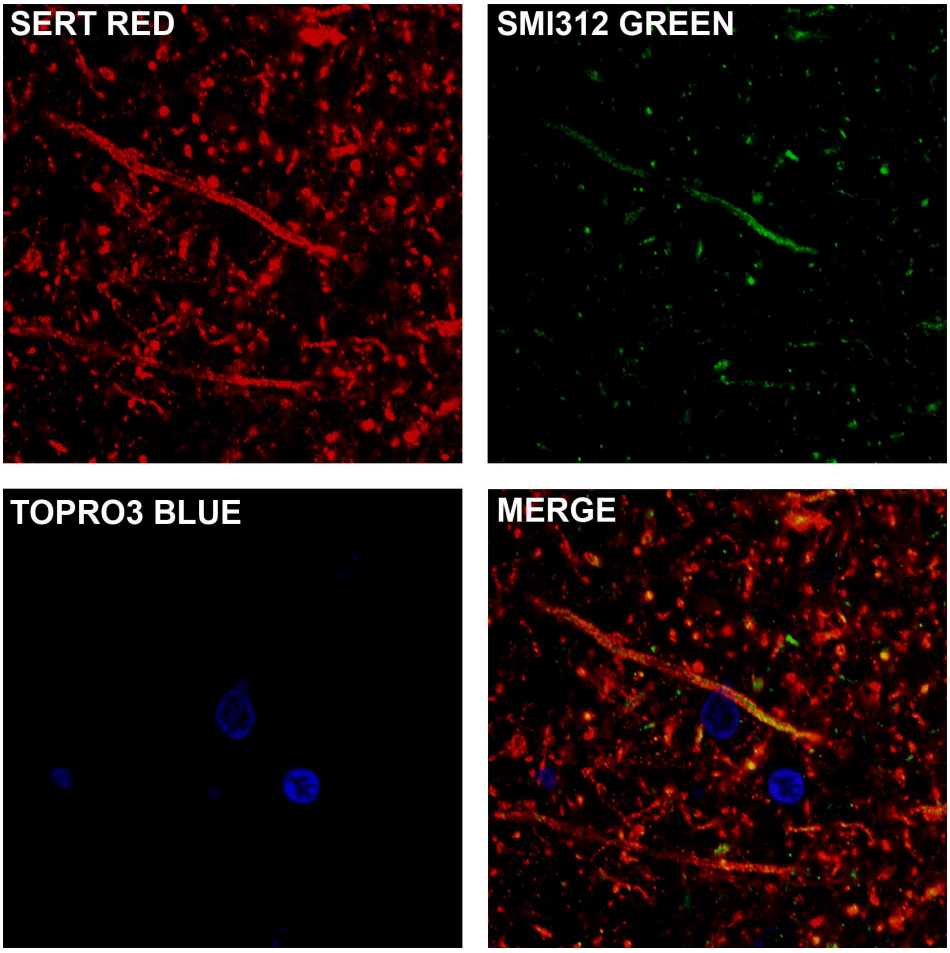

Fig. 16. SERT in dendrites and axons in DRN of autistic subject. SERT immunostaining with mAb ST51 (red) reflects dense network of dendrites and axons of serotonergic neurons in 15-year old autistic subject (M3-10). Relatively few SMI312-positive axons (green) are shown in upper right micrograph. Merged image (bottom right) illustrates distribution of SERT within serotonergic cell axons (yellow). Nuclear staining with TOPRO (blue). 100x.

Figure 17 shows bundles of SERT-positive fibers in 15 year old control subject (M8-10; panel A) and in autistic subject (M3-10; panel B) in neuronal projections outside of raphé nuclei perimeter. Staining for SMI312 shows numerous transversly cut axons detectable at high magnification. Only the central bundle represented axons of serotonergic raphé neurons.

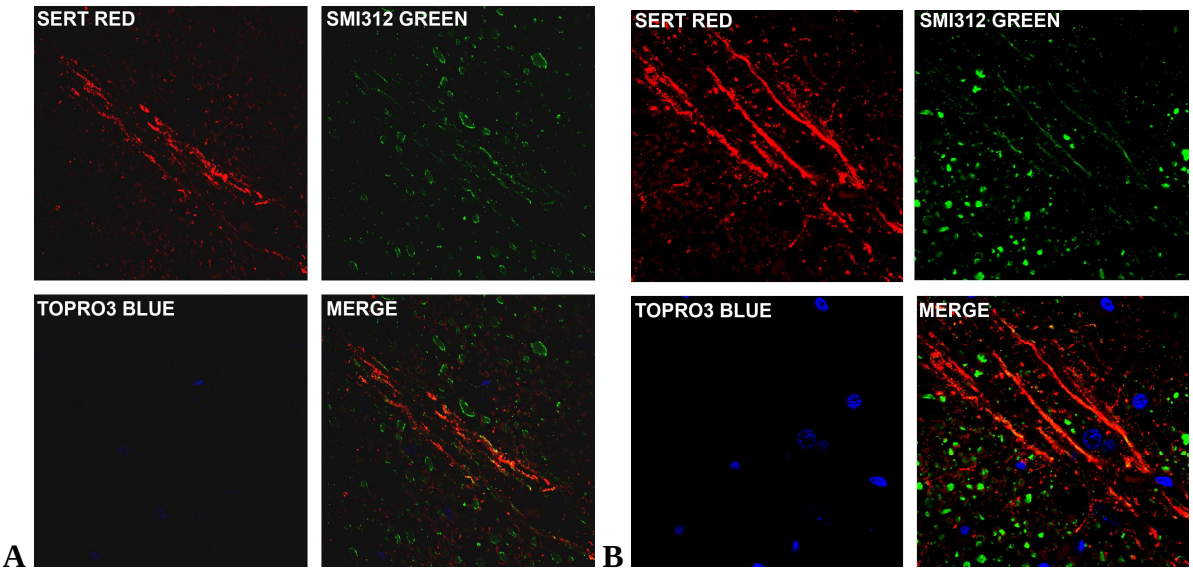

Fig. 17. Bundles of SERT (+) and (-) fibers in vinicity of DRN. Comparison of SERT(+) bundles (red/yellow) with SERT(-) SMI312(+) axons (green). TOPRO labeling of cell nuclei (blue). 100x. (A: M8-10, B: M3-10)

4.6. Altered TPH expression in autistic subjects in immunofluorescence- based quantitative study

Standardization of methods of background subtraction. The critical factor for estimation of neuronal TPH was standardization of both immunolabeling and quantitative evaluation of the amount of intracellular TPH. Four methods of background detection and subtraction were applied including: equal background correction for all 8 examined cases, pairwise background correction, individual background correction, and correction based on subtraction of only cytoplasmic background. I have attempted to work around the difficulties associated with human postmortem formalin fixed tissue and produce meaningful data using several approaches which have been applied systematically to all the human brainstems. The results and limitations of all these approaches were compared.

Equal background correction in all 8 cases.

Image correction by subtraction of one average background value established for all 8 subjects results in distortion of results with loss of almost all existing signal in two control subjects (values of 2.6 and 0.8 arbitrary units, respectively), and similar loss of signal in two autistic subjects (0.7 and 11.9). The mean signal in two older control and two autistic subjects (Figs. 18-20) was disproportionately high (65 and 266 in control subjects, and 403 and 1304 in autistic subjects, respectively).

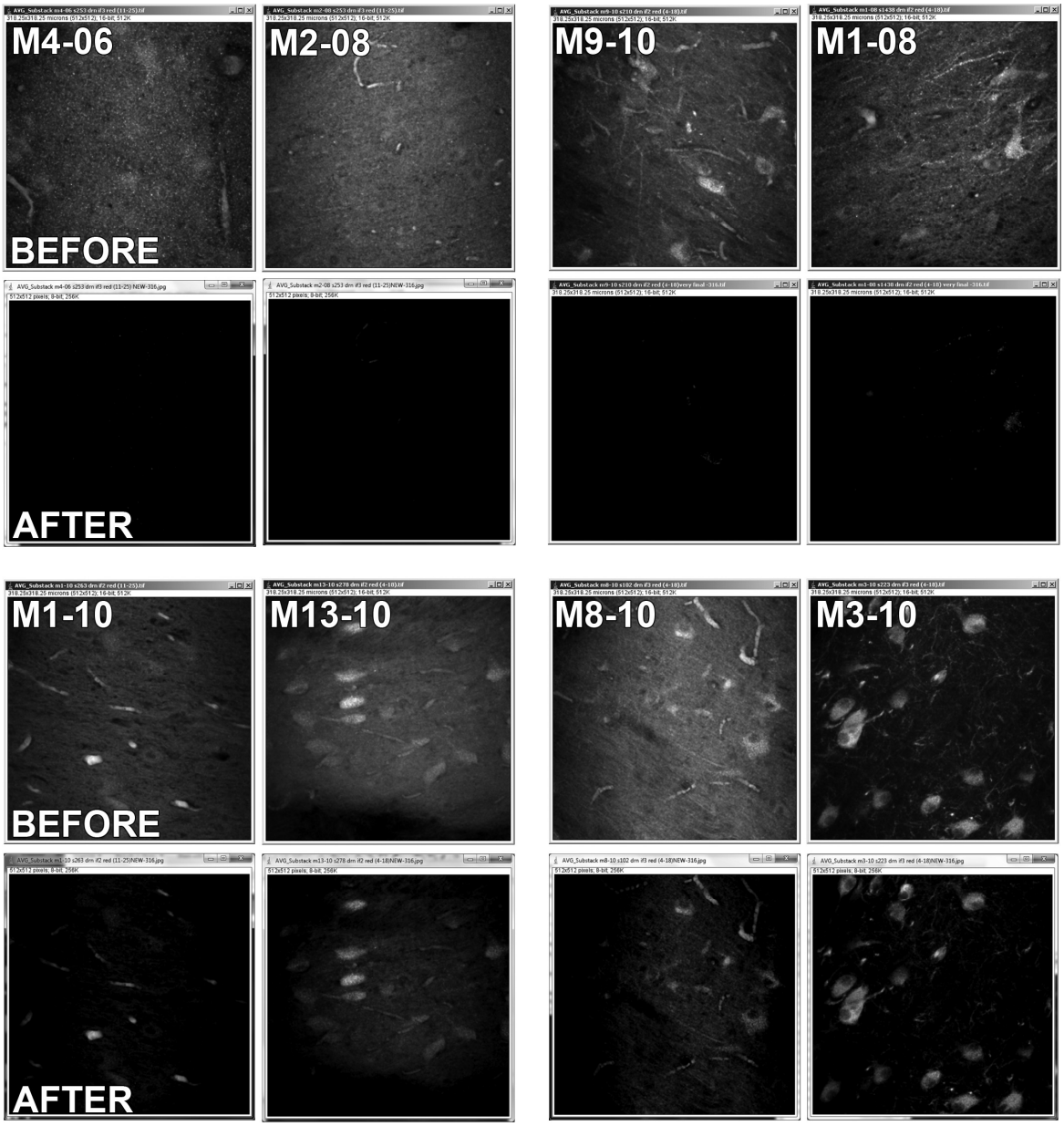

Fig. 18. Equal background subtraction. The DRN IF nucleus immunolabeled with mAb PH8 (TPH labeling) in pairs of control and autistic subjects before equal background correction and after correction. Equal background subtraction established for all 8 subjects with significant clinical and neuropathological differences, as well as differences in vessels and neuropil signal intensity dramatically distorted PH8 intensity readings shown as a loss of signal in two control and autistic subjects (upper panel, images after subtraction).

It should be noted that the autistic subject in pair one (M2-08) always had weak staining (including at all tested concentrations/times in colorimetric staining) and the subject had a

premature birth. The subject's mother was hypoglycemic and suffered from low blood pressure as well as fainting during pregnancy. These, as well as premature birth may have contributed to hypoxia and permanent injury to some brainstem neuronal populations.

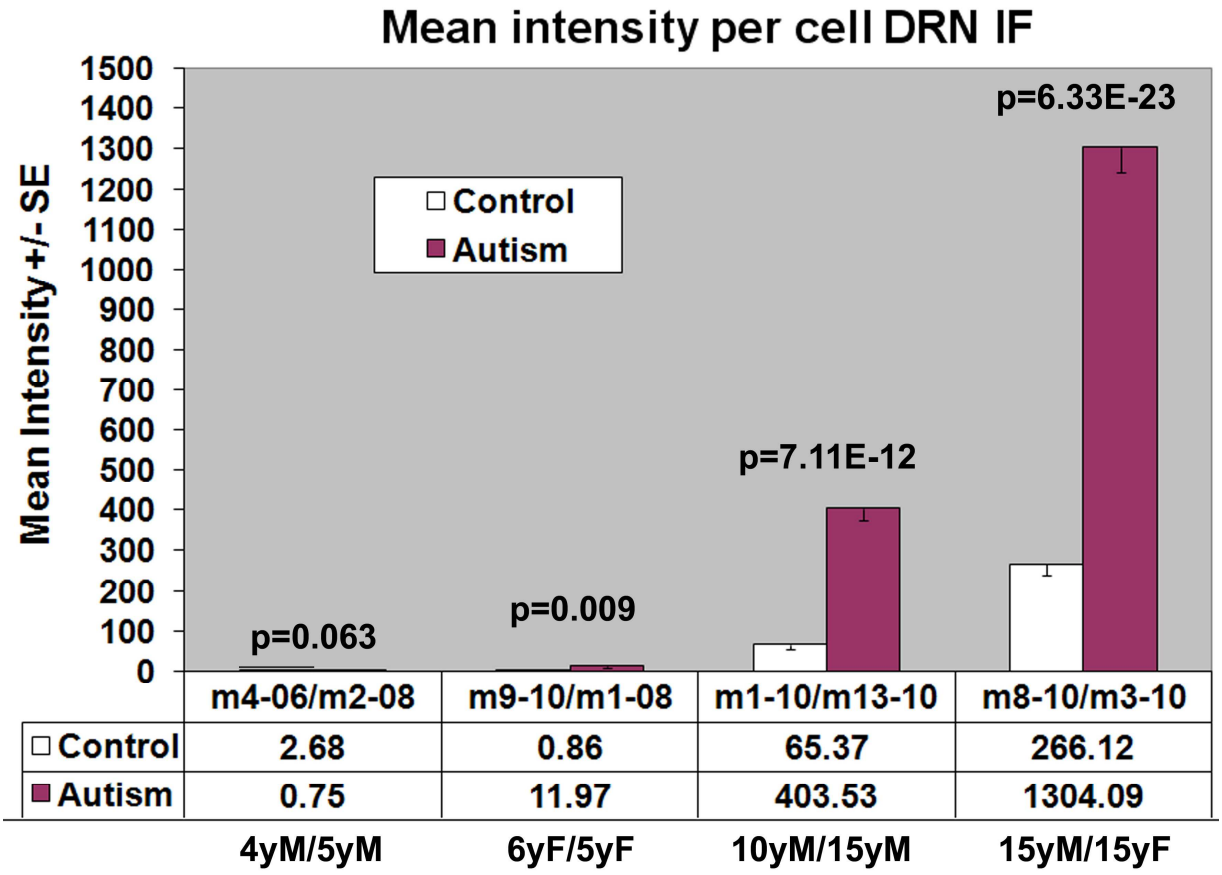

Fig. 19. Mean neuron soma TPH IF after equal background subtraction (bar graph). Mean soma intensity results of application of equal background subtraction in 8 examined cases. Significant signal increase in 3 out of 4 autistic cases. Extremely low values in two youngest subjects and extremely high value in M3-10.

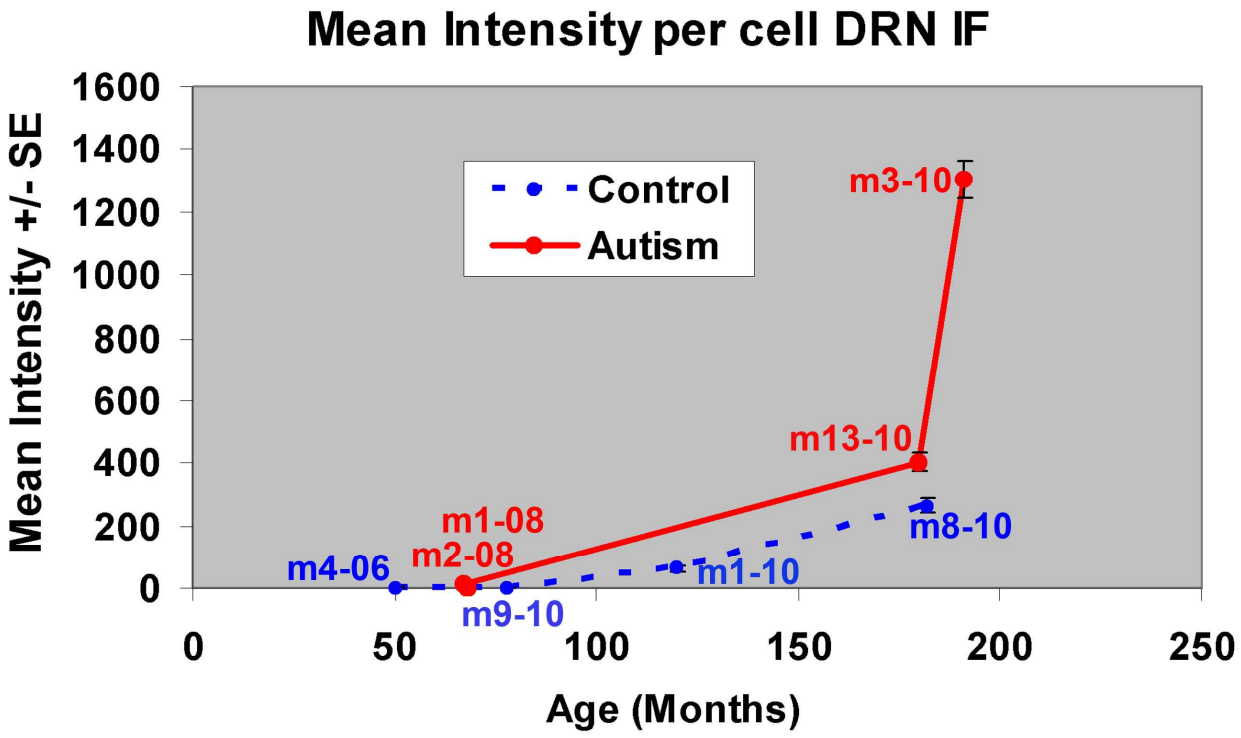

Fig. 20. Mean neuron soma TPH IF after equal background subtraction (line graph). This graph illustrates in a different way the distortion of TPH immunofluorescence with equal background subtraction. Distortion is most noticeable in two youngest pairs. M4-06: 4y M, M2-08: 5y M, M9-10: 6y F, M1-08: 5y F, M1-10: 10y M, M13-10: 15y M, M8-10: 15y M, M3-10: 15y F

The result of this correction was a signal reduction by 72% (p=0.063) in the first autistic subject (M2-08), and signal increase in second autistic subject (M1-08) of 1286% (p=0.009), in autistic subject three (M13-10) of 517%, (p=7.11E-12), and in autistic subject four (m3-10) of 390%, (p=6.33E-23) (Fig. 21).

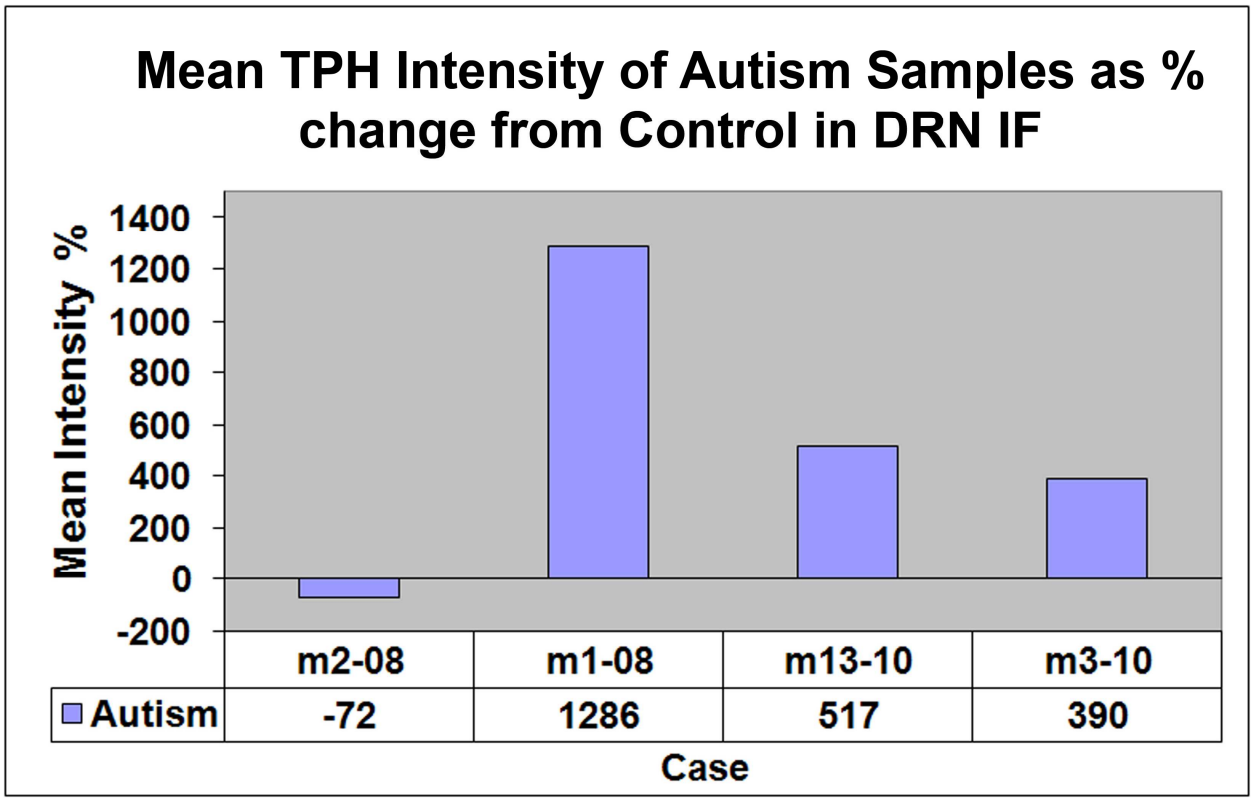

Fig. 21. Mean neuron soma TPH IF in autistic subjects as percent change from control after equal background subtraction. Proportions between control and autistic subject immunofluorescence after equal background subtraction.

In this method, the average soma intensity per group measured 91 arbitrary units for the control group and 563 arbitrary units for the autistic group. There was a significant increase in the autistic group ($P < 0.001$). (Fig. 22)

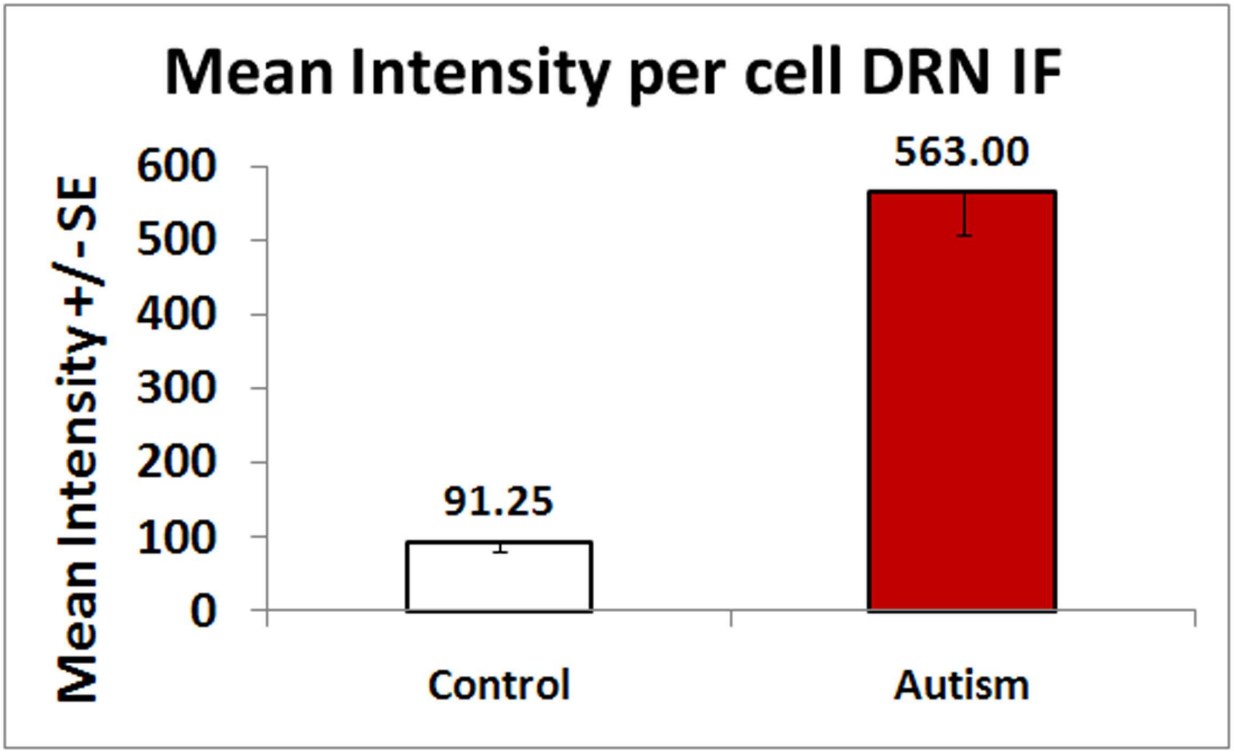

Fig. 22. Increase in mean cell TPH IF in autistic group after equal background subtraction. Equal background subtraction results in a very high (6.2x) disproportion between immunofluorescence in autism and in control group.

The Spearman correlation coefficient for the equal background correction approach measured 0.8 for the control group and 0.8 for the autistic group.

The results of application of equal background subtraction in all cases (Figs. 18-22) indicated that equal background subtraction did not effectively correct the existing signal but on the contrary, resulted in distortion. The method of uniform background correction resulted in the least constant background intensity and the highest loss of signal from a large number of cells with lower signal values (which in many cases is equal to complete loss of existing neuronal signal). Lost neurons contributed to the low mean intensities for a given case and large percentage differences between those cases and those where intensity values did not bottom out at 0. Standard deviations were also large. Results of this test indicate that both direct cell body

fluorescence measurements (uncorrected background) and measurements corrected by subtraction of a constant background value from all subjects are biased.

The variations in background intensity at constant confocal settings (Fig. 23) seen in TPH negative controls without primary antibody contributed to the ineffectiveness of the equal background correction method.

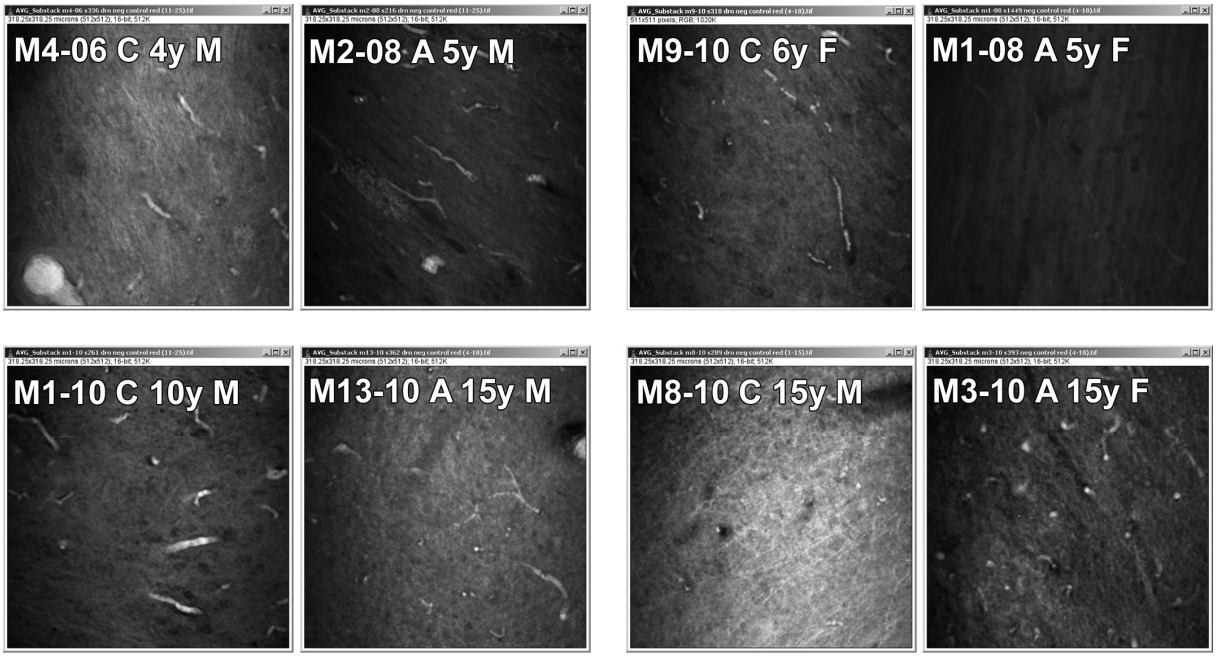

Fig. 23. DRN IF TPH negative controls (no primary antibody). Images of negative control tissue for each subject's DRN taken at constant settings illustrating variation in background.

Pairwise background correction in four pairs of autistic and control subjects.

In the pairwise approach, following the chosen method did not result in preserving all cells from disappearing nor keeping the background consistent due to existence of background intensity variations.

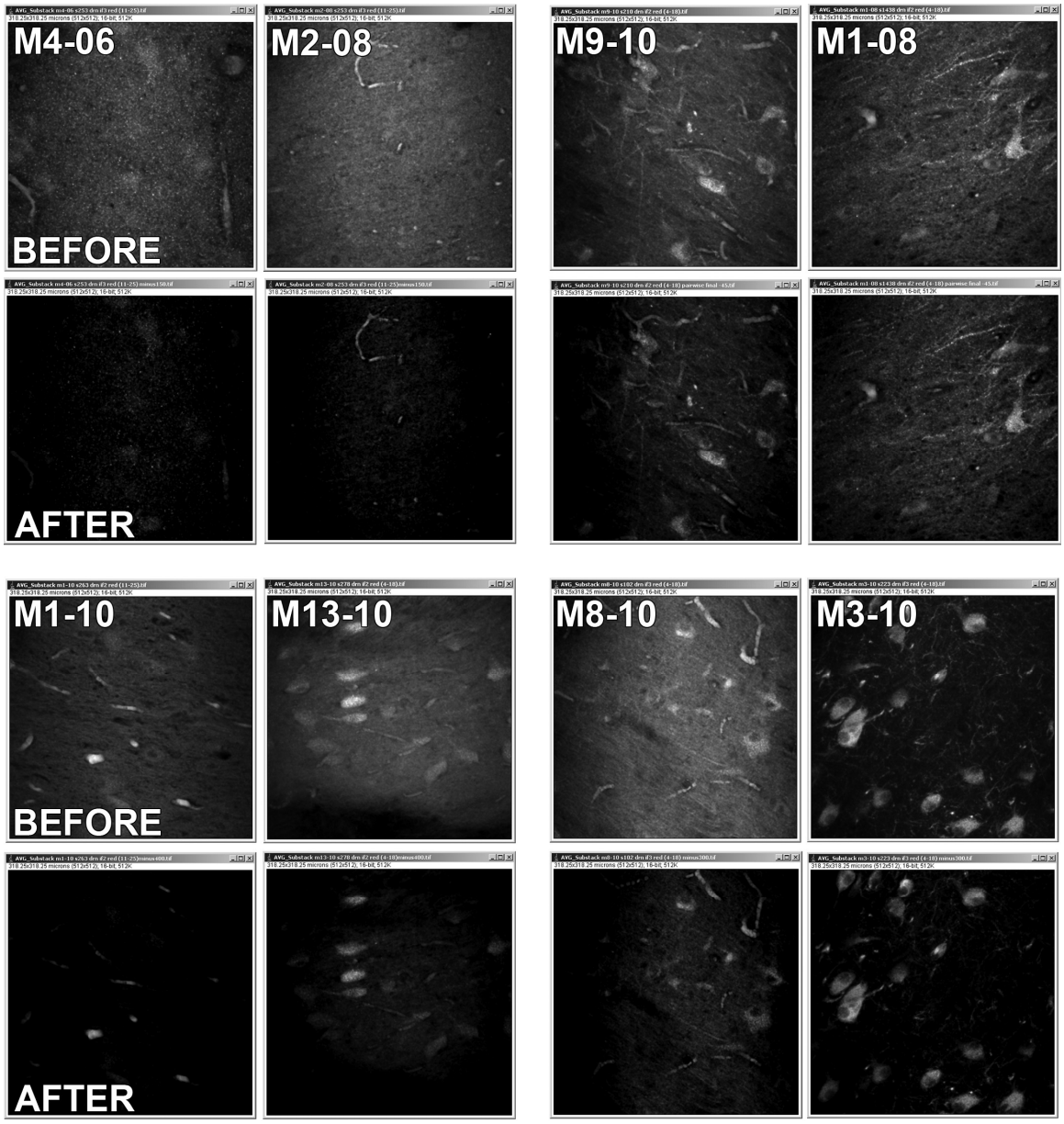

Fig. 24. Pairwise background subtraction. DRN IF immunolabelled with mAb PH8 (TPH labeling) in pairs of control and autistic subjects before and after pairwise background correction.

The second method showed that tryptophan hydroxylase immunofluorescence measured in arbitrary units per neuron body area was decreased in autistic subject in the interfascicular subdivision of the dorsal raphé nucleus in pair 1 (-31%, p=0.025), but increased in autistic

subject in pair 2 (+53%, p=0.001), pair 3 (+1248%, p=7.12E-11), and pair 4 (+306%, p=4.22E-25). The average increase for three autistic subjects was 536% (Figs. 25-27).

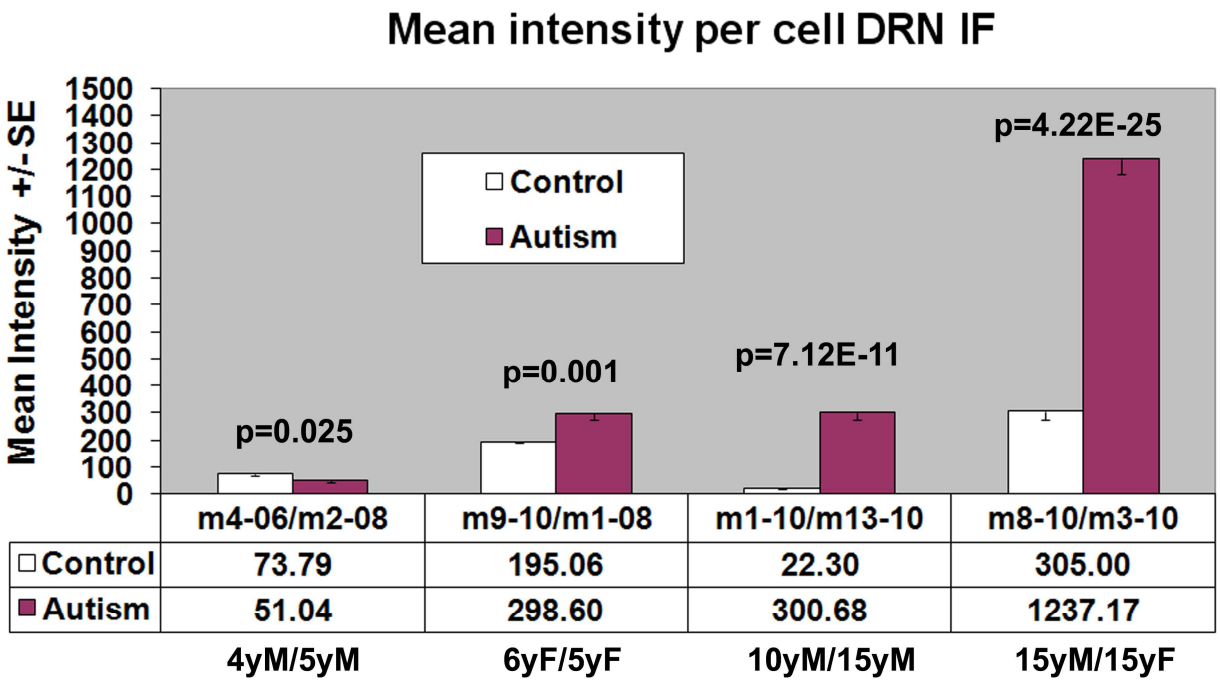

Fig. 25. Mean neuron soma TPH IF after pairwise background subtraction (bar graph). Mean soma intensity results of application of pairwise background subtraction in 8 examined cases. Significant signal increase seen in 3 out of 4 autistic cases.

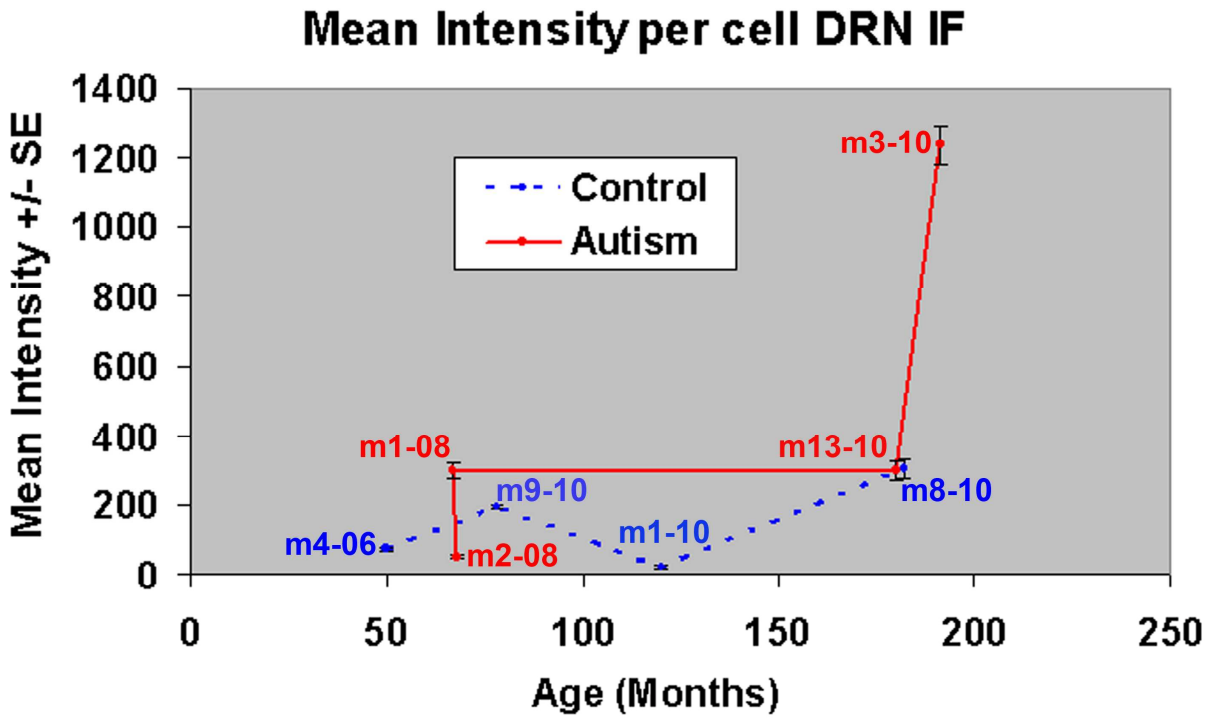

Fig. 26. Mean neuron soma TPH IF after pairwise background subtraction (line graph). Mean soma intensity results of application of pairwise background subtraction in 8 examined cases. M4-06: 4y M, M2-08: 5y M, M9-10: 6y F, M1-08: 5y F, M1-10: 10y M, M13-10: 15y M, M8-10: 15y M, M3-10: 15y F

The mean intensity percent change in autistic subjects was -31% (M2-08), 53% (M1-08), 1248% (M13-10), and 306% (M3-10) (Fig. 27).

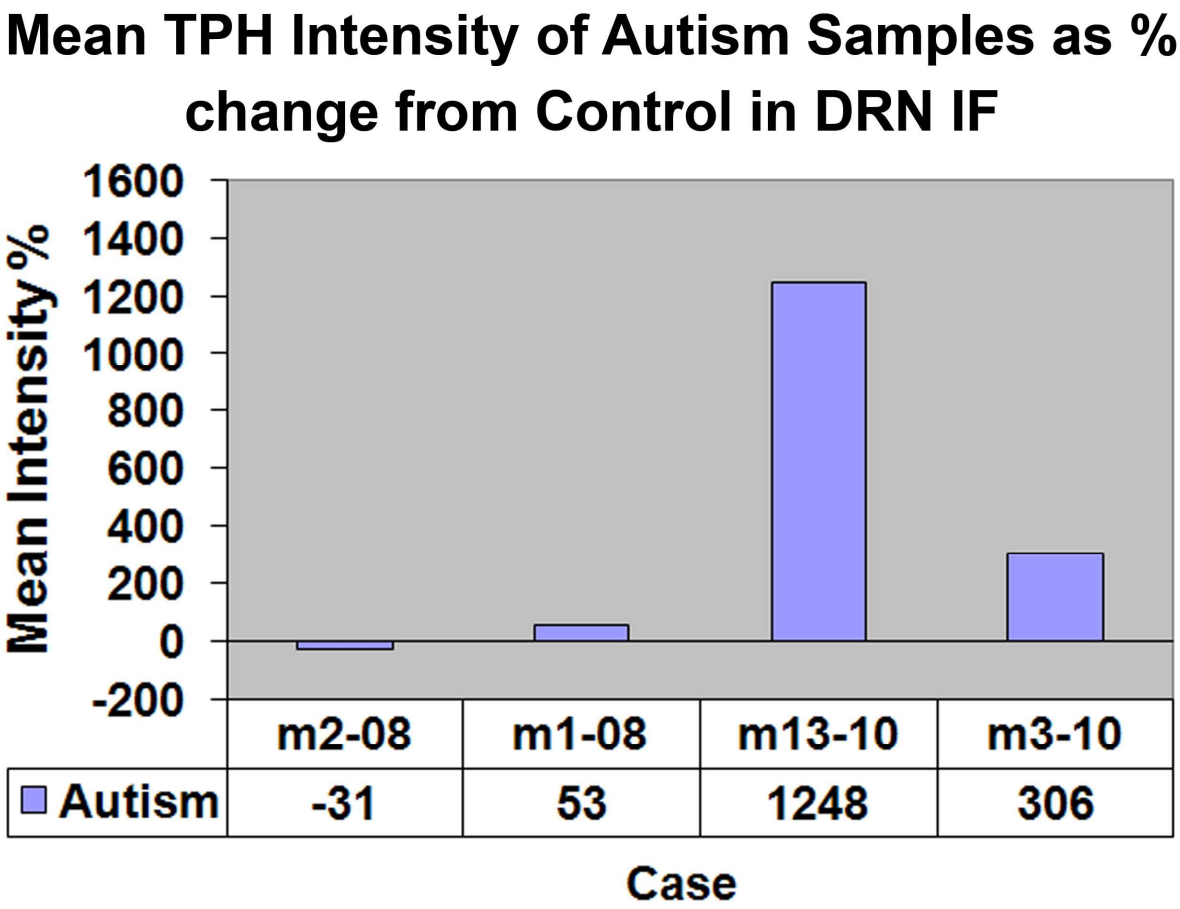

Fig. 27. Mean neuron soma TPH IF in autistic subjects as percent change from control after pairwise background subtraction. Correction results in distortion of proportions between control and autistic subjects, especially large in the pair of M13-10 (autism) and M1-10 (control).

In this method, the average soma intensity per group measured 160 arbitrary units for the control group and 684 arbitrary units for the autistic group. There was a significant increase in the autistic group ($P < 0.001$). (Fig. 28)

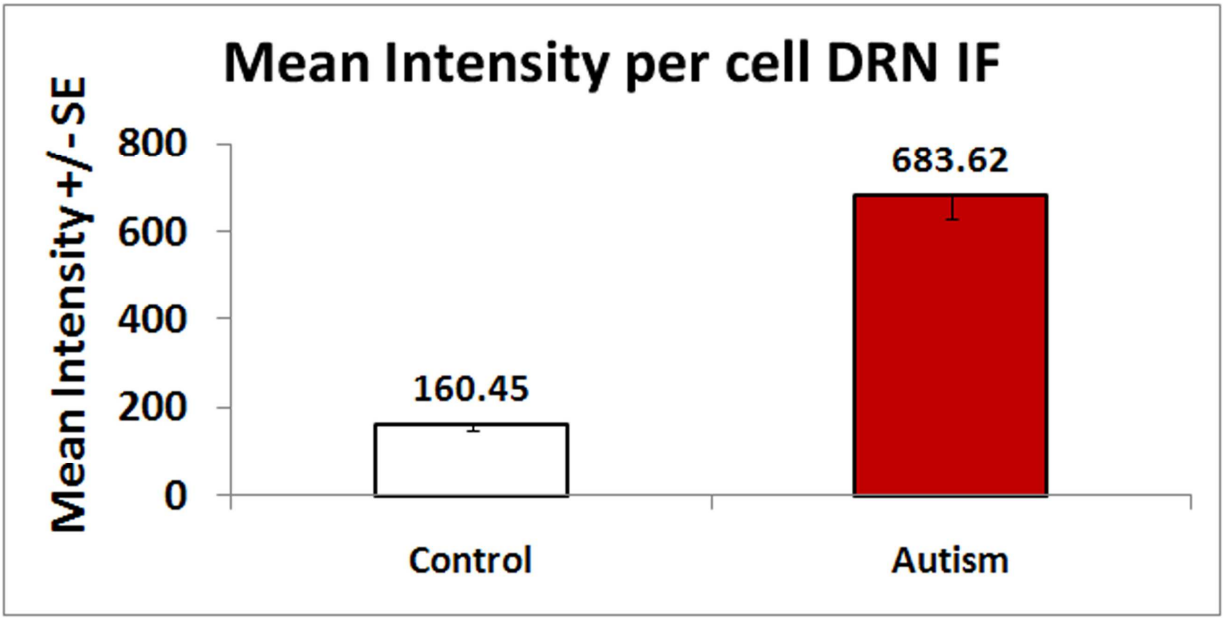

Fig. 28. Increase in mean cell TPH IF in autistic group after pairwise background subtraction. The ratio between average immunfluorescence in autistic and control subjects is in range of 4.3x.

The Spearman correlation coefficient for the pairwise background correction approach measured 0.4 for the control group and 0.8 for the autistic group.

Again, an almost 14- fold higher immunofluorescence in control subject M8-10 than in M1-10 suggests that these results do not reflect TPH cellular concentration in examined cases but rather a distortion created by subtraction of a background factor calculated for pairs of subjects with different tissue properties.

Individual background correction.

In the third method, there was variation in background even with correction value set for each individual brain. There is variation even between stacks of the same brain. Due to the fact that .tif files are used, however, there are enough grayscale levels to record non-zero intensity values for cells, which may have become invisible to the eye. (Fig. 29)

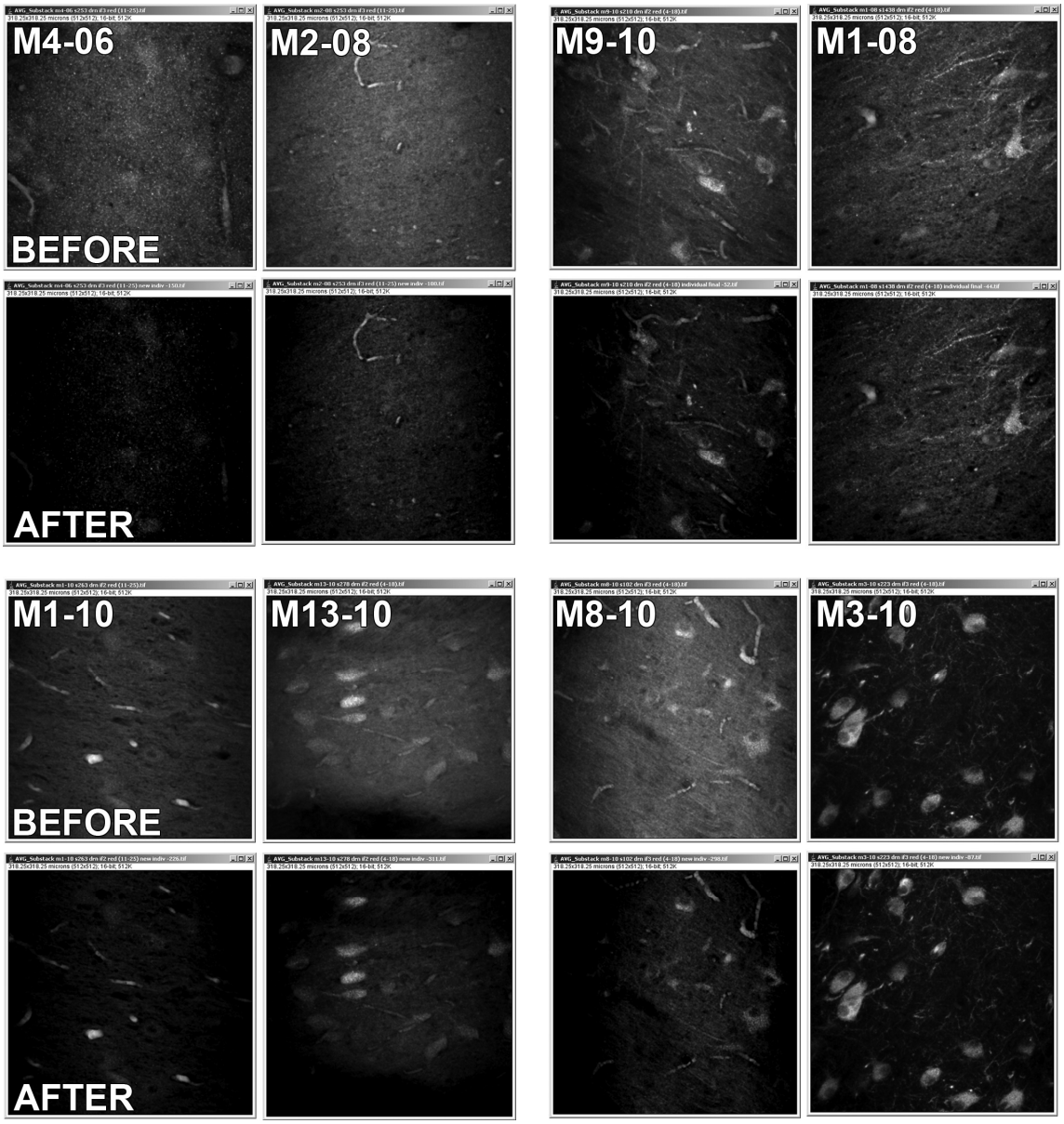

Fig. 29. Individual background subtraction. DRN IF immunolabelled with mAb PH8 (TPH labeling) in pairs of control and autistic subject cases before individual background correction and after correction.

This method showed that tryptophan hydroxylase immunofluorescence measured in arbitrary units per neuron body area was decreased in autistic subject in the interfascicular subdivision of the dorsal raphé nucleus in pair 1 (-6%, p=0.542), but increased in autistic subject

in pair 2 (+29%, p=0.01), pair 3 (+148%, p=1.18E-10), and pair 4 (+386%, p =2.23E-33). The average increase for the autistic subjects, which increased in intensity was 187% (Figs. 30-32).

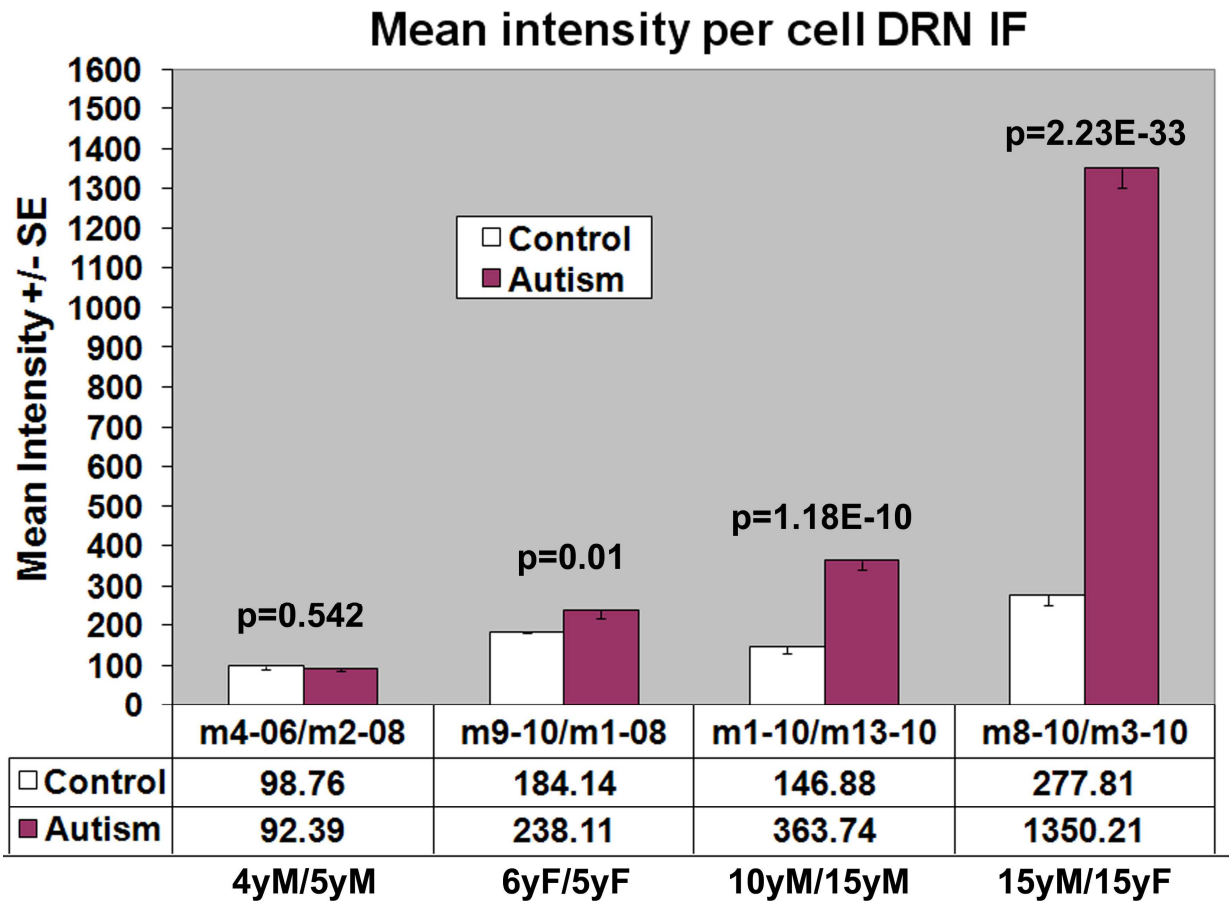

Fig. 30. Mean neuron soma TPH IF after individual background subtraction (bar graph). Mean soma intensity results of application of individual background subtraction in 8 examined cases. Significant signal increase in 3 out of 4 autistic cases.

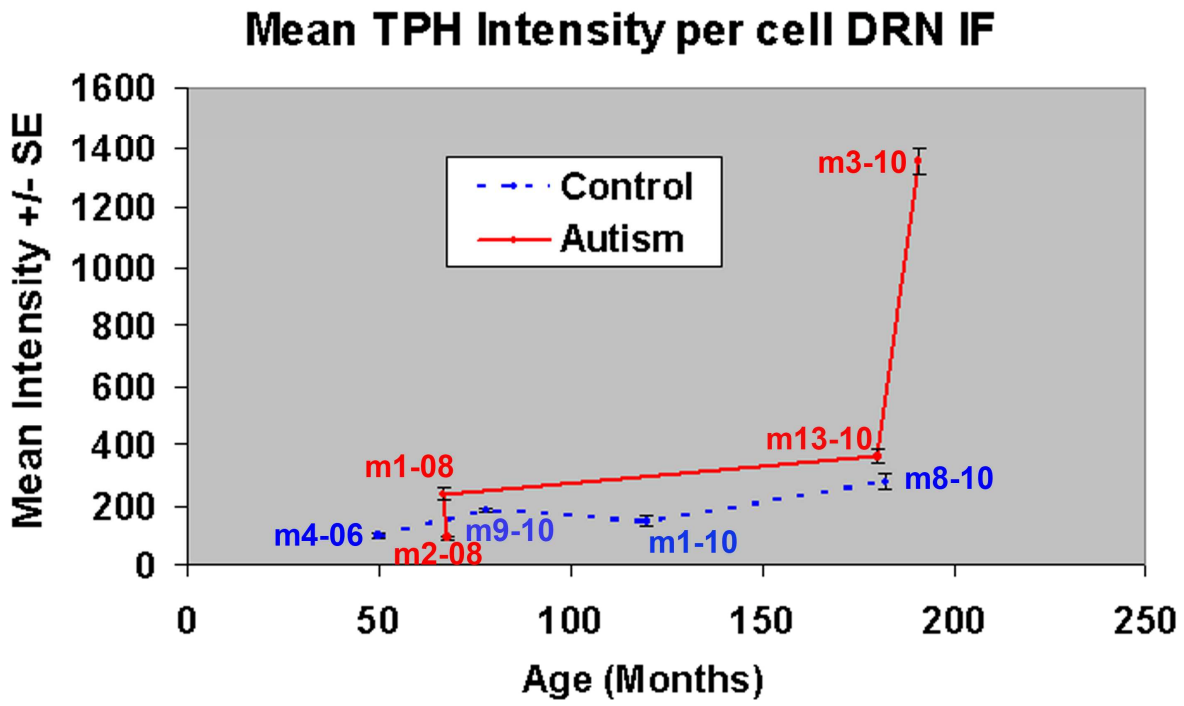

Fig. 31. Mean neuron soma TPH IF after individual background subtraction (line graph). Signal increase in autistic group expressed as line graph**.** M4-06: 4y M, M2-08: 5y M, M9-10: 6y F, M1-08: 5y F, M1-10: 10y M, M13-10: 15y M, M8-10: 15y M, M3-10: 15y F

The mean intensity percent change in autistic subjects was -6% (M2-08), 29% (M1-08), 148% (M13-10), and 386% (M3-10) (Fig. 32.) There was a significant difference in TPH signal in age-matched pairs between control and autistic cases in the individual correction method.

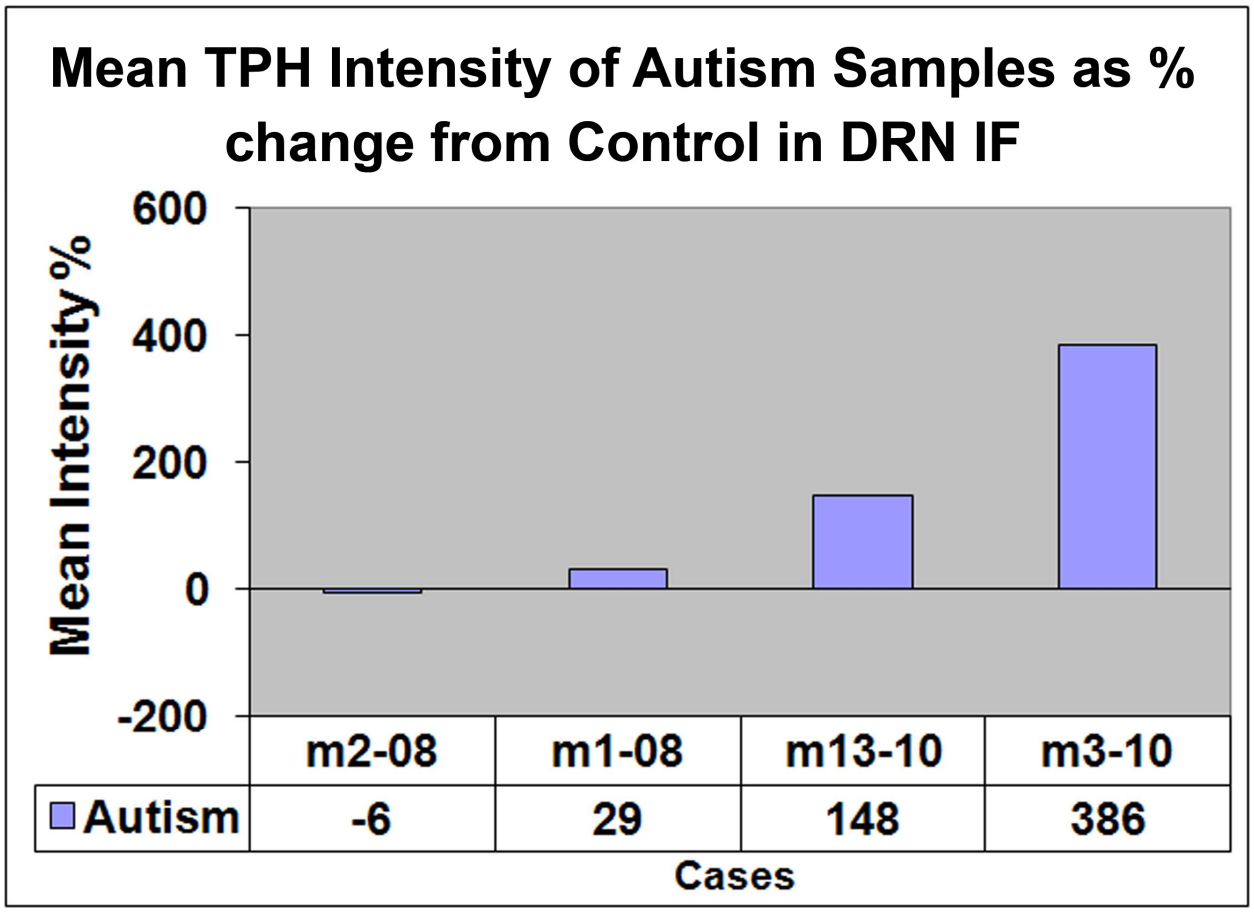

Fig. 32. Mean neuron soma TPH IF in autistic subjects as percent change from control after individual background subtraction. Signal increased in autistic group.

In this method, the average soma intensity per group measured 183 arbitrary units for the control group and 658 arbitrary units for the autistic group. There was a significant increase in the autistic group ($P < 0.001$). (Fig. 33)

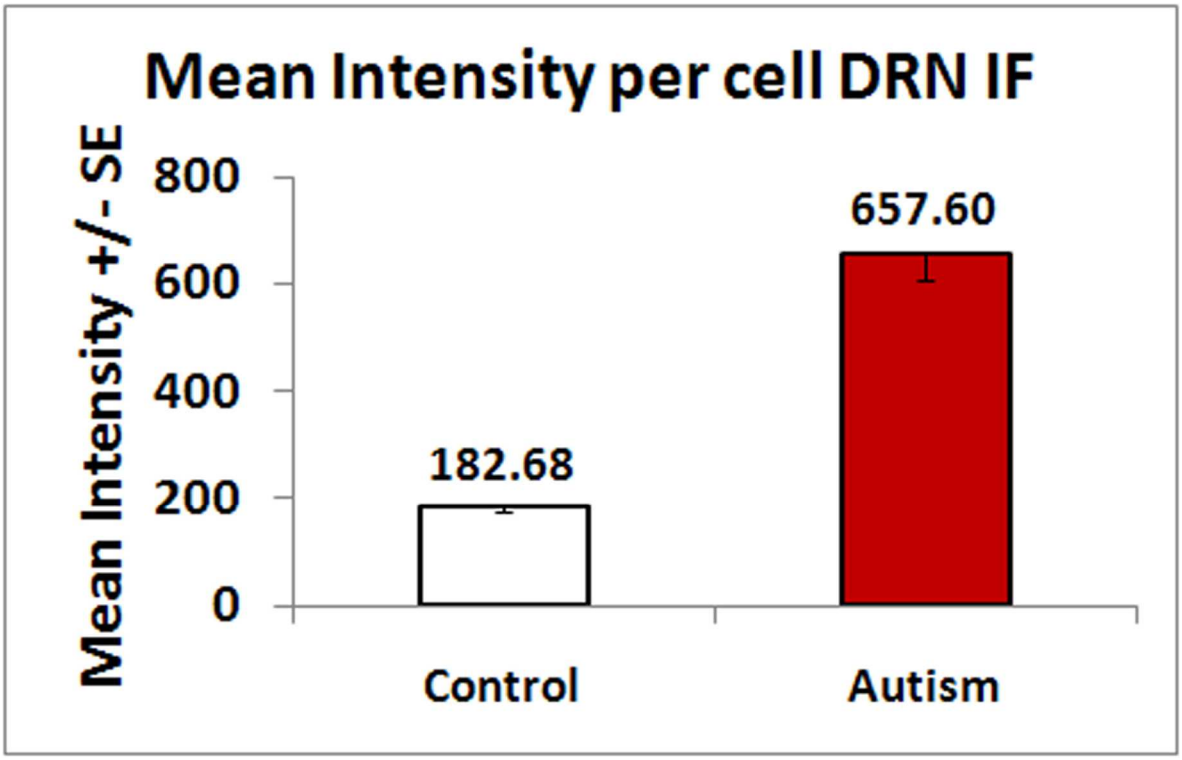

Fig. 33. Increase in mean cell TPH IF in autistic group after individual background subtraction. The ratio between immunofluorescence in autistic and control subjects is approximately 3.6x

The Spearman correlation coefficient for the individual background correction approach measured 0.8 for the control group and 0.8 for the autistic group.

Results of immunofluorescence based estimation of TPH levels in neurons of control and autistic subjects after individual background correction.

Intracellular immunofluorescence estimated after individual background subtraction in four control cases combined revealed a normal distribution of 132 measurements with a mean value of 183 arbitrary units (SE, 10; SD, 111), whereas in autistic group the mean value of 156 measurements was higher by 360% (658 arbitrary units; SE, 49; SD, 607) (t-test for two samples with unequal variances; p=1.41E-17).

A bimodal distribution within the autistic group suggested heterogeneity reflected in detachment of measurements above ~700 arbitrary units (Fig. 34, 35). Analysis of individual records revealed that all neuronal measures of subject diagnosed with autism associated with dup15 were in range from 704 to 2356 a.u. without overlap with any control or idiopathic autism case. All these readings correspond to the second normal but lower, bell-like distribution. Mean fluorescence level in neurons of autism/dup15 (M3-10; 1,350 a.u.) was 485% more than age matched control case (M8-10; 278 a.u., $p< 2.23E-33$).

Further analysis of differences between autistic subjects revealed that consistently with observations, readings in case M2-08 are 2.3 and 3.9x less than in two other cases of idiopathic autism (M1-08 and M13-10), respectively), and slightly less ($p<0.542$) than in age-matched control subject (M4-06).

Immunofluorescence-based evaluation of the cytoplasmic level of TPH detected in neurons in the interfascicular nucleus of the dorsal raphé with mAb PH8 revealed significant heterogeneity in pattern of changes. They reflect the role of the genetic causative factor in autism associated with dup15. The role of epigenetic factors is considered in case M2-08 with the impact of *in utero* exposure to mother's hypoglycemia, low blood pressure and fainting, as well as premature child birth. All these factors could directly affect development of raphé neurons, known to be sensitive to anoxia and hypoxia. Frequent agitation, screaming and crying, significant sleep disorder, sensory alterations, and laughter for no apparent reason appear to be related to raphé developmental injury. On the other hand, patient treatment with prozac for 3 years and valium occasionally might be another epigenetic factor modifying raphé neuron biochemistry and function, including tryptophan hydroxylase expression.

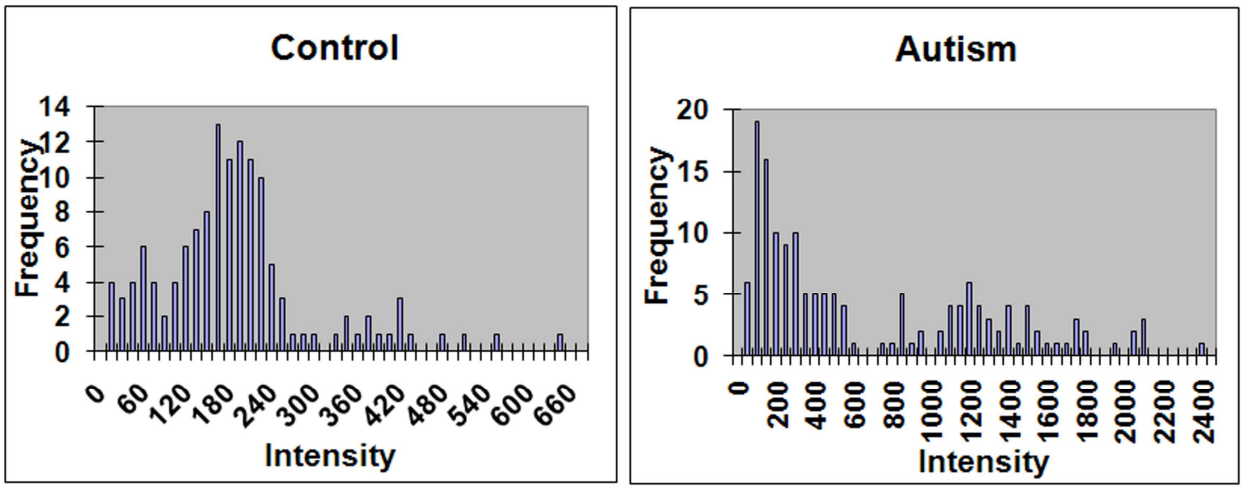

Fig. 34. Distribution of TPH IF in neuron soma in 4 control and 4 autistic subjects. Normal distribution in control group but bimodal distribution in autistic group with all readings in range from ~700 to 2,400 arbitrary units observed only in autistic subject with dup15 and not observed in control group.

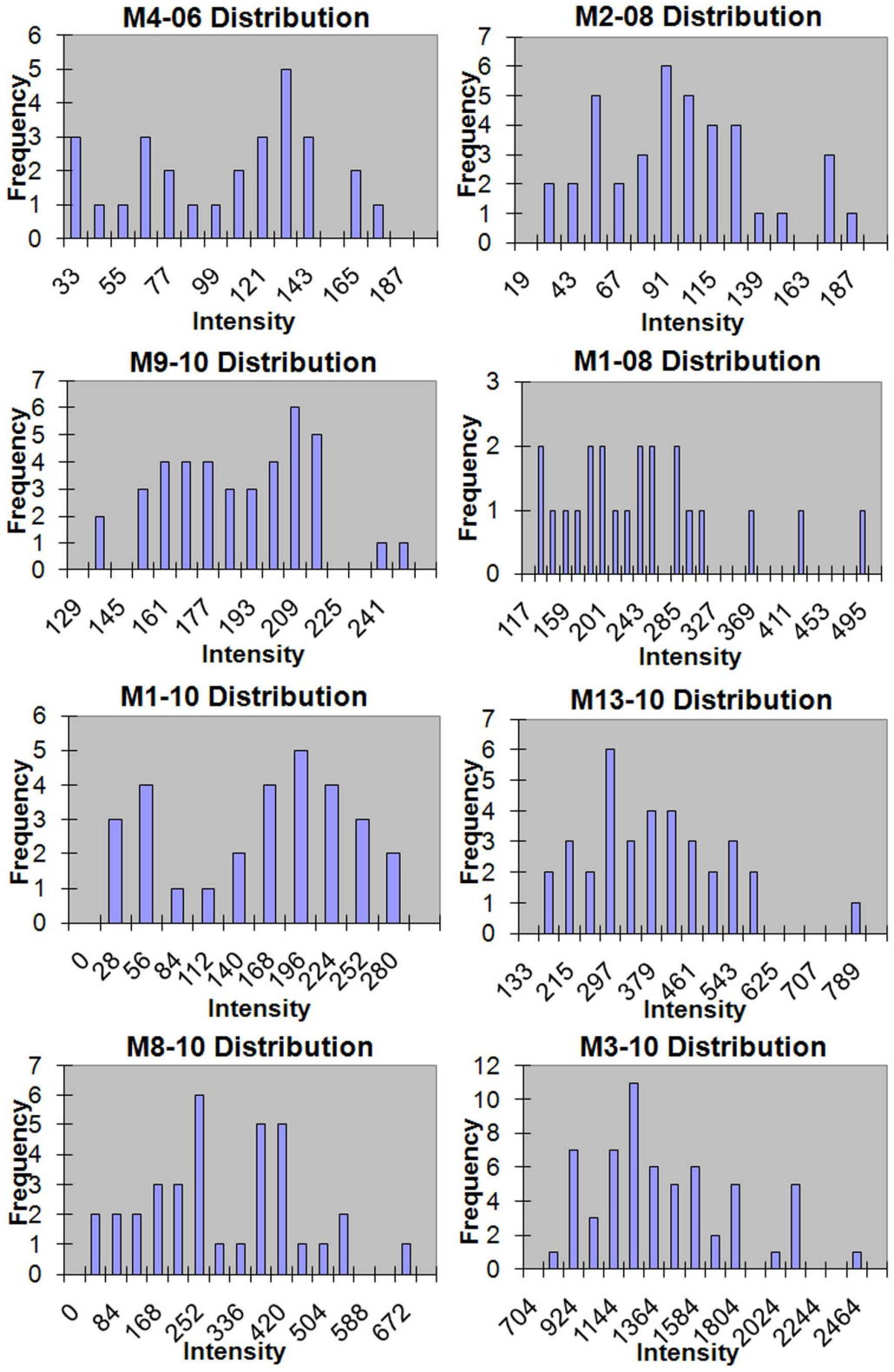

Fig. 35. Individual distributions of TPH IF in neuron soma in 4 control (left column) and 4 autistic subjects (right column).

Subtraction of cytoplasmic background of serotonergic neurons measured in adjacent sections processed without primary and secondary antibodies.

All TPH-immunofluorescence measurements are limited to the serotonergic neuron soma excluding the TPH-negative nucleus. Therefore, the fourth method of defining background and background subtraction was limited to the soma of neurons in the nucleus interfascicularis. Two adjacent brainstem sections from each subject were treated with one of two protocols: (a) immunostaining with primary antibody and secondary antibody conjugated with fluorochrome, and (b) omitting the primary antibody and secondary antibody conjugated with fluorochrome (control). Both sections were examined in identical conditions in confocal microscope. Measurements were limited to the cytoplasm of neurons in both sections. Mean value of signal from control section neuron soma was subtracted from signal measurements in individual neuron soma in immunostained section.

Several arguments support application of this method as appropriate for background correction in the cytoplasm in raphé neurons. Measurements are performed on adjacent sections of the same subject which eliminates variation related to the difference between control and autistic subject sample. Measurements are restricted to the cytoplasm, which eliminates variation of neuropil signals. In this method, cytoplasmic signal including lipofuscin autofluorescence is detected in the laser channel used for detection of AlexaFluor 555 used in measurements in immunostained sections. The protocol repeats all steps and timing of tissue treatment but omits the primary and the secondary antibody conjugated with fluorochrome, which preserves all cell cytoplasm signals, including lipofuscin autofluorescence.

For each of 4 control and four autistic subjects, a panel of three images illustrates background fluorescence in section processed without application of primary and secondary

antibodies (Ab-), section incubated with primary antibody (PH8 detecting TPH) and secondary antibody conjugated with AlexaFluor 488 (Ab+). The third image (Ab+ After) reflects immunofluorescence (Ab+) after subtraction of mean fluorescence detected in the cytoplasm in Ab- section. Subtraction of mean neuron cytoplasmic signal measured in Ab- section ultimately reduces neuropil signal but this artifact does not affect measurements and corrections restricted to neuron cytoplasm as intended (Fig. 36).

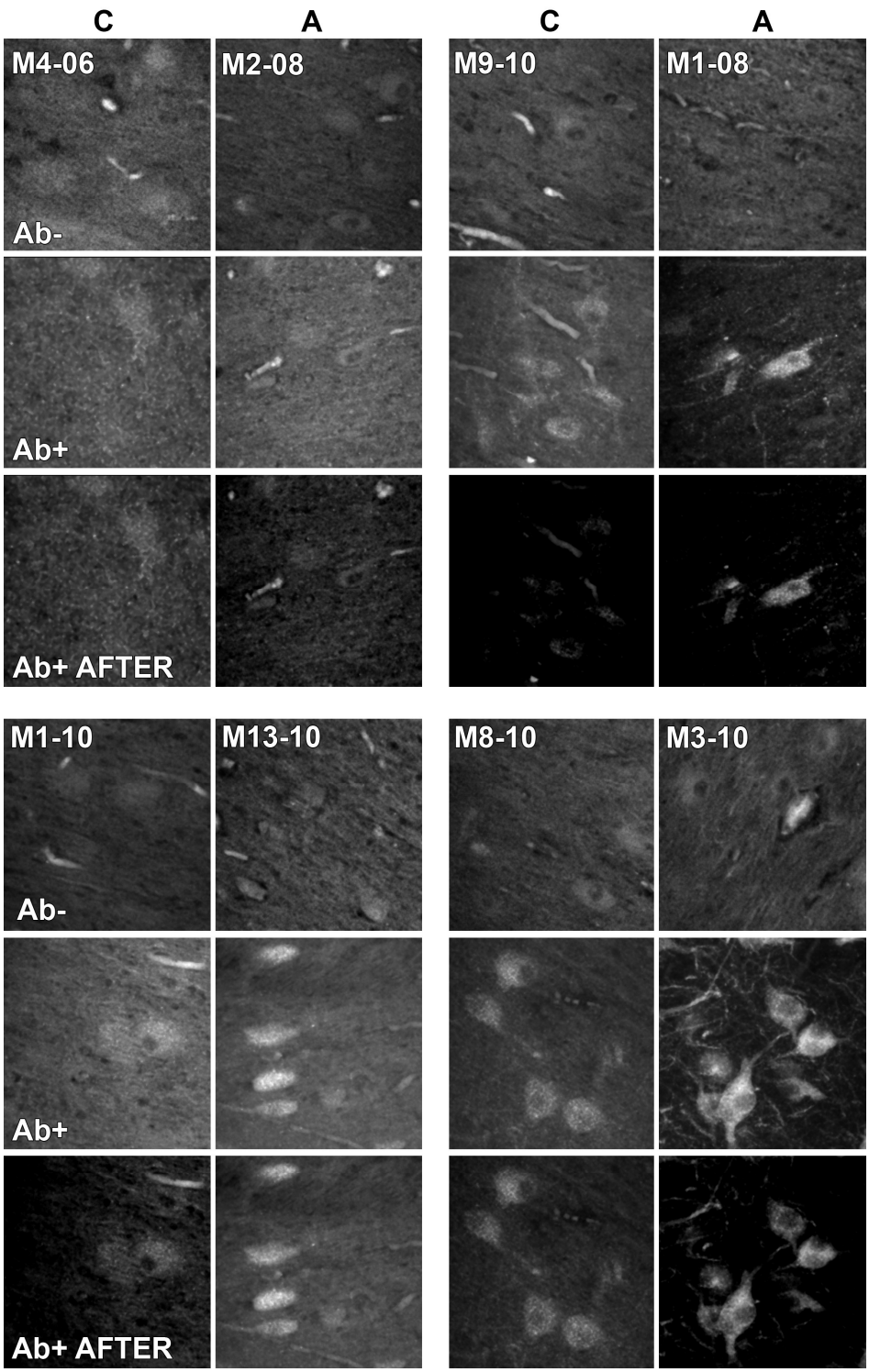

Fig. 36. External background subtraction. Subtraction of cytoplasmic background in DRN IF automatically affects neuropil fluorescence, but neuropil signal is not measured in this approach. Ab- (omission of primary and secondary ab), Ab+ (PH8 primary and secondary), Ab+ After (PH8 primary and secondary ab minus background). 40x, magnified.

In this method, the mean intensity of TPH immunofluorescence in neurons in autistic subjects was reduced in M2-08 case by 48%, but increased by 105%, 249% and 90% ($p<0.001$) in three autistic subjects (M1-08, M13-10, and M3-10, respectively) in comparison to age-matched control subjects (Figs. 37-39).

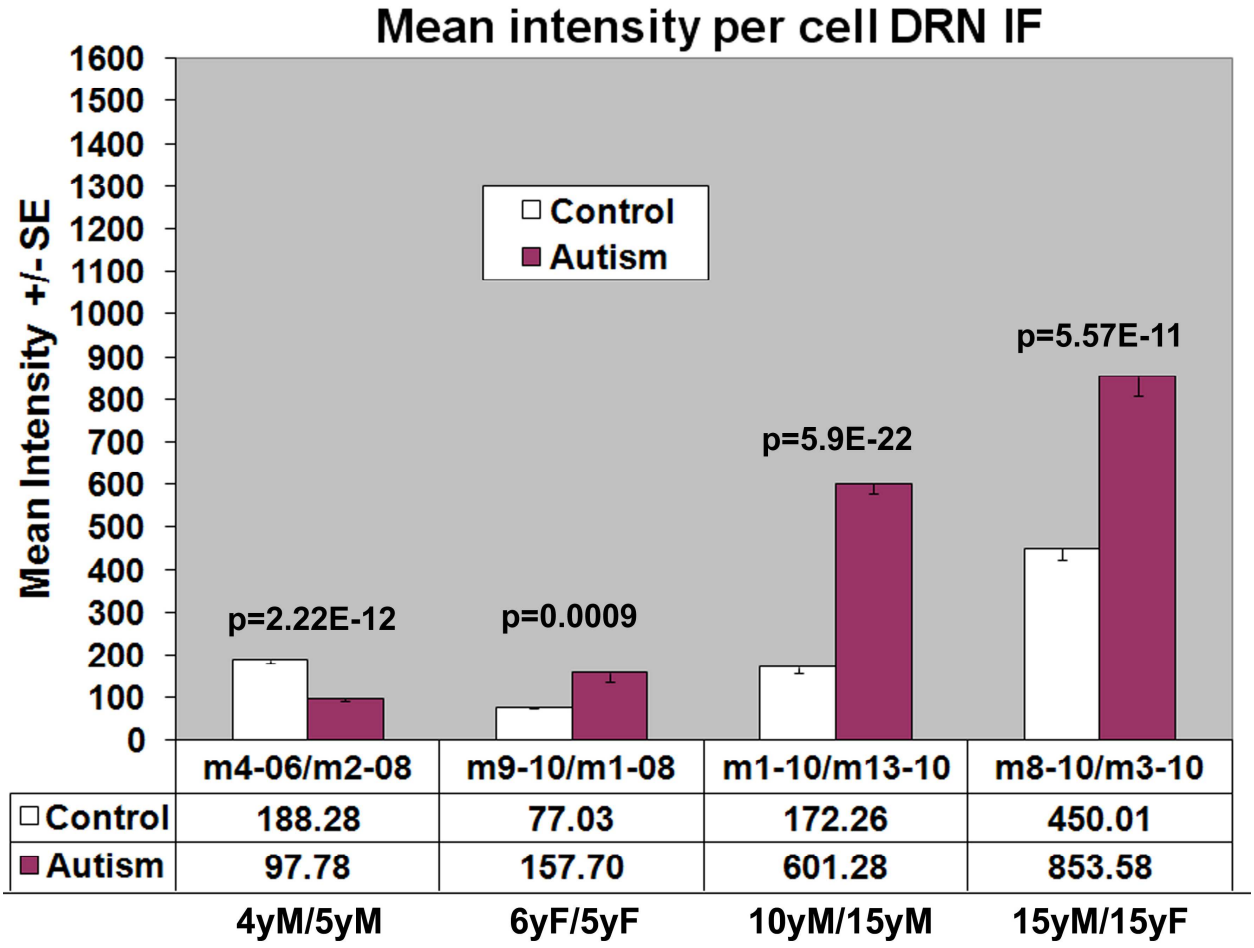

Fig. 37. Mean neuron soma TPH IF after external background subtraction (bar graph). Mean soma intensity results of application of external background subtraction in 8 examined cases. Significant signal increase in 3 out of 4 autistic cases.

Immunofluorescence within cytoplasm of one idiopathic autism case (M13-10) and in autistic subject with dup15 is much stronger than in third autistic subject (M1-08). The

immunofluorescence in autistic subject M2-08 is the lowest in comparison to all autistic subjects and reflects most likely permanent neuronal injury caused by hypoxia during fetal life (Fig. 38).

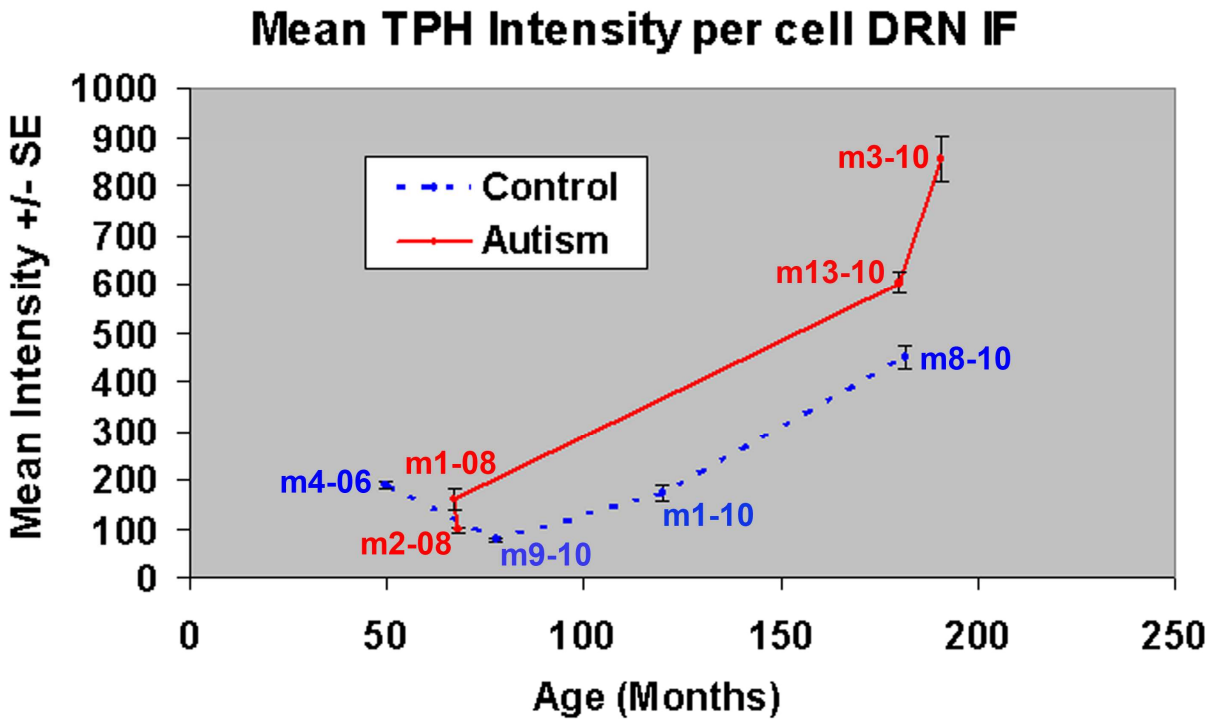

Fig. 38. Mean neuron soma TPH IF after external background subtraction (line graph). Graph reflects increase of signal in both older autistic subjects in comparison to two younger subjects. Increase in control group is observed only in 15 year old control, whereas 3 younger controls are in the same range of TPH fluorescence. M4-06: 4y M, M2-08: 5y M, M9-10: 6y F, M1-08: 5y F, M1-10: 10y M, M13-10: 15y M, M8-10: 15y M, M3-10: 15y F

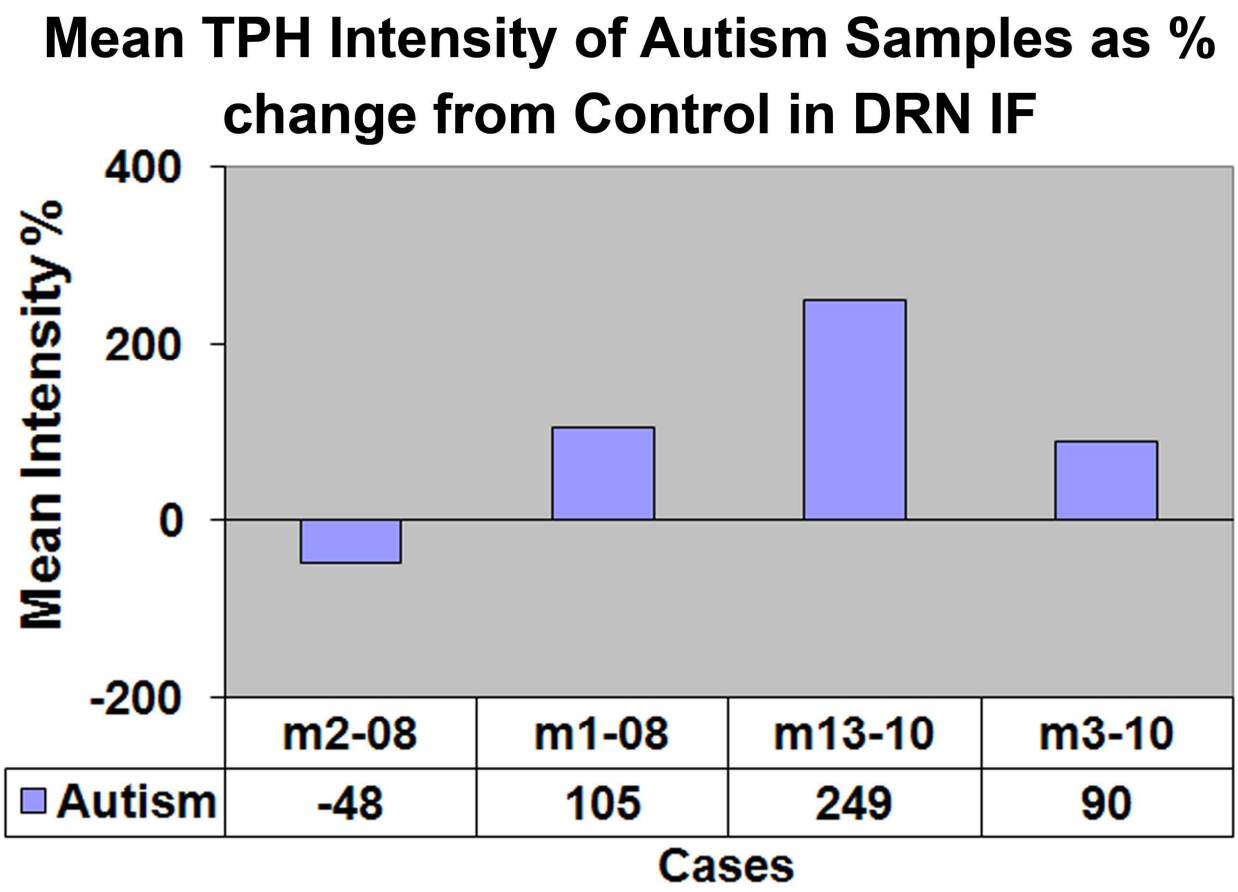

Fig. 39. Mean neuron soma TPH IF in autistic subjects as percent change from control after external background subtraction. The increase in autistic subjects is almost identical in M1-08 and M3-10 (105% and 90% respectively). The increase by 249% in M13-10 and decrease by 48% in M2-08 reflect expected significant interindividual differences and may explain different patient responses to treatments.

In this method, the average soma intensity per group measured 219 arbitrary units for the control group and 518 arbitrary units for the autistic group. There was a significant increase in the autistic group ($P < 0.001$). (Fig. 40)

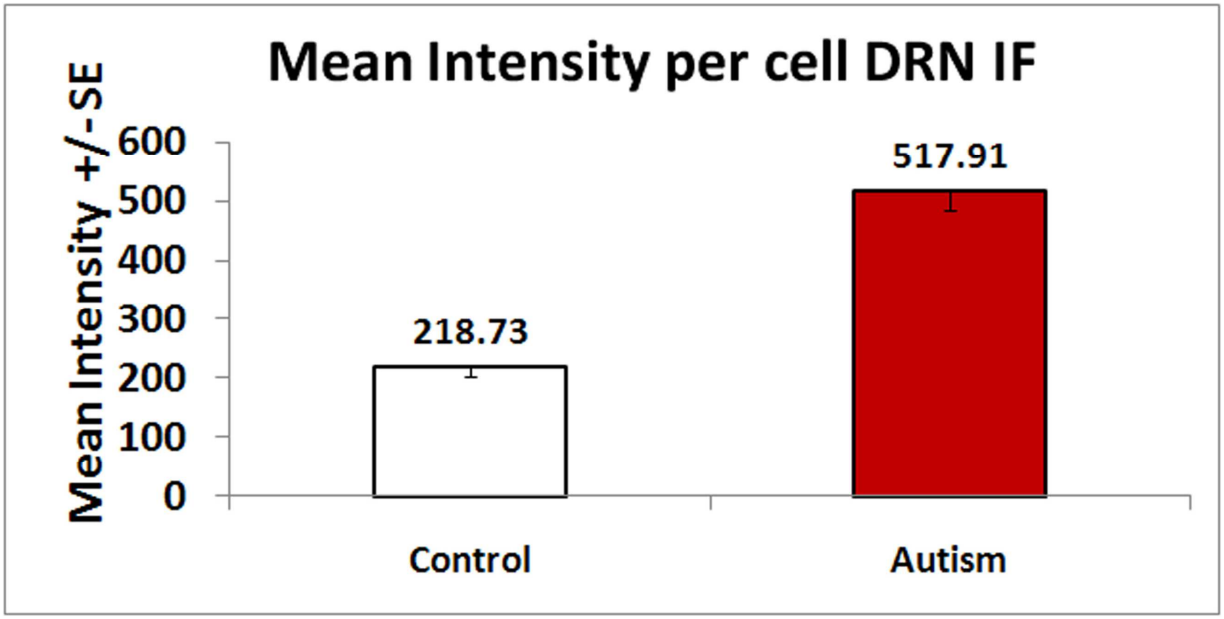

Fig. 40. Increase in mean cell TPH IF in autistic group after external background subtraction. The graph illustrates the general trend in examined group of autistic subjects.

The Spearman correlation coefficient for the external background correction approach measured 0.4 for the control group and 0.8 for the autistic group.

4.7. Abnormal neuron soma volume in autistic subjects

Reduced size of neurons in the cerebral cortex, subcortical structures, and in the brainstem is a commonly reported developmental defect observed in autism. Increased size of neurons in the inferior olive in the brainstem of 9 to 12 year old and decreased size in 22 to 29 year old autistic subjects were reported by Bauman and Kemper (1994). However, these studies were not performed with unbiased morphometric methods. The majority of individuals diagnosed with ASD demonstrate some degree of auditory dysfunction ranging from deafness to difficulty listening with background noise (Greenspan and Wieder 1997, Tomchek and Dunn 2007) suggesting dysfunction of the lower auditory brainstem and disrupted encoding of simple sounds. Kulesza's study of the auditory system in the brainstem of autistic subjects revealed

reduced size of neuron soma in the medial superior olive (Kulesza and Manguanay 2009) as well as a neuronal deficit and reduced neuron size in the superior olivary complex (Kulesza et al. 2011). The human superior olivary complex includes two principal nuclei, the medial and lateral superior olives, which have essential roles in sound localization (Kulesza 2007).

Defects of growth of neurons in the brain cortex, cerebellum and in the brainstem superior and inferior olives suggest that other brainstem nuclei, including raphé nuclei, may be affected by developmental alterations.

Application of the Nucleator probe revealed only small interindividual differences in mean volume of neuronal soma in the dorsal raphé nucleus of control subjects: 10,067 μm^3 (M4-06), 9,573 μm^3 (M9-10) and 10,558 μm^3 (M1-10). The volume of neuronal soma was much less in the three autistic subjects: 7,828 μm^3 (M2-08), 7,920 μm^3 (M1-08), 7,319 μm^3 (M13-10) (Fig. 41). The mean volume of neuron soma in dorsal raphé nuclei was less in autistic subjects by 24% (7,689 μm^3) than in control group (10,066 μm^3) ($p<0.006$) (Fig. 42). P values in pairs were: M4-06/M2-08: 1.35E-11, M9-10/M1-08: 0.0007, M1-10/M13-10: 1.02E-14.

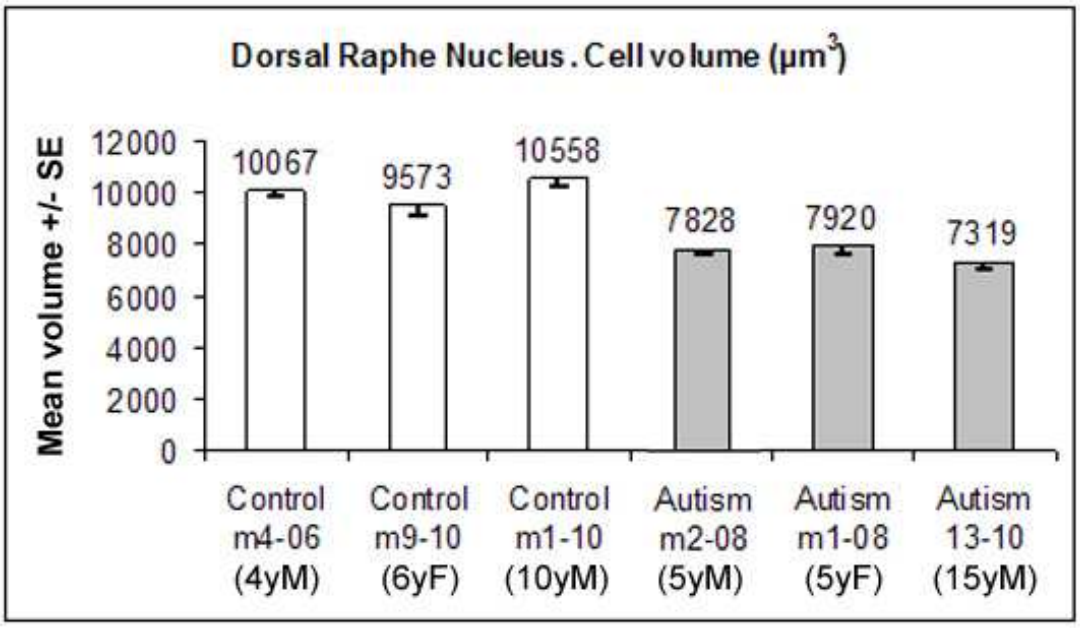

Fig. 41. **Individual characteristics of neuron volume deficit in DRN.** Application of Nucleator revealed lower mean volume of PH8-positive neurons soma in DRN of all three examined subjects and small interindividual differences in DRN neuron volume within control and autistic groups.

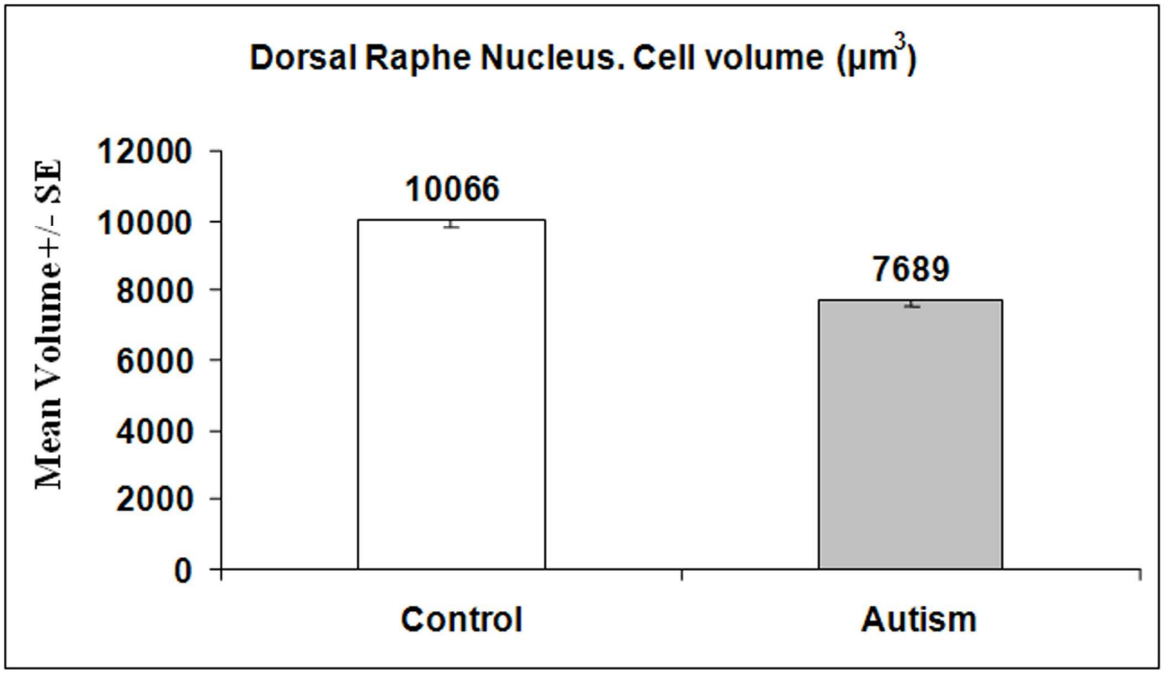

Fig. 42. Mean neuron soma volume deficit in autistic subjects. Consistent reduction of neuron soma volume in all three subjects allows generalization of individual observations. Mean neuron soma volume reduced on average by 24% reflects developmental neuron growth defect in all three examined autistic subjects regardless of clinical differences.

A histogram of frequency distribution shows that the volume of 77% of neurons in the DRN of autistic subjects is less than 10,000 μm^3, whereas in control subjects only 53% of neurons are less than 10,000 μm^3 (cumulative %) (Fig. 43).

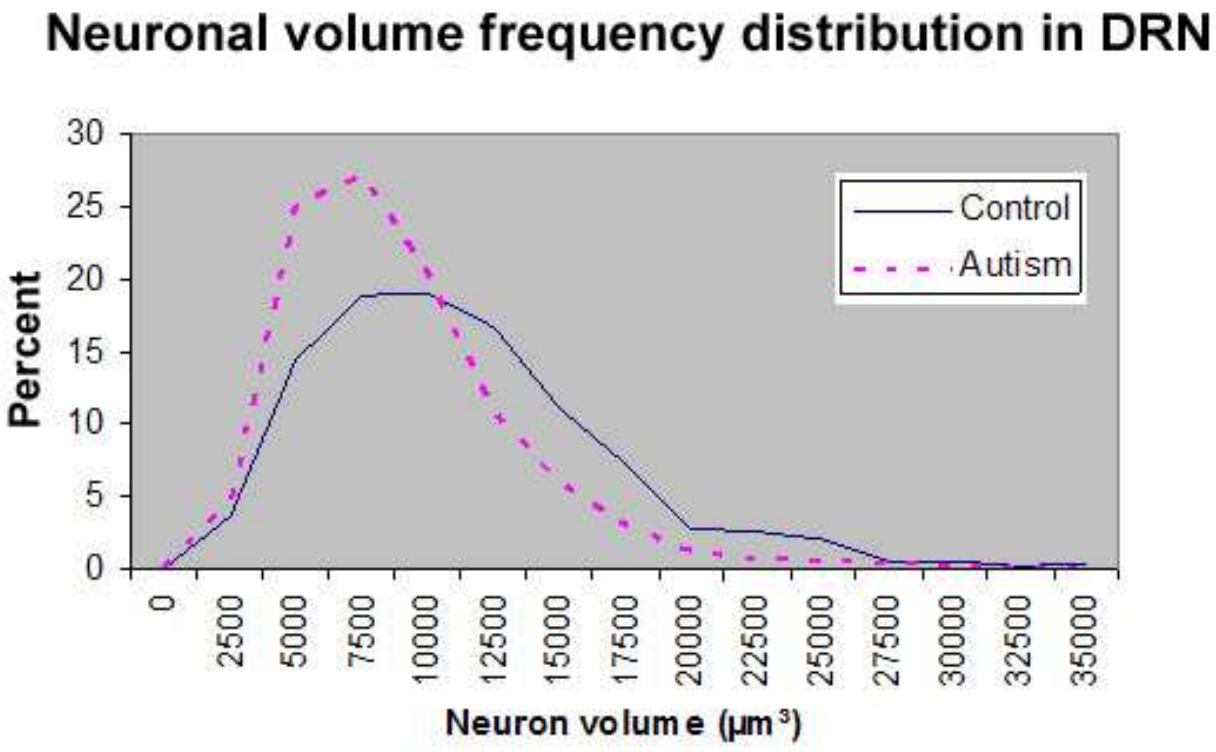

Fig. 43. Neuronal volume frequency distribution in DRN in control and autistic subjects. The graph illustrates a shift of a large percentage of autistic DRN neurons to a smaller than control group volume.

4.8. Numerical density of PH8-positive neurons

Increase in the number of neurons in the prefrontal cortex by 67% (Courchesne et al. 2011) but reduced number of neurons in the fusiform gyrus (van Kooten et al. 2008) and in the amygdala (Schuman and Amaral 2006), as well as reduced number of Purkinje cells (Bailey et al. 1998, Fatemi et al. 2002, Whitney et al. 2008, 2009) and neurons in the superior colliculus

(Kulesza et al. 2011) suggest that defects of brain development may include a developmental deficit and/or defects of apoptosis regulating size of neuronal populations in early childhood. Detection of an enhanced level of cytoplasmic TPH required evaluation of the number of neurons in raphé nuclei to determine raphé capacity to produce serotonin.

In control subjects, the mean numerical density in the dorsal raphé nucleus was 5,207/mm^3, whereas numerical density in autistic subjects measured 4,852/mm^3. These values were not statistically different (Fig. 44).

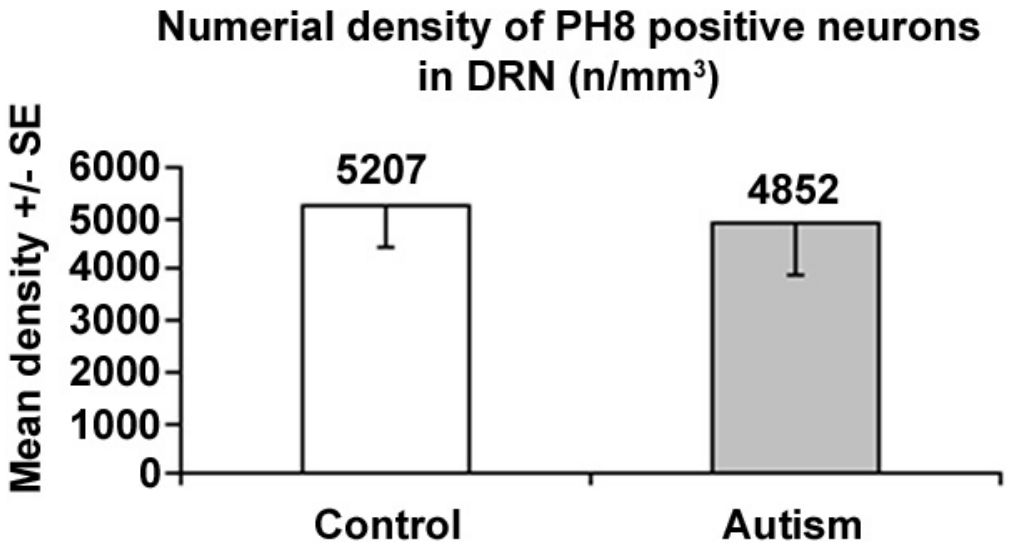

Fig. 44. Numerical density of PH8 (+) neurons in DRN of control and autistic subjects. No significant difference in numerical density of PH8-positive neurons in DRN between control and autistic group was seen.

5. DISCUSSION

5.1. Tissue preservation for raphé studies in autism

Application of clinical, pathological, and technical inclusion and exclusion criteria resulted in reduction of the autistic group from 9 to 4 cases and control group from 6 to 4 cases (four age- and gender-matched pairs). Due to a partial lack of the caudal complex of nuclei (magnus, pallidus and obscurus) caused by inappropriate brainstem dissection during autopsy, the study was concentrated on three anterior (CLN, DRN, and MRN) nuclei, and then limited to the DRN for reasons given. Due to postmortem degradation of serotonin, the project was limited to immunocytochemical detection of TPH, SERT and SMI312. The need for numerous modifications reflects research limits in the raphé serotonergic system in routinely formalin fixed brain of autistic subjects.

Progress in brainstem research, especially research on raphé nuclei of autistic and control subjects is limited by:

a. A very low number of postmortem brain donations of autistic subjects of any age;

b. A limited number of pediatric control donations;

c. Distribution of brain samples to many unrelated projects resulting in lack of material for global studies of serotonergic system abnormalities including those of raphé nuclei, and target structures regulated developmentally and functionally by raphé nuclei originating serotonin;

d. Application of brainstem dissection protocols designed for neuropathological diagnosis (midsaggital or transverse cut) that result in loss of anatomical integrity of the brainstem's serotonergic system.

Numerous studies indicate that alterations are raphé subregion- specific (Bonkale et al. 2004, 2006, Underwood 2004, 2007) but incomplete brainstem samples restrict research on disorder-specific topographic differences in the type and severity of pathology.

The optimal protocol of brainstem preservation for study of raphé nuclei requires:

a. Preservation of the entire brainstem from the anterior pole of the substantia nigra (anterior cut) to about 2 mm below the inferior olive (posterior cut);

b. Prevention of brainstem shape distortion during fixation and dehydration, and

c. Precise orientation of the long axis of the brainstem during serial section cutting.

Correction of routine protocols of brainstem preservation would provide material for quantitative studies of architecture of raphé nuclei in (a) normal development, maturation and aging, and (b) abnormal development, maturation and aging of autistic subjects.

Because of these limitations only a few complex studies of all human raphé nuclei have been accomplished and many were a result of cooperation of a few researchers from Australia and Switzerland using the same material (Stone et al. 1987, Baker et al. 1990, 1991ab, 1996, Törk and Hornung 1990, Halliday et al. 1993). They provided a comprehensive characterization of human raphé anatomy and cytoarchitecture in an unaffected brain but they were performed on a few samples preserved specially for the study of the brainstem. The most fundamental report,

which included anatomical and cytoarchitectonic parcellation of raphé nuclei, some morphometric procedures and a 3D raphé reconstruction, was based on examination of a single brainstem stained with PH8 (Törk and Hornung 1990). Due to similar technical limitations, the majority of recent studies are restricted mainly to dorsal raphé nuclei or a single raphé nucleus. In some studies only a few sections were used to compare affected and unaffected subjects (Baker et al. 1991ab, 1996, Halliday et al. 1993, Bonkale et al. 2004, 2006, Underwood et al. 2004, 2007).

In spite of hundreds of reports indicating that the serotonergic system is affected in autism, the alterations in raphé nuclei of autistic subjects are not studied yet. Therefore, this first study of raphé in autism required focus on obstacles limiting research of raphé in autism and methods of addressing the major restrictions. Technical problems addressed in this project included: use of PEG-protocol for brainstem embedding and cutting of 50-μm-thick serial sections, standardization of free floating section staining and immunostaining for stereological evaluation, application of stereological protocols for raphé studies, and standardization of immunofluorescence-based quantitative image analysis to detect autism associated developmental changes.

Therefore this study was focused on (1) improvement of raphé research design and implementing unbiased quantitative methods for detection of developmental changes and (2) evidence of structural and chemical abnormalities in raphé of 5 to 15 year old autistic subjects.

5.2. Justification for concentration on interfascicular nucleus.

Dual serotonergic innervation of human forebrain. Based on degeneration studies of raphé nuclei in the cat brainstem, Brodal et al. (1960) postulated that the dorsal raphé has

massive projections to the forebrain. Application of tritiated amino-acids (Azmitia and Segal 1978, Bobillier et al. 1976) for tracing of ascending raphé projections revealed that the dorsal and median raphé nuclei form two major bundles of fibers projecting to the forebrain: the bundle detected in the central gray matter and the second bundle detected in the ventral part of the tegmentum. Kosofsky and Molliver's (1987) studies of the rat serotonergic ascending fibers revealed that the fiber systems emerging from the dorsal and median raphé nuclei are morphologically different. Detection of fine axons with small fusiform varicosities emerging from the dorsal raphé and axons with large and round varicosities emerging from median nucleus suggests that these structural differences reflect presence of two parallel but functionally different serotonergic subsystems (Mulligan and Törk 1988). Cortical nonpyramidal neurons are the target of serotonergic fibers with large round varicosities (Mulligan and Törk 1988). Different response of these two types of fibers to neurotoxic compounds reflects structural, biochemical and functional differences in projections from dorsal and medial raphé nuclei. A dual innervation of the human cortex has been confirmed by Törk and Hornung's (1987) study of human biopsies and Kosofsky and Kowall (1989) study of human postmortem tissues.

The role of the interfascicular nucleus (dorsal division of the nucleus centralis superior) in brain serotonergic innervation. This study is concentrated on the interfascicular nucleus. Raphé nuclei form a superior group that mainly projects to the forebrain and an inferior group that projects to the spinal cord (Dahlstrom and Fuxe 1964). The dorsal raphé nucleus and the nucleus centralis superior are the main nuclei within the superior group. Nucleus centralis superior has two divisions: dorsal division (synonymous with interfascicular nucleus) and medial division (synonymous with the median raphé nucleus) (Azmitia 2012).

In rat, the fibers from the medial division of the nucleus centralis superior travel in the medial forebrain bundle (MFB) and innervate medial nuclei of the thalamus, septum, medial cortex and upper hippocampus (Azmitia and Segal 1978).

The fibers from the interfascicular nucleus (dorsal division of the nucleus centralis superior) travel in the lateral forebrain bundle (LFB) and innervate lateral regions of the hypothalamus, amygdala, striatum, frontal cortex and lower hippocampus (Azmitia and Segal (1978). Detection of fine axons with small fusiform varicosities emerging from the dorsal raphé (Mulligan and Törk 1988, Törk and Hornung 1990) suggests that the studied neuronal population in the interfascicular nucleus is contributing to one of two parallel serotonergic systems innervating key structures involved in all three diagnostic autism domains. A parallel study of the median nucleus would characterize the pattern of changes of the second serotonergic subsystem and its contribution to the autistic phenotype.

In addition to the role of the DRN IF in innervation of target structures related to autism diagnosis, the nucleus was chosen based on its characteristic cell orientation parallel to the midline, as well as its ease of delineation- being bordered on three sides by non raphé serotonergic neurons. Scarcity of tissue was another element which limited the choice of study material.

5.3. Distribution of TPH and SERT in confocal microscopy

In the examined material immunolabeling with PH8 antibody revealed intense immunofluorescence in the neuron soma. Lack of colocalization of TPH with axonal neurofilament marker (SMI312) in projections and presence of TPH in SMI312-negative processes demonstrates presence of TPH in neuron dendrites but not in axons in the particular

material studied. Ultrastructural studies revealed that TPH is diffusely distributed in raphé neuron cytoplasm. TPH localization in association with membranes of endoplasmic reticulum and Golgi apparatus possibly reflects the sites of this protein's synthesis. In processes in raphé nuclei the enzyme is primarily associated with microtubules (Joh et al. 1975). The association of both tryptophan hydroxylase and tyrosine hydroxylase with microtubules suggests transport of these enzymes from cell body (site of synthesis) to axons (Pickel et al. 1975). However, in contrast to well detected TPH in soma, potential axonal TPH appears to be masked and does not have an immunocytochemically detectable equivalent as shown in results.

It has long been believed that serotonin is released and taken up exclusively at the synaptic junction (synaptic neurotransmission). However, in the past decade research has provided evidence that serotonin reuptake is not restricted to the synaptic junction, but occurs at perisynaptic sites and along the axonal membrane. This study of serotonin transporter distribution in human raphé nuclei indicates that SERT detected with mAb ST51 is present in several clusters of granular material in cell soma that may correspond to endoplasmic reticulum and/or Golgi apparatus. A small amount of immunoreactive material is detected in the cellular membrane in neuron soma and a large amount in dendrites and axons. Confocal microscopy with SMI312 selectively detecting axonal neurofilaments and ST51 detecting SERT demonstrates transporter in the axolemma. A merging of fluorescent images results in focal overlap but proximity rather than a real colocalization is responsible for this yellow fluorescence. These results are consistent with ultrastructural studies demonstrating the majority of SERT in the membrane of axons (on the cytoplasmic site of axolemma), and in the membrane of axon varicosities but not in the axoplasm. Presence of a significant portion of SERT outside synaptic junctions suggests that SERT is involved in serotonin level regulation through extrasynaptic

(volume) transmission (Zhou et al. 1998). In situ hybridization studies in human (Austin et al. 1994, 1999), rat (Blakely et al. 1991, Fujita et al. 1993) and cat (Charnay et al. 1996), and immunocytochemical studies of animal brainstem (Qian et al. 1995, Sur et al. 1996) indicate that raphé neurons express both serotonin transporter messenger RNA and protein. Presence of SERT in the cell perikaryon and perinuclear enhancement of SERT immunoreactivity, similar to those in human neurons, has been reported in rat raphé nuclei (Sur et al. 1996). The somatic staining around unstained cell nucleus extends into the dendritic tree of rat raphé neurons (Qian et al. 1995). Immunoreactivity with mAb ST51 within the cell cytoplasm, especially in the perinuclear area, known as the location of the cell protein synthesis apparatus in rough endoplasmic reticulum, processing in smooth endoplasmic reticulum and Golgi apparatus, may correspond to the site of SERT synthesis before transport to the cell soma, dendritic and axonal membranes. The studies of rat brain show a pattern of SERT expression in raphé nuclei similar to that obtained by labeling adjacent sections with 5-HT antisera (Qian et al. 1995).

Microdialysis reveals extrasynaptic serotonin in the brain (Auerbach et al. 1989, Matos et al. 1992). Serotonin released in synapses spills out of the synaptic cleft and diffuses away from synapses to distances up to 20 μm, several times farther than diffusion of dopamine (Garris et al. 1994), glutamate and GABA (Clements 1996). Only a portion of serotonin is picked up by perisynaptic SERT (Zhou et al. 1998), whereas the majority is picked up by axonal SERT, including SERT of axonal varicosities. It may suggest that axonal SERT has a limited role in regulation of serotonin synaptic transmission but may play a major role in recollecting and conserving serotonin which has diffused from the synaptic cleft.

Enhanced immunofluorescence corresponding to increased levels of tryptophan hydroxylase per cell suggests that small, immature neurons may produce disproportionally large

amount of serotonin. One may speculate that it can result in enhanced levels of extracellular serotonin in autistic children.

An attempt was made at measuring the intensity of fluorescent SERT staining per region of interest (randomized areas of raphé subnuclei). However, all SERT immunopositive material cannot be outlined such as with PH8 stained cell bodies. SERT is present in numerous neuronal processes and in a small amount in cell body cytoplasmic membrane. There are also issues with strongly reacting blood vessels with SERT positive platelets, in addition to all the tissue and background related problems faced with PH8.

5.4. Interindividual differences

Detection of a combination of interindividual differences (reflecting etiological, clinical and pathological heterogeneity) and common denominators which reflect the mainstream pathology regardless of differences between examined subjects are the main findings which require modifications in research design in the future. Differences in the clinical phenotype and pathological heterogeneity of changes in raphé in the four examined autistic subjects suggest that in a larger group, at least 3 subpatterns of changes can be expected. They will reflect (a) pathology in idiopathic autism without detectable genetic and/or epigenetic etiology (illustrated by changes in 2 subjects examined: M1-08 and M13-10), (b) pathology linked to epigenetic factors active during in utero development (one subject: M2-08), and (c) pathology linked to dup15 (one subject: M3-10). Duplications of chromosome 15q11-q13 account for approximately 0.5 to 3% of ASD and are considered the single most common identifiable cause of autism (Schroer et al. 1998). Clinical studies indicate that 69% of individuals with dup(15) are diagnosed with autism, and most is associated with maternal origin of dup(15) (Rineer et al.

1998). The review of 107 cases of dup(15) revealed that microcephaly is more common than macrocephaly but both are reported (microcephaly in 17% and macrocephaly in 3%) (Schroer et al.1998). In a group of 126 children with idiopathic autism, 15% of subjects were diagnosed as microcephalic (Fombone et al. 1999). The examined dup(15) case's (M3-10) low brain weight (1,125g) qualified this subject as microcephalic.

Analysis of power indicated that a minimum group size of 5 is required in morphometric studies of TPH immunoreactivity in raphé nuclei in alcoholics (Underwood et al. 2007). However, the link between type, topography, and severity of serotonergic system alterations and numerous behavioral and neurological abnormalities defining the subject's phenotype can be determined only in large group postmortem studies. The list of these most common clinical cofactors includes: intellectual deficits defining low to high functioning autism (Mazzone et al. 2012), prevalence of seizures, significant differences in level of anxiety, aggression, self-injurious behavior, depression, attention disorder, sleep pattern alterations, sensory abnormalities, and common medications often targeting the serotonergic system, including selective serotonin reuptake inhibitors (Sasayama et al. 2009, Shanahan et al. 2011, Kolevzon et al. 2010, Nakamura et al. 2010, King et al. 2009). They may all contribute to inter-individual differences in the raphé subregion and raphé global alterations detected in postmortem studies as observed in depression, psychoses or alcoholism (Halliday et al. 1993, Baker et al. 1996, Underwood et al. 1999, 2004, 2007, Boldrini et al. 2005, Bonkale et al. 2004, 2006).

Another major cofactor are gender-specific differences in serotonergic regulation during development (Chandana et al. 2005; Chugani et al. 1999), combined with a 52% higher rate of 5-HT biosynthesis in the male over female brain (Nishizawa et al. 1997), and the increased susceptibility of males to early insults imposed by elevated levels of 5-HT. These may contribute

to the four-fold higher propensity of males to develop autism as compared to females. A higher rate of serotonin biosynthesis in the male might be reflected in a higher level of TPH in control and autistic males.

5.5. Spectrum of morphological developmental abnormalities

This study of raphé nuclei in four autistic subjects suggests that the spectrum of morphological developmental defects includes:

- Enhanced TPH immunoreactivity in neuron soma
- Reduced volume of neuron soma
- Clinical and pathological heterogeneity

5.5.1. Enhanced TPH immunoreactivity in neuron soma

Morphometric methods estimating the volume of neuronal body and TPH immunoreactivity are commonly used methods of detection of disease-associated alterations. However, different protocols of tissue preservation, immunostaining and estimating TPH immunoreactivity may contribute to differences between published results. The most complex methodology has been developed by three groups including Baker et al. (1996) Underwood et al. (1999, 2004, 2007), and Bonkale et al. (2004, 2006) to study pathology in depression, psychoses and alcoholism. Serotonin is implicated in the regulation of alcohol preference and intake in humans (Underwood et al. 2004, Wong et al. 2003). Serotonin reuptake inhibitors decrease the desire to drink in a dose dependent manner (Cornelius et al. 1995, 1997, Naranjo and Brenner 1993). Selective increase of TPH-immunoreactivity was reported in neurons in dorsal raphé subnucleus using immunoautoradiography in alcohol-dependent depressed suicides (Bonkale et

al. 2006). A similar increase in TPH-IR in alcohol-dependent depressed suicides was detected by Underwood et al. (2007).

This raphé study revealed increased immunofluorescence of cytoplasmic TPH in autistic cases. Because tryptophan hydroxylase is the rate-limiting enzyme for serotonin biosynthesis, the observed increase in TPH immunofluorescence in neuron soma is considered a marker of an enhanced level of serotonin production and release. In autism, developmental alterations in different raphé nuclei with projections to different brain regions may contribute to differences in structural changes in target brain structures such as amygdala, caudate, putamen, globus pallidus, n. accumbens and different cortical regions reported in qualitative and morphometric studies (Bauman and Kemper et al. 2005, Courchesne et al. 2005a, Van Kooten et al. 2008, Schumann et al. 2004, Schumann and Amaral 2006). The relatively low level of PH8 immunostaining in M2-08 may reflect interindividual differences in genetic and epigenetic factors contributing to differences in the morphological and functional phenotype.

The pattern of higher TPH fluorescence in autism for 3 out of 4 studied pairs was seen in all background correction approaches utilized. There also appeared to be an increase in TPH signal intensity in neurons with increasing age. However, the study consisted of a limited number of cases with varying etiologies. Interindividual differences in this small group may account for an unknown amount of the observed differences. The patterns based on this small sample appear to be independent of sex of subjects, as pairs studied included both males and females in various combinations.

Several studies suggest that regional increase in TPH level in raphé nuclei is typical of psychiatric disorders. Serotonin dysfunction has been implicated in alcoholism, depression, and suicide. Bonkale et al. (2006) revealed a 46% TPH increase in the dorsal subnucleus of the dorsal

raphé in depressed suicide victims with alcohol dependence, while the increase in other dorsal subnuclei was not significant. However, tryptophan hydroxylase immunoreactivity was normal in dorsal raphé of depressed suicide victims (Bonkale 2004). Topography and severity of response to a toxic insult is species- and insult-specific. In rats chronically treated with alcohol, the number of tryptophan hydroxylase- positive neurons was decreased in the dorsal raphé (Casu et al. 2004, Jang et al. 2002). Similarly, these neurons were decreased in the DRN of subjects with chronic alcoholism and Wernicke's encephalopathy or Korsakoff's psychosis (Baker et al. 1996, Halliday et al. 1993). Bonkale et al. (2006) speculated that the increase in TPH-immunoreactivity in the dorsal subnucleus in depressed alcohol-dependent suicide subjects is an attempt to elevate TPH biosynthesis to compensate for reduced serotonin neurotransmission in specific cortical or subcortical terminal fields (Mantere et al. 2002, Underwood et al. 2004).

Morphometric methods of estimation of TPH expression in human raphé nuclei. Underwood (2007) examined raphé nuclei in 10 control subjects 17 to 74 years of age, and 9 alcoholic individuals 16-66 years of age. The brainstem was separated with a transverse cut at the anterior border of the superior colliculi, fixed in 10% formalin, cryoprotected and 50-um-thick sections were incubated with PH8 antibody diluted 1:50,000 for 7 days. The product of immunostaining was visualized with DAB. The subtraction of the area of the labeled neuron soma from the total area of immunolabeling resulted in the estimate of immunoreactivity corresponding to PH8-positive processes. Neuron number and the average size of neurons were similar in alcoholics and control subjects. However, the area occupied by PH8-positive processes was 2.2-fold greater in alcoholic individuals compared to controls suggesting that alcohol affects serotonergic system and causes neuron process sprouting. Moreover, optical density of TPH

reaction was 42% higher in alcoholic individuals than in control subjects (Underwood et al. 2007).

Autoradiographic method of estimating TPH –immunoreactivity in human raphé nuclei. Bonkale et al. (2004) estimated TPH immunoreactivity in dorsal raphé nuclei in depressed suicide victims brainstem obtained in the course of routine autopsies performed by a medical examiner. Two tissue blocks with midbrain/pons and caudal medulla blocks were frozen in isopentane and stored at –80C. 20 μm-thick sections were cut and fixed in 4% paraformaldehyde. The TPH primary antiserum (PH8) was applied at 1:10,000 dilution for 48h. Sections were incubated with the [^{125}I] labeled secondary antibody and radioactivity was determined within individual DR nuclei. The quantitative autoradiographic measurements of TPH-IR from control subjects revealed regional differences in TPH-IR concentration among the DR nuclei: Drif>DRv>DRvl>DRd, but differences between depressed and control subjects were found not significant (Bonkale et al. 2004). However, the study of depressed suicide victims with alcohol dependence revealed a selective significant increase in TPH-IR levels (by 46%) in the dorsal subnucleus when compared with controls.

These results indicate that abnormalities in 5-HT biosynthesis in the brain of depressed alcoholic suicide subjects are restricted within distinct regions of the DR (Underwood et al. 1999, Bonkale et al. 2006).

Methods applied in this study of raphé nuclei in autism. The study of TPH immunofluorescence was concentrated on the interfascicular nucleus. Within the dorsal raphé, the ventrolateral and interfascicular nuclei contain the greatest number of tryptophan hydroxylase mRNA-positive neurons (Austin and O'Donnell 1999). Moreover, localization of

the interfascicular nucleus between the left and right medial longitudinal fasciculus reduces the risk of incorrect delineation of the border of ROI.

In contrast to Bonkale and Underwood protocols, formalin fixed as opposed to frozen tissue was used in this study. The brainstem was embedded in PEG and cut into 50-µm-thick sections in a transverse plane. Antigen retrieval at 65C in 2x SSC buffer in free-floating sections was applied. TPH was detected with mAb PH8 diluted 1:5000 and secondary antibody linked to fluorochrome (Alexa 555). Detection of PH8 immunofluorescence was a reflection of TPH distribution.

At 40x, four image stacks distributed systematically in one column covered almost completely one half of the IF nucleus. The total thickness of the stack was 15µm and corresponded to 15 images per stack. The single image area was selected to have 10+ neurons for TPH-immunoreactivity evaluation. The volume of individual stack was approximately 170 larger than the average neuron volume. Fluorescence intensity was measured per neuron soma after outlining the soma of each neuron with cell nucleus exclusion. Therefore, individual neuron soma PH8 immunoreactivity could be considered a measure of individual neuron involvement in 5-HT synthesis at the time of tissue fixation. To perform measurements average projections were created from each stack.

Background subtraction. The intensity of background might be specific for each case due to postmortem changes, different time of tissue fixation in formalin, PEG exposure, and subtle differences in section immunolabeling in spite of rigorous standardization. Four approaches were tested to correct for background.

1. Across the board background subtraction
2. Subtracting background pair wise

3. Subtracting background individually

4. Cytoplasm background subtraction

The first three methods of background subtraction were based on background measured in the neuropil (outside of neuron soma). Subtraction of neuropil background distorted cytoplasmic TPH immunofluorescence measurements. Distortion is caused by measurement and subtraction of neuropil signal which is the equivalent of average signal/noise from astrocytes, microglia and oligodendrocyte bodies and processes; bodies, axons and dendrites of non-serotonergic neurons residing in the raphé nuclei- all artifacts related to formalin fixation by variable period of time and tissue exposure to PEG. All these factors become components of "background" to be subtracted from TPH-immunofluorescence in serotonergic neuron cytoplasm. The second type of distortion is associated with inability of detection and subtraction of neuron cytoplasmic signal, including neuronal lipofuscin autofluorescence. The fourth method eliminates these distortions.

Measurement of background in the cytoplasm of neurons in the region of interest in sections treated without primary and secondary antibody is the most specific. This method results in detection of neuron cytoplasm- specific type and strength of background. Among others, this background includes a measure of lipofuscin autofluorescence, therefore subtraction of signal from control section (not treated with antibodies) results in measure of cytoplasmic TPH immunofluorescene only.

Age and TPH intensity correlation analysis. Spearman's correlation coefficient was calculated for age and TPH intensity for both control and autistic groups in four background correction approaches. Spearman correlation analysis is a non-parametric approach and unlike Pearson correlation does not require a linear relationship between variables. The Spearman

correlation coefficient in this study ranged from 0.4 to 0.8, which might be suggestive of a weak to moderate correlation. However, since the sample is quite small (n=4 in each group), these correlation results should be considered only as indications of a general agreement between age and TPH intensity. Since only a perfect rank agreement would produce a significant result ($p<0.05$) using a sample of four, even strong rank correlations would be statistically insignificant.

5.5.2. Higher TPH immunoreactivity versus reduced neuron soma volume and unmodified neuronal numerical density

The decrease in neuron volume in studied autistic group is on the order of 24%, whereas the average increase in TPH fluorescence in autism in the four approaches including reversed case is +530% (equal background correction), +394% (pairwise background correction), +139% (individual background correction), and +99% (neither antibody background correction). Therefore, even if one were to make the argument that a smaller neuron concentrates the staining in a smaller space and this is the reason for the intensity increase, the average intensity increase is several times higher than the decrease in volume.

One may assume that increased cytoplasmic TPH immunofluorescence reflects enhanced serotonin synthesis in developmentally defective raphé neurons, an increased level of cytoplasmic and potentionally axonal serotonin, as well as enhanced serotonin level in target structures as shown by Azmitia et al. (2011a,b).

Moreover, the unchanged numerical density of neurons in the dorsal raphé nucleus, combined with ~24% reduction of neuron soma volume and increase of TPH expression in 3 subjects suggests that in the majority of autistic subjects TPH, and possibly serotonin, are

overexpressed and that in autism neuron soma volume is not a predictor of raphé neuron serotonin synthesis.

These data are the first indicator that reduced size of neuron soma reported in many brain regions is not equal to reduced neuron protein synthesis. However, this information can't be generalized and only specific protein estimates may define how synthesis of cell cytoskeletal proteins, receptors, and transporters are modified in autistic subject neurons. Cautious interpretation of results indicates that in some autistic subjects reduced neuron soma volume is paralleled by disproportional increase of TPH and possibly serotonin levels.

The lower than normal volume of DRN neurons detected in 3 autistic subjects 5 to 15 years of age examined in this project suggests that regardless of etiological, clinical, and pathological differences, alterations in neuron growth are a consistent feature of autistic children raphé neurons and are a marker of global encephalopathy associated with autism. One may expect that dynamic changes in neuron soma or permanent defects of raphé neuron growth will be reflected in patterns of structural and functional changes in target brain structures, altered function and their contribution to the autism clinical phenotype.

Several studies indicate that serotonin plays an important role in normal development of the central nervous system and that it induces neurogenesis and neuronal differentiation. As a trophic factor serotonin is involved in neuron growth and maturation in the brain cortex and subcortical structures (Buznikov 1984, Chubakov et al. 1986, Whitaker-Azmitia et al. 1991, 1996, Azmitia 2012). Therefore, developmental defects of raphé nuclei may result in secondary alterations of neurogenesis, differentiation and maturation with brain structure-specific functional changes.

5.5.3. Clinical and neuropathological heterogeneity

Examination of medical records of four subjects diagnosed with autism revealed clinical, genetic and epigenetic heterogeneity. Two subjects represented idiopathic autism without detectable genetic etiology (M1-08, M13-10). The youngest autistic subject (M2-08) represented autism with both a complex history of multiple disorders in the family suggesting genetic autism etiology, and complex history of fetal exposure to mothers medications and diseases suggesting contribution of epigenetic factors to autistic phenotype. The fourth subject (M3-10) represented a subpopulation of autistic subjects with known autism etiology (autism linked to dup15).

Unique pattern of developmental alterations in 5-year old autistic subject. The 5-year old autistic male's (M2-08) medical records and family medical history reveal complex and heterogeneous etiology and links between neuropathological changes and clinical manifestations of autism (Fig.32). He did not follow the trend seen in other autistic subjects. He had a striking deficit of TPH as shown in all tested pretreatments, antibody dilutions and times of incubation in colorimetric and fluorescence methods. The pattern of changes suggests that this is an example of an individual rather than group pathology. Regional pathology, rather than pathology affecting all raphé nuclei is consistent with numerous studies of alcoholism, depression, and suicidal behaviors (Young et al. 2008, Underwood et al. 2007). However, in this case pre- and postnatal exposure to noxius factors appears to be the cause of neuron injury, changes in cell biochemistry and most likely function.

He experienced immune system deficiencies such as infections (chronic ottitis media) and allergies (milk, soy, other food leading to frequent swelling, indicating immune system alterations). He displayed an abnormal gaze, possibly related to cerebellar floccular dysplasia

detected in postmortem study. His intellectual deficits could be related to defects of cellular migration and defects of cytoarchitecture detected in postmortem study as multifocal cortical dysplasia and hypocellularity. His frequent agitation, crying, reduced sensory response, and severe sleep disorder might be related to serotonergic system alterations, including region-restricted neuron loss or deficit, and tryptophan hydroxylase and serotonin transporter deficit.

His agitation required chronic treatment with prozac and valium, whereas severe sleep disorder required treatment with melatonin.

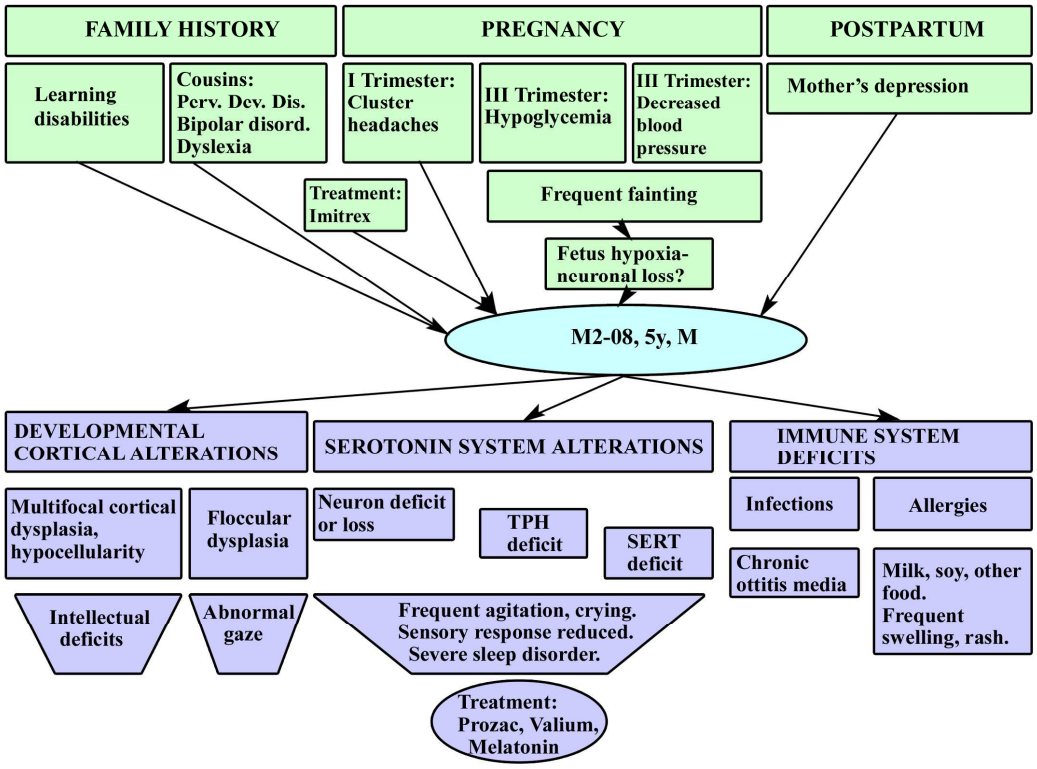

Fig. 45. Link between genetic factors, brain pathology, serotonergic system abnormalities and clinical phenotype. Genetic factors and epigenetic factors acting during all three trimesters appear to cause:
(a) developmental brain abnormalities with multifocal cortical dysplasia contributing to autistic phenotype and intellectual deficit;
(b) floccular dysplasia associated with abnormal gaze;
(c) serotonergic system pathology including deficit of tryptophan hydroxylase
(d) immune system deficits resulting in chronic infections and severe allergies.

The etiology of these clinical abnormalities might be linked to several mechanisms, including genetic and epigenetic factors. Family history consisted of pervasive developmental disorder, bipolar disorder, dyslexia in cousins and learning disabilities. The mother suffered from cluster headaches in the first trimester of pregnancy and was treated with Imitrex. In the third trimester she was diagnosed with hypoglycemia and decreased blood pressure resulting in frequent fainting. This suggests that the mother's hypoxia lead to fetus' hypoxia and hypoxia-related neuronal loss as well as distortion of neuronal networks with postnatal structural and functional consequences. Premature birth, at 37 weeks, was an indication that fetus development was affected by pregnancy complications. The mother's post partum depression was another sign of imbalance of mother's health during gestation and after delivery.

The potential links between mother's health during pregnancy and child autism are supported by other reports. Numerous gestation complications, mother's metabolic changes and/or psychological factors may increase risk for autism including: bleeding during pregnancy (Brimacombe et al. 2007), long labor (Glasson et al. 2004), pre-term and induced labor (Brimacombe et al. 2007), anxiety and fear (Beversdorf et al. 2005), sadness (Zhang et al. 2010), fear of abortion (Glasson et al. 2004).

Hypo- and hyperserotonemia in autism. Hyperserotonemia, identified as an increase in the serotonin level in blood platelets by 25% to 50% is a frequent finding in autism (Anderson 2002). The first report of hyperserotonemia in autism by Schain and Freedman (1961) was confirmed by other studies of blood serotonin in autism (Hanley et al. 1977, Anderson et al. 1990, Cook 1996, McBride et al. 1998, Mulder et al. 2004, Hranilovic et al. 2007, Melke et al. 2008). Clinical studies reveal that tryptophan depletion can worsen repetitive behaviors of autistic subjects (McDougle 1993). Imaging studies demonstrate signs of impairment of the

serotonergic system in autism (Chugani et al. 1997, 1999, Makkonen et al. 2008) and justify clinical applications of serotonin- enhancing drugs such as serotonin reuptake inhibitors (Mehlinger et al. 1990, McDougle et al. 1993, Fatemi et al. 1998, Kolevzon et al. 2006). However, lack of improvement or worsening of clinical status in the majority of patients (Brodkin et al. 1997, King et al. 2009, Williams et al. 2010) contradicts SSRIs application. The first postmortem study of serotonergic fibers (Azmitia et al. 2011ab) revealed an increase in the number of serotonin axons in forebrain pathways and in cortex of autistic donors. The detected signs of over-activity of the serotonergic system may explain adverse effects observed in clinical trials and suggest that use of serotonin antagonists may be a more advantageous therapeutic strategy (Azmitia et al. 2011ab).

However, there is no report characterizing serotonin level in raphé neurons of autistic subjects to fill the gap between imaging studies showing reduction in brain serotonin (Chugani et al. 1997, 1999) and histopathological studies showing an increase in serotonin transporter-positive fibers (Azmitia et al. 2011ab). This study of raphé nuclei of autistic subjects indicates that cells may have a smaller volume, decreased tryptophan hydroxylase (and probably serotonin) levels detected in one autistic subject, or significantly increased levels of tryptophan hydroxylase detected in three autistic subjects.

In the 5-year old autistic male (M2-08), the detected pattern of postmortem pathology indicates deficits of tryptophan hydroxylase, reflecting most likely hyposerotonemia in raphé nuclei, as well as in brain cortex and subcortical structures innervated by the altered anterior raphé nuclei. This pattern of developmental defects was strikingly different than in three other autistic subjects with signs of enhanced tryptophan hydroxylase level in raphé and most likely in projection areas in the cerebral cortex and subcortical structures. The pattern detected in these

three subjects may correspond to raphé and brain hyperserotonemia. Medical family history and clinical records of M2-08 suggest a link between severe and diverse insults during fetal development and appear to explain causes of severe clinical manifestations of autism on one hand and a unique pattern of morphological changes in raphé nuclei on the other hand. The detected diversity of clinical and postmortem observations in this small group of 4 autistic subjects appears to be a reflection of etiological, clinical, and neuropathological heterogeneity. Moreover, this diversity may explain the striking differences in response of autistic subjects to treatments targeting SERT.

Clinical differences in responses to selective serotonin reuptake inhibitors (SSRIs). SSRIs are used to reduce binding of serotonin to transporter. Azmitia (2011) demonstrated an increase in the number of serotonin-positive axons in cortex and pathways of autism patients which suggests that currently common use of serotonin enhancing drugs such as SSRIs in autism may not be the correct approach (Azmitia et al. 2011 a,b). DeLong reported that SSRIs enhanced learning and memory in a group of 2-7 year olds with idiopathic autism but individual treatment responses varied widely. Out of nearly 40 children, after continued fluoxetine treatment of mean duration 21 months, 30% had a very good response and were able to join regular classrooms. Another 30% had a good response although remained autistic. However, in 40% of treated autistic subjects, there was no improvement or significant negative response was observed, and treatment needed to be discontinued due to enhanced aggression, agitation, hyperactivity, or lethargy. Several other studies revealed positive response to selective serotonin reuptake inhibitors (Mehlinger et al. 1990, Fatemi et al. 1998, Kolevzon et al. 2006). However, Brodkin et al. (1997) reported adverse effects (seizures, agitation, constipation, weight gains) in 37% of 35 young adults treated with clomipramine for 3 months. Impulsiveness, decreased

concentration, hyperactivity, enhanced stereotypic behavior, and insomnia were reported after treatment with Citalopram (King et al. 2009). It may indicate that applied SSRIs in some patients enhance reuptake of serotonin in an already hyperactive serotonergic system leading to a negative patient response.

All the children studied by DeLong had a normal development until a time of regression in language, cognition, and social functions (1-3 years of age). In the group that had an excellent response, "vestiges of their condition remained". Excellent response meant appropriate social interactions, improvements in language, and normalized movement. In those with a negative response, changes for the worse were seen anywhere from immediately to months into treatment. In some cases both negative and positive changes were seen in the same individual. In certain cases there was no long-term benefit even though initially the patients seemed to respond well. Stopping of treatment usually meant a regression of symptoms, sometimes within weeks or months. There was no measure of whether they regressed below treatment baseline. Regression after discontinuation of SSRIs is an indication that treatment has a functional positive effect, but pathology which is the cause of functional alterations is intact and treatment does not have a permanent positive structural and functional outcome. Regression toward pretreatment baseline shortly after discontinuation of "successful" treatment suggests that (a) clinical improvement is transient and functional, (b) biochemical/structural changes in the serotonergic system are permanent, (c) they are the cause of clinical alterations and deficits, and (d) treatment does not correct structural/biochemical developmental alterations.

Signs of genetic diversity contributing to phenotype and response to treatment. In 21 children studied by DeLong, a family history of major affective disorder (bipolar or schizoaffective disorder or major depression) was found. In children whose family history

showed no psychopathology, 40% had excellent, 20% good, and 40% poor outcome. Of 10 children with a positive psychiatric family history not including major affective disorder, only one had a positive response. One patient with no positive outcome was quoted as responding with “increased nervous energy, increased obsessive behavior, increased frustration, decreased communication” (DeLong 1998).

6. CONCLUSIONS

1. The study of raphé nuclei of 5 to 15 year old autistic subjects revealed:
    a) Significant interindividual differences of the pattern of morphological changes, most likely reflecting contribution of genetic and pre- and postnatal alterations to postmortem detected changes.
    b) Increase in TPH immunoreactivity per cell body that appears to reflect increased level of serotonin in interfascicular nucleus.
    c) Reduced volume of neuron soma in DRN consistent with numerous reports published in past two decades demonstrating small neuron size in cerebral cortex, subcortical structures, and cerebellum in autistic subjects.

2. The study recognized several limitations of research on raphé nuclei of autistic subjects:
    a) Very low number of postmortem brain donations of autistic subjects of all ages;
    b) Limited number of pediatric control donations;
    c) Lack of brainstem samples with preserved anatomical integrity of brainstem serotonergic system due to routine methods of brainstem dissection in midsaggital or transverse plane designed for neuropathological diagnosis;
    d) Lack of material for global studies of serotonergic system abnormalities due to brain sampling for non-integrated projects.

Standardization of brainstem preservation, immunostaining and methods for quantitative analysis, especially immunofluorescence-based measurements of key proteins reflecting raphé structure and function, will contribute to detection and characterization of serotonergic system alterations in autism.

Diversity of detected alterations might be a reflection of genetic and/or epigenetic factors. One may expect that a study of the brainstem of 16 to 20 autistic subjects would identify patterns of interindividual differences and provide data for a preliminary subclassification of patterns according to genetic and epigenetic factors, gender and age, and clinical phenotype.

7. REFERENCES

Aitken AR, Törk I. Early development of serotonin-containing neurons and pathways as seen in wholemount preparations of the fetal rat brain. J Comp Neurol 1988, 274, 32-47

Akbari HM, Kramer HK, Whitaker-Azmitia PM et al. Prenatal cocaine exposure disrupts the development of the serotonergic system. Brain Res 1992, 572, 57-63

American Psychiatric Association. Diagnostic and Statistical Manual of Mental Disorders DSM-IV-TR. Washington, DC: American Psychiatric Association, 2000

American Psychiatric Association. DSM-5 development: autism spectrum disorder. Available at http://www.dsm5org/ProposedRevisions/Pagesproposedrevision.aspx?rid=94. 2012

Anderson GM, Freedman DX, Cohen DJ, Volkmar FR, Hoder EL, McPhedran P, Minderaa RB, Hansen CR, Young JG. Whole blood serotonin in autistic and normal subjects. J Child Psychol Psychiatry 1987, 28, 885-900

Anderson GM, Horne WC, Chatterjee D, Cohen D J. The hyperserotonemia of autism. Ann. NY Acad Sci. 1990, 600, 331-340

Anderson GM. Genetics of childhood disorders: XLV. Autism, part 4: Serotonin in autism. J Am Acad Child Adolesc Psychiatry 2002, 41, 1513-1516

Arango V, Mann JJ. Relevance of serotonergic postmortem studies to suicidal behavior. Int Rev Psychiatry 1992, 4, 131-140

Arato M, Tekes K, Tothfalusi L, Magyar K, Palkovits M, Frecska E, Falus A, MacCrimmon DA. Reversed hemispheric asymmetry of imipramine binding in suicide victims. Biol Psychiatry 1991, 29, 699-702

Assal F, Valenza N, Landis T, Hornung JP (2000) Clinicoanatomical correlates of a Fou rire prodromique in a pontine infarction. J Neurol Neurosurg Psychiatry 69: 697-698.

Auerbach SB, Minzenberg MJ, Wilkinson LO. Extracellular serotonin and 5-hydroxyindole acetic acid in hypothalamus of the unanesthesized rat measured by electrochemical detection: dialysate serotonin reflects neuronal release. Brain Res 1989, 499, 281-290

Austin MC, Bradley CC, Mann JJ, Blakely RD. Expression of serotonin transporter messenger RNA in the human brain. J Neurochem 1994, 62, 2362-2367

Austin MC, O'Donnell SM. Regional distribution and cellular expression of tryptophan hydroxylase messenger RNA in postmortem human brainstem and pineal gland. J Neurochem 1999, 72, 2065-2073

Azmitia EC, Segal M. An autoradiographic analysis of the differential ascending projections of the dorsal and median raphe nuclei in the rat. J Comp Neurol 1978, 179, 641-668

Azmitia EC, Gannon PJ. The primate serotonergic system: a review of human and animal studies and a report on Macaca fascicularis. Adv Neurol 1986, 43, 407-46

Azmitia EC. Serotonin neurons, neuroplasticity, and homeostasis of neural tissue. Neuropsychopharmacology. 1999, 21(2 Suppl), 33S-45S

Azmitia EC. Modern views on an ancient chemical: serotonin effects on cell proliferation, maturation, and apoptosis. Brain Res Bull 2001, 56, 413-424

Azmitia EC, Singh JS, Hou XP, Wegiel J. Dystrophic serotonin axons in postmortem brains from young autism patients. Anat Rec 2011a, 294, 1653-1662

Azmitia EC, Singh JS, Whitaker-Azmitia JM. Increased serotonin axons (immunoreactive to 5-HT transporter) in postmortem brains from young autism donors. Neuropharmacology 2011b, 60, 1347-1354

Azmitia EC. Serotonin. In: eLS. John Wiley & Sons, LTD: Chichester. 2012 1-12. DOI: 10.1002/9780470015902.a0000124.pub2

Bailey A, Le Couteur A, Gottesman I et al. Autism as a strongly genetic disorder: evidence from a British twin study. Psychol Med 1995, 25, 63-77

Bailey A, Luthert P, Dean A et al. A clinicopathological study of autism. Brain 1998, 121, 889–905

Baker KG, Halliday GM, Törk I. Cytoarchitecture of the human dorsal raphé nucleus. J. Comp Neurol 1990, 301, 147-161

Baker KG, Halliday GM, Hornung JP, Geffen LB, Cotton RGH, Törk I. Distribution, morphology and number of monoamine-synthesizing and substance O-containing neurons in the human dorsal raphe nucleus. Neuroscience 1991a, 42: 757-775.

Baker KG, Halliday GM, Halasz P, Hornung J-P, Geffen LB, Cotton RGH, Tork I. Cytoarchitecture of serotonin-synthesizing neurons in the pontine tegmentum of the human brain. Synapse 1991b, 7, 301-320

Baker KG, Halliday GM, Harper CG. Effect of chronic alcohol consumption on the human locus coeruleus. Alcohol Clin Exp Res 1994, 18, 1491-1496

Baker KG, Halliday GM, Krill JJ, Harper C. Chronic alcoholics without Wernicke-Korsakoff syndrome or cirrhosis do not lose serotonergic neurons in the dorsal raphe nucleus.Alcohol Clin Exp Res 1996, 20, 61-66

Banerjee P, Mehta M, and Kanjilal B. The 5-HT_{1A} Receptor: A Signaling Hub linked to Health and Emotional Balance. Frontiers in Neuroscience (CRC Press) (Ed. A. Chattopadhyay) (Series Ed. S.A. Simon, and M.A.L. Nicolelis) 2007, p133-155

Baranek GT, David FJ, Poe MD, Stone WL, Watson LR. Sensory Experiences Questionnaire: discriminating sensory features in young children with autism, developmental delays, and typical development. J Child Psychol Psychiatry 2006, 47, 591-601

Baron-Cohen, S. The cognitive neuroscience of autism. J Neurol Neurosurg Psychiatr 2004, 75, 945-948

Bartol TM, Land BR, Salpeter EE, Salpeter MM. Monte Carlo simulation of miniature endplate current generation in the vertebrate neuromuscular junction. Biophys J 1991, 59, 1290-1307

Bauman ML, Kemper TL. Histoanatomic observations of the brain in early infantile autism. Neurology 1985, 35, 866-874

Bauman ML, Kemper TL. Neuroanatomic observations of the brain in autism. In: The neurobiology of autism. Edited by M.L. Bauman and T.L. Kemper. John Hopkins Univ Press 1994, 119-145

Bauman ML, Kemper TL. Neuroanatomic observations of the brain in autism: a review and future directions. Int J Dev Neurosci 2005, 23, 183–187

Beitz AJ. Central gray. In: The human Nervous System. Ed. G. Paxinos. Academic Press, Inc., San Diego, 1990, 307-320

Bel N, Figueras G, Vilaro MT, Sunol C, Artigas F. Antidepressant drugs inhibit a glial 5-hydroxytryptamine transporter in rat brain. Europ J Neurosc 1997, 9, 1728-1738

Berner NJ, Grahn DA, Heller HC. 8-OH-DPAT-sensitive neurons in the nucleus raphe magnus modulate thermoregulatory output in rats. Brain Res 1999, 831, 155-164

Beversdorf DQ, Manning SE, Hillier A, Anderson SL, Nordgren RE, Walters SE, Nagaraja HN, Cooley WC, Gaelic SE, Bauman ML. Timing of prenatal stressors and autism. J Autism Dev Disord 2005, 35, 471-478

Bianchi P, Ciani E, Guidi S, Trazzi S, Felice D, Grossi G, Fernandez M, Giuliani A, Calza L, Bartesaghi R. Early pharmacotherapy restores neurogenesis and cognitive performance in the Ts65Dn mouse model for Down syndrome. Neurobiol Dis 2010, 30, 8779-8769

Björklund A, Hökfelt T. GABA and neuropeptides in the CNS. Part I, Elsevier, Amsterdam, 1985

Björklund A, Hökfelt T. Kuhar MJ. Neuropeptides in the CNS. Part II, Elsevier, Amsterdam, 1985

Blakely RD, Berson HE, Fremeau RT, Jr, Caron MG, Peek MM, Prince HK, Bradley CC. Cloning and expression of a functional serotonin transporter from rat brain. Nature 1991, 354, 66-70

Blessing WW, and Gai WP. Caudal pons and medulla oblongata. *In* "The Primate Nervous System, Part 1, Handbook of Chemical Neuroanatomy, Vol. 13, Eds: F. E. Bloom, A. Björklund, and T. Hökfelt, pp. 139–186. Elsevier, Amsterdam, 1997

Bobillier P, Seguin S, Petijean F, Salvert D, Touret M and Jouvet M. The raphe nuclei of the cat brainstem: A topographical atlas of their efferent projections as revealed by autoradiography. Brain Res 1976, 113, 449-486

Boldrini M, Underwood MD, Mann JJ, Arango MC. More tryptophan hydroxylase in the brainstem dorsal raphe nucleus in depressed suicides. Brain Res 2005, 1041, 19-28

Bolton PF, Dennis NR, Browne CE, et al. The phenotypic manifestations of interstitial duplications of proximal 15q with special reference to the autistic spectrum disorders. Am J Med Genet 2001, 105, 675–685

Bolton PF, Veltman MWM, Weisblatt E, et al. Chromosome 15q11-13 abnormalities and other medical conditions in individuals with autism spectrum disorders. Psychiatr Genet 2004, 14, 131-137

Bonin A, Goeden N, Chen K, et al. A transient placental source of serotonin for the fetal forebrain. Nature 2011, 472, 347-350

Bonkale WL, Murdock S, Janosky J, Austin MC. Normal levels of tryptophan hydroxylase immunoreactivity in the dorsal raphe of depressed suicide victims. J Neurochem 2004, 88, 958-964

Bonkale WL, Turecki G, Austin MC. Increased tryptophan hydroxylase immunoreactivity in the dorsal raphe nucleus of alcohol-dependent, depressed sucide subjects is restricted to the dorsal subnucleus. Synapse 2006, 60, 81-85

Bou-Flores C, Lajard AM, Monteau R et al. Abnormal phrenic motoneuron activity and morphology in neonatal monoamine oxidase A-deficient transgenic mice: a possible role of serotonin excess. J Neurosci 2000, 20, 4646-4656

Braak H. Uber die Kerngebiete des menschlichen Hinstammes II. Die Raphékerne. Zeischrift Zellforsch 1970, 107, 123-141

Brimacombe M, Ming X, Lamendola M. Prenatal and birth complications in autism. Matern Child Health J. 2007, 11, 73-79

Brodal A, Taber E, Walberg F. The raphe nuclei of the brain stem in the cat. II. Efferent connections. J Comp Neurol 1960, 114, 239-259

Brodkin ES, McDougle CJ, Naylor ST, Cohen DJ, Price LH. Clomipramine in adults with pervasive developmental disorders: a prospective open-label investigation. J Child Adolesc Psychopharmacol 1997, 7, 109-121

Brown GL, Goodwin FK, Bunney WE Jr. Human aggression and suicide: their relationship to neuropsychiatric diagnoses and serotonin metabolism. Adv Biochem Psychopharmacol 1982, 34, 287-307

Brown WT. Genetics of autism. In: Autism: oxidative stress, inflammation, and immune abnormalities. Eds: A. Chauhan, V. Chauhan, and WR Brown. CRC Press Taylor and Francis Group, Boca Raton 2010, 61-72

Bruns D, Engert F, Lux HD. A fast activating presynaptic reuptake current during serotonergic transmission in identified neurons of Hirudo. Neuron 1993,10, 559-572

Buitelaar JK, Willemsen-Swinkels SHN. Medication treatment in subjects with autistic spectrum disorders. Europ Child Adolesc Psychiatry 2000, 9, 85-97

Bunin MA, Wightman RM. Quantitative evaluation of 5-hydroxytryptamine (5-HT) neuronal release and uptake: an investigation of extrasynaptic transmission. J Neurosci 1998, 18, 4854-4860

Butler MG, Dasouki MJ, Zhou XP, Talebizadeh Z, Brown M, Takahashi TN, Miles JH, Wang CH, Stratton R, Pilarski R, Eng C. Subset of individuals with autism spectrum disorders and extreme macrocephaly associated with germline PTEN tumour suppressor gene mutations J Med Genet 2005, 42, 318-321

Buznikov GA. The action of neurotransmitters and related substances on early embryogenesis. Pharmac Ther 1984, 25, 23-59

Carper RA, Moses P, Tigue ZD, Courchesne E., Cerebral lobes in autism: early hyperplasia and abnormal age effects. Neuroimage 2002, 16, 1038-1051

Casanova MF, Buxhoeveden DP, Switala AE, Roy E. Minicolumnar pathology in autism. Neurology 2002, 58, 428–432

Casanova MF, Buxhoeveden D, Gomez J. Disruption in the inhibitory architecture of the cell minicolumn: implications for autism. Neuroscientist 2003, 9, 496-507

Casanova MF, van Kooten IAJ, Switala AE, van Engeland H, Heinsen H, Steinbusch HWM, Hof PR, Trippe J, Stone J, Schmitz C. Minicolumnar abnormalities in autism. Acta Neuropathol. 2006, 112, 287-303

Casu MA, Pisu C, Lobina C, Pani L. Immunocytochemical study of the forebrain serotonergic innervation in Sardinian alcohol-preferring rats. Psychopharmacology 2004; 172: 341-351.

Centers for Disease Control and Prevention. Prevalance of autism in Brick Township, New Jersey, 1998. Community Report. Atlanta, GA: Department of Health and Human Services. 2000.

Centers for Disease Control and Prevention. Prevalence of autism spectrum disorders – Autism and Developmental Disabilities Monitoring Network, 14 sites, United States,
2002. MMWR 2007; 56 (No. SS-1):12-28
2006. MMWR 2009; 58 (No. SS-10)

Chandana SR, Behen ME, Juhasz C, Muzik O, Rothermel RD, Mangner TJ, Chakraborty PK, Chugani HT, Chugani DC. Significance of abnormalities in developmental trajectory and asymmetry of cortical serotonin synthesis in autism. Int J Dev Neurosci 2005, 23, 171-182

Charnay Y, Léger L, Vallet PG, Greggio B, Hof PR, Jouvet M, Bouras C. Mapping of serotonin transporter messenger RNA-containing nerve cell populations in the cat brainstem. J Chem Neuroanat 1996, 10, 93-100

Chen L, Hamaguchi K, Hamada S, Okado N. Regional differences of serotonin-mediated synaptic plasticity in the chicken spinal cord with development and aging. J Neural Transplant Plast 1997, 6, 41-48

Chess S. Autism in children with congenital rubella. J Autism Child Schizophr 1971, 1, 33-47

Chubakov AR, Gromova EA, Conovalov GV, Sarkisova EF, Chumasov EI. The effects of serotonin on the morpho-functional development of rat cerebral neocortex in tissue culture. Brain Res 1986, 369, 285-297

Chugani DC, Muzik O, Rothermel R, Behen M, Chakraborty P, Mangner T, da Silva EA, Chugani HT. Altered serotonin synthesis in the dentatothalamocortical pathway in autistic boys. Ann Neurol 1997, 42, 666-669

Chugani DC, Muzik O, Behen M, Rothermel R, Janisse JJ, Lee J, Chugani HT. Developmental changes in brain serotonin synthesis capacity in autistic and nonautistic children. Ann. Neurol 1999, 45, 287-295

Chugani DC. Role of altered brain serotonin mechanisms in autism. Mol Psychiatry 2002, 7, 16–17

Clark S et al. Fluoxetine rescues deficient neurogenesis in hippocampus of the Ts65Dn mouse model for Down syndrome. Exp Neurol 2006, 200, 256-261

Clements JD, Transmitter timecourse in the synaptic cleft: Its role in central synaptic function. Trends Neurosci 1996, 19, 163-171

Cochran WG. 1977. Sampling techniques. Third edition. New York: Wiley.

Cohen IL, Criterion related validity of the PDD Behavior Inventory. J Autism Dev Disord 2003, 33, 47-53

Cohen LS, Nonacs R, Viguera AC, Reminick A. Diagnosis and treatment of depression during pregnancy. CNS Spectr 2004, 9, 209-216

Connors SL, Matteson KJ, Sega GA et al. Plasma serotonin in autism. Pediatr Neurol 2006, 35, 182-186

Cook EH, Leventhal BL, Heller W, Metz J, Wainwright M, Freedman DX. Autistic children and their first-degree relatives: relationships between serotonin and norepinephrine levels and intelligence. J Neuropsychiatry Clin Neurosci 1990, 2, 268-274

Cook EH, Arora RC, Anderson GM, Berry-Kravis EM, Yan SY, Yeoh HC, et al. Platelet serotonin studies in hyperserotonemic relatives of children with autistic disorder. Life Sci 1993, 52, 2005-2015

Cook EH, Leventhal BL. The serotonin system in autism. Curr Opin Pediatr 1996, 8: 348-354.

Cook EH, Lindgren V, Leventhal BL, et al. Autism or atypical autism in maternally but not paternally derived proximal 15q duplication. Am J Hum Genet 1997, 60, 928–934

Cook, EH. Genetics of autism. Mental Retardation Dev Disabil Res Rev 1998. 4: 113-120.

Cook EH. Serotonergic mechanisms in self injurious behavior and related disorders. 1999. In: Paper presented at NICHD Conference on SIB. Dec 6-7, Rockville MD.

Coon H, Dunn D, Lainhart J, Miller J, Hamil C Battaglia A, Tancredi R, Leppert MF, Weiss R, McMahon W. Possible association between autism and variants in the brain-expressed tryptophan hydroxylase gene (TPH2). Am J Med Genet B Neuropsychiatr Genet 2005, 135B, 42-46

Corbett BA, Schupp CW, Levine S, Mendoza S. Comparing cortisol, stress and sensory sensitivity in children with autism. Autism Res 2009, 2, 39-49

Cornelius JR, Salloum IM, Cornelius MD, Perel JM, Ehler JG, Jarrett PJ, Levin RL, Black A, Mann JJ. Preliminary report: double-blind, placebo-controlled study of fluoxetine in depressed alcoholics. Psychopharmacol Bull 1995, 31, 297-303

Cornelius JR, Salloum IM, Ehler JG, Jarrett PJ, Cornelius MD, Perel JM, Thase ME, Black A. Fluoxetine in depressed alcoholics. A double-blind, placebo-controlled trial. Arch Gen Psychiatry 1997, 54,700-705

Côté F, Fligny C, Bayard E, et al. Maternal serotonin is crucial for murine embryonic development. PNAS 2007, 104, 329-334

Cotton R, McAdam W, Jennings I, Morgan F. A monoclonal antibody to aromatic amino acid hydroxylases. Identification of the epitope. Biochem J 1988, 25,193-196

Courchesne E, Hesselink JR, Jernigan TL, Yeung-Courchesne R. Abnormal neuroanatomy in a nonretarded person with autism. Unusual findings with magnetic resonance imaging. Arch Neurol 1987, 44, 335-341

Courchesne E, Karns CM, Davis HR, et al. Unusual brain growth patterns in early life in patients with autistic disorder. An MRI study. Neurology 2001, 57, 245–254

Courchesne E, Carper R, Akshoomoff N, Evidence of brain overgrowth in the first year of life in autism. JAMA 2003, 290, 3

Courchesne E, Pierce K. Why the frontal cortex in autism might be talking only to itself: local over-connectivity but long-distance disconnection. Curr Opin Neurobiol, 2005a, 15, 225-230

Courchesne E, Pierce K. Brain overgrowth in autism during a critical time in development: implications for frontal pyramidal neuron and interneuron development and connectivity. Int J Dev Neurosci 2005b, 23,153-170

Courchesne E, Pierce K, Schumann CM, Redcay E, Buckwalter JA, Kennedy DP, Morgan J. Mapping early brain development in autism. Neuron 2007, 56, 399-413

Courchesne E, Campbell K, Solso S. Brain growth across the life span in autism: Age-specific changes in anatomical pathology. Brain Res 2010, 9,101

Courchesne E, Mouton PR, Calhoun ME et al. Neuron number and size in prefrontal cortex of children with autism. JAMA 2011, 306, 2001-2010

Coutinho AM, Oliveira G, Morgadinho T, Fesel C, Macedo TR, Bento C, Marques C, Ataide A, Miguel T, Borges L, Vicente AM. Variants of the serotonin transporter gene (SLC6A4) significantly contribute to hyperserotonemia in autism. Mol Psychiatry 2004, 9, 264-271

Craske MG, Rauch SL, Ursano R, Prenoveau J, Pine DS, Zinbarg RE. What is an anxiety disorder? 2009. Depression and Anxiety2009, 26, 1066-1085

Croen LA, Grether JK, Yoshida CK, et al. Antidepressant use during pregnancy and childhood autism spectrum disorders. Arch Gen Psychiatry 2011, *doi:10.1001/archgenpsychiatry.2011.73.*

Cross S, Kim SJ, Weiss LA, et al. Molecular genetics of the platelet serotonin system in first-degree relatives of patients with autism. Neuropsychopharmacology 2008, 33, 353-360

Cuccaro ML, Wright HH, Abramson RK, Marsteller FA, Valentine J. Whole-blood serotonin and cognitive functioning in autistic individuals and their first-degree relatives. J Neuropsychiatry Clin Neurosci 1993, 5, 94-101

Dahlström A, Fuxe K. Evidence for the existence of monoamine-containing neurons in the central nervous system. I. Demonstration of monoamines in the cell bodies of brainstem neurons. Acta Physiol Scand 1964, 232, Suppl. 62, 1-55

Damasio H, Maurer RG, Damasio AR, Chui HC. Computerized tomographic scan findings in patients with autistic behavior. Arch Neurol 1980, 37, 504-510

Daniels JL. Autism and the environment. Environ Health Perspect 2006, 114, A396

Dave V, Kimelberg HK. Na (+)-dependent, fluoxetine-sensitive serotonin uptake by astrocytes tissue-printed from rat cerebral cortex. J Neurosci 1994, 14, 4972-4986

Davis E, Fennoy I, Laraque D, et al. Autism and developmental abnormalities in children with perinatal cocaine exposure. J Natl Med Assoc 1992, 84, 315-319

Dawson AJ, Mogk R, Rothenmund H, et al. Paternal origin of a small, class I inv dup(15) Am J Med Genet 2002, 107, 334-336

Delgado PL, Charney DS, Price LH, Aghajanian GK, Landis H, Heninger GR. Serotonin function and the mechanism of of antidepressant action. Reversal of antidepressant-induced remission by rapid depletion of plasma tryptophan. Arch Gen Psychiatry 1990, 47, 411-418

DeLong Robert G, Teague LA, Kamran MM. Effects of fluoxetine treatment in young children with idiopathic autism. Dev Med & Child Neurol. 1998, 40, 551-562

De Bruin EI, Ferdinand RF, Meester S, de Nijs PFA, Verheij F. High rates of psychiatric co-morbidity in PDD-NOS. 2007. J Aut Dev Dis 37, 877-886

Del Fiacco M, Dessi ML, Levanti MC. Topographical localization of substance P in the human post-mortem brainstem. An immunohistochemical study in newborn and adult tissue. Neuroscience 1984, 12, 141-150

Descarries L, Watkins KC, Garcia S, Beaudet A. The serotonin neurons in nucleus raphe dorsalis of adult rat: A light and electron microscope radioautographic study. J Comp Neurol 1982, 207, 239-254

Dickie VA, Baranek GT, Schultz B, Watson LR, McComish CS. Parent reports of sensory experiences of preschool children with and without autism: a qualitative study. Am J Occup Ther 2009, 63, 172-181

Ding Y-Q, Marklund U, Yuan Q, Yin J, Wegman L, Ericson J, Deneris E, Johnson RL, Chen Z-F, *Lmx1b* is essential for the development of serotonergic neurons. Nat Neurosci 2003, 6, 933-938

Eriksen JL, Gillespie R, Druse MJ Effects of ethanol and 5-HT_{1A} agonists on astroglial S100B. Brain Res Dev Brain Res 2002, 139, 97-105

Erde SM, Sherman D, Gershon MD. Morphology and serotonergic innervation of physiologically identified cells of the guinea pig's myenteric plexus. J Neurosci 1985, 5, 617-633

Faccidomo S, Bannai M, Miczek A. Escalated aggression after alcohol drinking in male mice: dorsal raphe and prefrontal cortex serotonin and 5-HT_{1B} receptors. Neuropsychopharm 2008, 33, 2888-2899

Fardin V, Oliveras JL, Besson JM. A reinvestigation of the analgesic effects induced by stimulation of the periaqueductal gray matter in the rat. I. The production of behavioral side effects together with analgesia. Brain Res 1984, 306, 105-123

Fatemi SH, Realmuto GM, Khan L, Thuras P. Fluoxetine in treatment of adolescent patients with autism: a longitudinal open trial. J. Autism Dev Disord. 1998, 28, 303-307

Fatemi SH, Halt AR, Realmuto G et al (2002) Purkinje cell size is reduced in cerebellum of patients with autism. Cell Molec Neurobiol 2002, 22, 171-175

Fils-Aime ML et al. Early onset alcoholics have lower cerebrospinal fluid 5-hydroxyindoleacetic acid levels than later onset alcoholics. Arch Gen Psychiatry 1996, 53, 211-216

Fitzgerald LW, Kaplinsky L, Kimelberg HK. Serotonin metabolism by monoamine oxidase in rat primary astrocyte cultures. J Neurochem 1990, 55, 2008-2014

Folstein SE, Rosen-Sheidley B. Genetics of autism: complex aetiology for a heterogeneous disorder. Nat Rev Genet 2001, 2, 943-955

Fombonne E, Roge B, Claverie J, et al. Microcephaly and macrocephaly in autism. J Autism Dev Disord 1999, 29, 113–9

Fombonne E. Epidemiological surveys of autism and other pervasive developmental disorders. J Autism Dev Disord 2003, 33, 365-382

Freitag CM. The genetics of autistic disorders and its clinical relevance: A review of the literature. Mol Psychiatry 2007, 12, 2-22

Friede, R. L. Developmental neuropathology. Berlin. Springer Verlag.1975

Fuchs AF, Kaneko CRS, Scudder CA. Brain stem control of saccadic eye movements. Ann Rev Neurosci 1985, 8, 307-337

Fujita M, Shimada S, Maeno H, Nishimuira T, Tohyama M, Cellular localization of serotonin transporter mRNA in the rat brain. Neurosci Lett 1993, 162, 59-62

Furness JB, Costa M. Neurons with 5-hydroxytryptamine-like immunoreactivity in the enteric nervous system: their projections in the guinea pig small intestine. Neuroscience 1982, 7, 341-350

Fuxe K, Agnati LF. Volume transmission in the brain: novel mechanisms for neural transmission. New York: Raven 1991.

Garris EL, Ciolkowski EL, Pastore P, Wingthman RM. Efflux of dopamine from the synaptic cleft in the nucleus accumbens of the rat brain. J Neurosci 1994, 14, 6084-6093

Garris PA, Wightman RM. Regional differences in dopamine release, uptake, and diffusion measured by fast-scan cyclic voltammetry. In: Neuromethods, Vol 27: Voltammetric methods in Brain Systems (Boulton AA, Baker G, Adams RN, eds.). Human Press, Clifton, New Jersey 1995, pp. 179-219

Gaspar P, Cases O, Maroteaux L. The developmental role of serotonin: news from mouse molecular genetics. Nat Rev Neurosci 2003, 4,1002-1012

Gershon MD, Drakontides AB, Ross LL. Serotonin: synthesis and release from the myenteric plexus of the mouse intestine. Science 1965, 149, 197-199

Gershon MD, Robinson R, Ross LL. Functional anatomy of the enteric nervous system. In: Johnson LR, Alpers DH, Jacobson ED, Walsh EH, editors. Physiology of the gastrointestinal tract. 3rd ed. New York: Raven Press, 1994, p. 381-422

Gershon MD. Review article: serotonin receptors and transporters -- roles in normal and abnormal gastrointestinal motility. Aliment Pharmacol Ther 2004, 20 Suppl 7, 3-14

Gershon MD, Tack J. The serotonin signaling system: from basic understanding to drug development for functional GI disorders. Gastroenterology 2007, 132, 397-414

Gillberg, C. Chromosomal disorders and autism. J Autism Dev Disord 1998, 28, 415-425

Gillberg C, Billstedt E. Autism and Asperger Syndrome: coexistence with other clinical disorders. Acta Psychiatr Scand 2000, 102, 321-330

Gilliam JE, Gilliam Autism rating Scale (GARS) Austin, Texas: Pro Ed, 1995.

Giros B, Jaber M, Jones SR, Wightman RM, Caron MG. Hyperlocomotion and indifference to cocaine and amphetamine in mice lacking the dopamine transporter. Nature 1996, 379, 606-612

Glasson EJ, Bower C, Petterson B, de Klerk N, Chaney G, Hallmayer JF. Perinatal factors and the development of autism: a population study. Arch Gen Psychiatry 2004, 61, 618-627

Gobbi M, Parazzoli A, Mennini T. In vitro studies on the mechanism by which (+)-norfenfluramine induces serotonin and dopamine release from the vesicular storage pool. Naunyn Schmiedebergs Arch Pharmacol 1998, 358, 323-327

Gomot, M, Giard MH, Adrien JL, Barthelemy C, Bruneau N. Hypersensitivity to acoustic change in children with autism: electrophysiological evidence of left frontal cortex dysfunctioning. Psychophysiol 2002, 39, 577-584

Gordon C, State R, Nelson J, Hamburger S, Rapoport J. A double-blind comparison of clomipramine, disipramine, and placebo in the treatment of autistic disorder. Arch Gen Psychiatry 1993, 50, 441-447

Green G, Brennan LC, Fein D. Intensive behavioral treatment for a toddler at high risk of autism. Behav Modification 2002, 26, 69-102

Green SA, Ben-Sasson A. Anxiety disorders and sensory over-responsivity in children with autism spectrum disorders: is there a causal relationship? J Autism Dev Disord 2010, 40, 1495-1504

Greenspan SI, Wieder S. Developmental patterns and outcomes in infants and children with disorders in relating and communicating: a chart review of 200 cases of children with autistic spectrum diagnoses. J Dev Learn Disord 1997, 1, 87-141

Grillon C. Models and mechanisms of anxiety: Evidence from startle studies. Psychopharmacology. 2008, 199, 421-437

Gundersen HJ. The nucleator. J Microsc 1988, 151, 3-21

Haan EA, Jennings IG, Cuello AC, Nakata H, Fujisawa H, Chow CW, Kushinsky R, Brittingham J, Cotton RGH. Identification of serotonergic neurons in human brain by a monoclonal antibody binding to all three aromatic amino acid hydroxylases. Brain Res 1987, 426, 19-27

Hadjikhani N. Serotonin, pregnancy and increased autism prevalence: Is there a link? Medical Hypotheses 2010, 74, 880-883

Hagerman RJ. The Physical and Behavioral Phenotype. In Fragile X syndrome: Diagnosis, treatment, and research. R. J. Hagerman and P. J. Hagerman, editors. Johns Hopkins University Press, Baltimor. 2002, 206-248

Hajos M, Sharp T, Newberry NR. Intracellular recordings from burst-firing presumed serotonergic neuronsin the rat dorsal raphe nucleus in vivo. Brain Res 1996, 737, 308-312

Halasz J, Toth M, Kallo I, Liposits Z, Haller J. The activation of prefrontal cortical neurons in aggression-a double labeling study. Behav Brain Res 2006, 175, 166-175

Halliday GM, and Törk I. Comparative anatomy of the ventromedial mesencephalic tegmentum in the rat, cat, monkey, and human. J Comp Neurol 1986, 252, 423-445

Halliday GM, Li YW, Joh TH, Cotton RGH, Howe PRC, Geffen LB, Blessing WW. Distribution of monoamine-synthesizing neurons in the human medulla oblongata. J Comp Neurol 1988a, 273, 301-317

Halliday GM, Li YW, Joh TH, Cotton RGH, Howe PRC, Geffen LB, Blessing WW. Distribution of substance P-like immunoreactive neurons in the human medulla oblongata: co-localization with monoamine-synthesizing neurons, Synapse 1988b, 2, 353-370

Halliday GM, Li YW, Blumbergs PC, Joh TH, Cotton RG, Howe PR, Blessing WW, Geffen LB. Neuropathology of immunohistochemically identified brainstem neurons in Parkinson's disease. Ann Neurol 1990, 27, 373-385

Halliday G, Ellis J, Heard R, Caine D, Harper C, Brainstem serotonergic neurons in chronic alcoholics with and without the memory impairment of Korsakoff's psychosis. J Neuropathol Exp Neurol 1993, 52, 567-579

Hanley HG, Stahl SM, Freedman DX. Hyperserotonemia and amine metabolites in autistic and retarded children. Arch Gen Psychiatry 1977, 34, 531-531

Harris, S. R., L. L. MacKay, and J. A. Osborn. Autistic behaviors in offspring of mothers abusing alcohol and other drugs: a series of case reports. Alcohol Clin Exp Res 1995, 19, 660-665

Hashimoto, T., M. Tayama, K. Mori, K. Fujino, M. Miyazaki, and Y. Kuroda. Magnetic resonance imaging in autism: preliminary report. Neuropediatrics 1989, 20, 142-146

Hashimoto, T., M. Tayama, M. Miyazaki, K. Murakawa, and Y. Kuroda. Brainstem and cerebellar vermis involvement in autistic children. J. Child Neurol 1993, 8, 149-153

Heinz A, Ragan P, Jones DW, Hommer D, Williams W, Knable MB, Gorey JG, Doty L, Geyer C, Lee KS, Coppola R, Weinberger DR, Linnoila M. Reduced central serotonin transporters in alcoholism. Am J Psychiatry 1998, 155, 1544-1549

Henderson LA. Caudal midline medulla mediates behaviourally-coupled but not baroreceptor-mediated vasodepression. Neuroscience 2000, 98, 779-792

Hérault J, Petit E, Martineau J et al. Serotonin and autism: Biochemical and molecular biology features. Psychiatry Res 1996, 65, 33-43

Hertz-Picciotto I, Deliche L. The rise in autism and the role of age at diagnosis. Epidemiology 2009, 20, 84-90

Hery F, Ternaux JP. Regulation of release processes in central serotoninergic neurons. J Physiol (Paris) 1981, 77, 287-301

Hirst WD, Price GW, Rattray M, Wilkin GP. Serotonin transporters in adult rat brain astrocytes revealed by [^{3}H]5-HT uptake into glial plasmalemmal vesicles. Neurochem Int 1998b, 33, 11-22

Hoffman BJ, Mezey E, Brownstein MJ. Cloning of serotonin transporter affected by antidepressants. Science 1991, 254, 579-580

Hollander E, Phillips A, Chaplin W, et al. A placebo controlled crossover trial of liquid fluoxetine on repetitive behaviors in childhood and adolescent autism. Neuropsychopharmacology 2005, 30, 582-589

Hornung J-P, Kraftsik R. Three-dimensional reconstruction procedure using GKS primitives and software transformations for anatomical studies of the nervous system. In "Proceedings of the Computer Graphics International Meeting" (N. Magnenant-Thalmann and D. Thalmann, Eds.) Springer-Verlag, Berlin 1988, 555-564

Hornung J-P. The human raphé nuclei and the serotonergic system. J Chem Neuroanat 2003, 26, 331-343

Hoyer D, Clarke DE, Fozard JR, Hartig PR, Martin GR, Mylecharane EJ, Saxena PR, Humphrey PPA. International union of pharmacology classification of receptors for 5-hydroxytryptamine (serotonin) Pharmacol Rev 1994, 46, 157-203

Hranilovic D, Bujas-Petkovic Z, Vragovic R, Vuk T, Hock K, Jernej B, Hyperserotonemia in adults with autistic disorder. J Autism Dev Disord 2007, 37, 1934-1940

Hrdina PD, Foy B, Hepner A, Summers RJ. Antidepressant binding sites in brain: autoradiographic comparison of [3H] paroxetine and [3H] imipramine localization and relationship to serotonin transporter. J Pharmacol Exp Ther 1989, 252, 410-418

Iqbal K, Braak H, Braak E, et al. Silver labeling of Alzheimer neurofibrillary changes and brain ß-amyloid. J Histotech 1993,16, 335-42

Iravani MM, Kruk ZL. Real-time measurement of stimulated 5-hydroxytryptamine release in rat substantia nigra pars reticulata brain slices. Synapse 1997, 25, 93-102

Jacobowitz DM, MacLean PD. A brainstem atlas of catecholaminergic neurons and serotonergic perikarya in a pygmy primate (*Cebuella pygmaea*) J Comp Neurol 1978, 153, 385-398

Jacobs B, Gannon PJ, Azmitia EC. Atlas of serotonergic cell bodies in the cat brainstem: An immunohistochemical study. Brain Res Bull 1984, 13, 1-31

Jacobs BL, Martín-Cora FJ, Fornal CA. Activity of medullary serotonergic neurons in freely moving animals. Brain Res 2002, 40, 45-52

Jacot-Descombes S, Uppal N, Wicinski B, et al Decreased pyramidal neuron size in Brodmann areas 44 and 45 in patients with autism. Acta Neuropathol 2012, 124, 67-79

Jakab R, Goldman-Rakic P. 5-Hydroxytryptamine$_{2A}$ serotonin receptors in the primate cerebral cortex: possible site of action of hallucinogenic and antipsychotic drugs in pyramidal cell apical dendrites. Proc Natl Acad Sci USA 1998, 95, 735-740

Jang MH, Shin MC, Lee TH, Kim YP, Jung SB, Shin DH, Kim H, Kim SS, Kim EH, Kim CJ. Alcohol and nicotine administration inhibits serotonin synthesis and tryptophan hydroxylase expression in dorsal and median raphe of young rats. Neurosci Lett 2002, 329, 141-144

Janusonis S, Anderson GM, Shifrovich I, Rakic P. Ontogeny of brain and blood serotonin levels in 5-HT receptor knockout mice: potential relevance to the neurobiology of autism. J Neurochem 2006, 99, 1019-1031

Janusonis S. Origin of the blood hyperserotonemia of autism. Theor Biol Med Model. 2008, 5, 10

Jennes L, Stumpf WE, Kalivas PW. Neurotensin: topographical distribution in rat brain immunohistochemistry. J Comp Neurol 1982, 210, 211-224

Joh TH, Shikimi T, Pickel VM, Reis DJ. Brain tryptophan hydroxylase: Purification of, production of antibodies to, and cellular and ultrastructural localization in serotonergioc neurons of rat midbrain. Proc Natl Acad Sci USA 1975, 72, 3575-3579

Jones BE, Yang TZ. The efferent projections from the reticular formation and locus coeruleus studies by the anterograde and retrograde axonal transport in the rat. J Comp Neurol 1985, 242, 56-92

Jones SR, O'Dell SJ, Marshall JF, Wightman RM. Functional and anatomical evidence for different dopamine dynamics in the core and shell of the nucleus accumbens in slices of rat brain. Synapse 1996, 23, 224-231

Jou, RJ, Minshew, NJ, Melhem, NM. Brainstem volumetric alterations in children with autism. Psychological Medicine 2009, 39, 1347-1354

Joyce D. Changes in the 5-hydroxytryptamine content of rat, rabbit, and human brain after death. BrJ Pharmac 1962,18, 370-380

Kaminsky KA, Tang T, Wang SC, Ptak C, Oh GH, Wong AH, Feldcamp LA, Virtanen C, Halfvarson J, Tysk C, McRae AF, Visscher PM, Montgomery GW, Gottesman II, Martin NG, Petronis A. DNA methylation profiles in monozygotic and dizygotic twins. Nat Genet 2009, 41, 240-245

Kandel ER, Schwartz JH, Jessell TM. Principles of neural science. 3rd Ed, p 875, New York, Elsevier Science 1991

Kanner L. Autistic disturbances of affective contact. Nervous Child 1943, 2.217-250

Karmel BZ, Gardner JM, Meade LS, Cohen IL, London E, Flory MJ, Lennon EM, Miroshnichenko I, Rabinowitz S, Parab S, Barone A, Harin A. Early medical and behavioral characteristics of NICU infants later classified with ASD. Pediatrics 2010, 126, 457-467

Katayama Y, Tsubokawa T, Abekura M, Hayes RL, Becker DP. Coma induced by cholinergic activation of a restricted region in the pontine reticular formation-a model of reversible form of coma. Neurol Med Chir (Tokyo) 1986, 26, 1-10

Katz B, Miledi R. The binding of acetylcholine to receptors and its removal from the synaptic cleft. J Physiol (London) 1973, 231, 549-573

Katz DM, Kimelberg HK. Kinetics and autoradiography of high affinity uptake of serotonin by primary astrocyte cultures. J Neurosci 1985, 5, 1901-1908

Kemper, T. L. and M. L. Bauman. The contribution of neuropathologic studies to the understanding of autism. Neurol. Clin. 1993, 11, 175-187

Kent, L., J. Evans, M. Paul, and M. Sharp. Comorbidity of autistic spectrum disorders in children with Down syndrome. Dev. Med. Child Neurol. 1999, 41,153-158

Kimelberg HK and Katz DM. High-affinity uptake of serotonin into immunocytochemically identified astrocytes. Science 1985, 228, 889-891

King BH, Hollander E, Sikich L, McCracken JT, Scahill L, Bregman JD, Donelly CL, Anagnostou E, Dukes K, Sullivan L, Hirtz D, Wagner A, Ritz L. STAART Psychopharmacology Network. 2009. Lack of efficacy of citalopram in children with autism spectrum disorders and high levels of repetitive behavior: citalopram ineffective in children with autism. Arch Gen Psychiatry 2009, 66, 583-590

Kinney HC, Filiano JJ, White WF, Medullary serotonergic network deficiency in the sudden infant death syndrome: review of a 15-year study of a single dataset. J Neuropath Exp Neurol 2001, 60, 228-247

Kinney HC, Paterson DS. Sudden infant death syndrome. In: Golden J, Harding B. eds. Pathology and Genetics: Developmental neuropathology. Basel, Switzerland, Neuropath Press 2004

Kirchgessner A. L., Liu M. T., Raymond J. R. and Gershon M. D. Identification of cells that express 5-hydroxytryptamine1A receptors in the nervous systems of the bowel and pancreas. J. Comp. Neurol. 1996, 364, 439–455

Kolevzon A, Mathewson KA, Hollander E. Selective serotonin reuptake inhibitors in autism: a review of efficacy and tolerability 2006, 67, 407-414

Kolevzon A, Newcorn JH, Kryzak L, Chaplin W, Watner D, Hollander E, Smith CJ, Cook EH Jr. Silverman JM. Relationship between whole blood serotonin and repetitive behaviors in autism. Psychiatry Res 2010,175,274-276

Kölliker A. Handbuch der Gewebelehre des Menschen. Vol 2. Engelmannn, Leipzig, 1893

Kondoh M, Shiga T, Okado N. Regulation of dendrite formation of Purkinje cells by serotonin through serotonin1A and serotonin2A receptors in culture. Neurosci Res 2004, 48,101-109

Kontur PJ, Leranth C, Redmond DE, Roth RH, Robbins RJ. Tyrosine hydroxylase immunoreactivity and monoamine and metabolite levels in cryopreserved human fetal ventral mesencephalon. Exp Neurol 1993, 121, 172-180

Kosofsky BE, Molliver ME. The serotonergic innervation of cerebral cortex: different classes of axon terminals arise from dorsal and median raphe nuclei. Synapse 1987, 1, 153-168

Kosofsky BE, Kowall NW. Demonstration of two morphologic classes of serotonergic fibers in human cortex. Soc Neurosci Abstract 1989,15, 5

Kramer, K., E. C. Azmitia, and P. M. Whitaker-Azmitia. In vitro release of [3H]5-hydroxytryptamine from fetal and maternal brain by drugs of abuse. Brain Res. Dev. Brain Res. 1994, 78, 142-146

Krammer EB, Rath T, Lischka MF. Somatotopic organization of the hypoglossal nucleus: a HRP study in the rat. Brain Res 1979, 170, 533-537

Kulesza RJ. Cytoarchitecture of the human superior olivary complex: medial and lateral superior olive. Hear Res 2007, 225, 80-90

Kulesza RJ, Mangunay K. Morphological features of the medial superior olive in autism. Brain Res 2009, 1200, 132-137

Kulesza RJ, Lukose R, Stevens LV. Malformation of the human superior olive in autistic spectrum disorders. Brain Res 2011, 1367, 360-371

Kuperman, S., J. Beeghly, T. Burns, and L. Tsai. Association of serotonin concentration to behavior and IQ in autistic children. J. Autism Dev. Disord. 1987, 17, 133-140

Lainhart JE, Bigler ED, Bocian M, Coon H, Dinh E, Dawson G, Deutsch CK, Dunn M, Estes A, Tager-Flusberg H, Folstein S, Hepburn S, Hyman S, McMahon W, Minshew N, Munson J, Osann K, Ozonoff S, Rodier P, Rogers S, Sigman M, Spence MA, Stodgell CJ, Volkmar F. Head circumference and height in autism: a study by the Collaborative Program of Excellence in Autism. Am J Med Genet A. 2006, 140, 2257-2274

Lam KS, Aman MG, Arnold LE. Neurochemical correlates of autistic disorder: a review of the literature. Res Dev Disabil 2006, 27, 254-289

Landrigan PJ. What causes autism? Exploring the environmental contribution. Curr Opin Pediatr 2010, 22, 219-225

Lauder JM, Liu J, Grayson DR. In utero exposure to serotonergic drugs alters neonatal expression of 5-HT(1A) receptor transcripts: a quantitative RT-PCR study. Int J Dev Neurosci 2000, 18, 171-176

Lesch K-P, Wolozin BL, Estler HC, Murphy DL, Riederer P. Isolation of a cDNA encoding the human brain serotonin transporter. J Neural Transm 1993, 91, 67-72

Lemberger L, Fuller RW, Zerbe RL. Use of specific serotonin uptake inhibitors as antidepressants. Clin Neuropharmacol 1985, 8, 299-317

Levallois C, Valence C, Baldet P, Privat A. Morphological and morphometric analysis of serotonin-containing neurons in primary dissociated cultures of human rhombencephalon: a study of development. Dev Brain Res 1997, 99, 243-252

Lidov, H. G. and M. E. Molliver. Immunohistochemical study of the development of serotonergic neurons in the rat CNS. Brain Res Bull. 1982, 9, 559-604

Limperopoulos C, Bassan H, Sullivan NR, Soul JS, Robertson RL, Jr., Moore M, Ringer SA, Volpe JJ, du Plessis AJ. Positive screening for autism in ex-preterm infants: prevalence and risk factors. Pediatrics 2008, 121, 758-765

Liposits A, Gorcs T, Trombitas K. Ultrastructural analysis of central serotonergic neurons immunolabeled by silver-gold-intensified diaminobenzidine chromogen. J Histochem Cytochem 1985, 33, 604-610

Liu, Zerubavel, Baerman. Social demographic change and autism. Demography 2010, 47, 327

Lopez-Hurtado E, Prieto JJ. A microscopic study of language-related cortex in autism. Am J Biochem. Biotechn. 2008, 4, 130-145

Lord C, Rutter M, Le Couteur A. Autism diagnostic interview-revised: A revised version of a diagnostic interview for caregivers of individuals with possible pervasive developmental disorders. J Autism Dev Disord 1999, 24, 659-685

Lord, C., S. Risi, L. Lambrecht, E. H. Cook, Jr., B. L. Leventhal, P. C. DiLavore, A. Pickles, and M. Rutter. The autism diagnostic observation schedule-generic: a standard measure of social and communication deficits associated with the spectrum of autism. J. Autism Dev. Disord. 2000, 30, 205-223

Lucki I. The spectrum of behaviors influenced by serotonin. Biol Psychiatry 1998, 44, 151-162.

Maciag D, Simpson KL, Coppinger D, Lu Y, Wang Y, Lin RCS, Paul IA. Neonatal antidepressant exposure has lasting effects on behavior and serotonin circuitry. Neuropsychopharmacol 2006, 31, 47-57

Maeshima T, Shutoh F, Hamada S, Senzaki K, Hamaguchi-Hamada K, Ito R, Okado N. Serotonin2A receptor-like immunoreactivity in rat cerebellar Purkinje cells. Neurosci Lett 1998, 252, 72-74

Magleby KL, Terrar DA. Factors affecting the time course of decay of end-plate currents: a possible cooperative action of acetylcholine on receptors at the frog neuromuscular junction. J Physiol (London) 1975, 244, 467-495

Makkonen I, Riikonen R, Kokki H, Airaksinen MM. Kuikka JT. Serotonin and dopamine transporter binding in children with autism determined by SPECT. Dev Med Child Neurol 2008, 50, 593-597

Malberg JE, Eisch AJ, Nestler EJ, Duman RS. Chronic antidepressant treatment increases neurogenesis in adult rat hippocampus. J Neurosci 2000, 20, 9104-9110

Mamounas LA, Mullen CA, O'Hearn E, Molliver ME. Dual serotoninergic projections to forebrain in the rat: Morphologically distinct 5-HT axon terminals exhibit differential vulnerability to neurotoxic amphetamine derivatives. J Comp Neurol 1991, 314, 558-586

Mann JJ, Brent DA, Arango V. The neurobiology and genetics of suicide and attempted suicide: a focus on the serotonergic system. Neuropsychopharmacology 2001, 24, 467-477

Mantere T, Tupala E, Hall H, Sarikioja T, Rasanen P, Berstrom K, Callaway J, Tiihonen J. Serotonin transporter distribution and density in the cerebral cortex of alcoholic and nonalcoholic comparison subjects: A whole-hemisphere autoradiography study. Am J Psychiatry 2002, 159, 599-606

Mantyh PW. The midbrain periaqueductal gray in the rat, cat and monkey: A Nissl, Weil and Golgi analysis. J Comp Neurol 1982,204,349-363

Martel F. Recent advances on the importance of the serotonin transporter SERT in the rat intestine. Pharmacol Res 2006, 54, 73-76

Martin GR, Humphrey PPA. Receptors for 5-hydroxytryptamine: current perspectives on classification and nomenclature. Neuropharmacology 1994, 33, 261-273

Mayser W, Betz H, Schloss P. Isolation of cDNAs encoding a novel member of the neurotransmitter transporter gene family. Fedn Eur Biochem Socs Lett 1991, 295, 203-206

Mazzone L, Ruta L, Reale L. Psychiatric comorbidities in Asperger syndrome and high functioning autism: diagnostic challenges. Annals Gen Psychiatry 2012, 11, 1-16

McBride PA, Anderson GM, Hertzig ME, Snow ME, Thompson SM, Khait VD et al. Effects of diagnosis, race, and puberty on platelet serotonin levels in autism and mental retardation. J Am Acad Child Adolesc Psychiatry 1998, 37, 767-776

McDougle CJ, Naylor ST, Goodman WK, Volkmar FR, Cohen DJ, Price LH. Acute tryptophan depletion in autistic disorder: a controlled case study. Biol Psychiatry 1993, 33, 547-550

McDougle C, Naylor S, Cohen D, Volkmar F, Heninger G, Price L. A double-blind, placebo controlled study of fluvoxamine in adults with autistic disorder. Arch Gen Psychiatry 1996, 56, 1001-1008

McEachin JJ, Smith T, Lovaas OI. Long-term outcome for children with autism who received early intensive behavioral treatment. Am J Ment Ret 1993, 4, 359-372

McNamara IM, Borella AW, Bialowas LA, Whitaker-Azmitia PM. Further studies in the developmental hyperserotonemia model (DHS) of autism: social, behavioral and peptide changes. Brain Res 2008, 1189, 203-214

Mehler MF. Epigenetics and the nervous system. Ann Neurol 2008, 64, 602-617

Mehler WR, Feferman ME, Nauta WJH. Ascendin axon degeneration following anterolateral cordotomy. An experimental study in the monkey. Brain 1960, 83,718-750

Mehlinger R, Scheftner WA, Poznanski E. Fluoxetine and autism. J Am Acad Child Adolesc Psychiatry 1990, 29, 985

Melke J, Goubran-Botros H, Chaste P, Betancur C, Nygren G, Anckarsäter H, Rastam M, Ståhlberg O, Gillberg IC, Delorme R, Chabane N, Mouren-Simeoni M-C, Fauchereau F, Durand CM, Chevalier F, Drouot X, Collet C, Launay J-M, Leboyer M, Gillberg C, Bourgeron T. Abnormal melatonin synthesis in autism spectrum disorders. Mol Psychiatry 2008, 13, 90-98

Miczek KA, Faccidomo S, de Almeida RMM, Bannai M, Fish EW, DeBold JF. Escalated aggressive behavior: pharmacotherapeutic approaches and opportunities. Ann NY Acad Sci 2004, 1036, 336-355

Miczek KA, Fish EW. Monoamines, GABA, Glutamate and Aggression. 2006. In: Nelson RJ (ed.) Biology of Aggression. Oxford University Press: New York, pp 114-149

Miles, J.H., T.N.Takahashi, S. Bagby, P.K. Sahota, D.F. Vaslow, C.H. Wang, R.E. Hillman, J.E. Farmer. Essential versus complex autism. Am J Med Genet 2005, 135, 171-180

Miles JH. Autism spectrum disorders – A genetic review. Genetics in Med 2011, 13, 278- 294

Miller MT, Strömland K, Ventura L et al. Autism associated with conditions characterized by developmental errors in early embryogenesis: a mini review. Int J Dev Neurosci 2005, 23, 201-219 and 629-642

Morrison AR, Reiner PB. A dissection of paradoxical sleep. In “Brain Mechanisms of Sleep”. Editors: DJ McGinty, R, Druker-Colin, A. Morrison and PL Parmeggiani. Raven Press, New York, 1985, pp 97-110

Mosko SS, Haubrich D, Jacobs BL. Serotonergic afferents to the dorsal raphe nucleus: evidence from HRP and synaptosomal uptake studies. Brain Res 1977, 119, 269-290

Moukhles H, Bosler O, Bolam JP, Vallee A, Umbriaco D, Geffard M, Doucet G. Quantitative morphometric data indicate precise cellular interactions between serotonin terminals and postsynaptic targets in rat substantia nigra. Neuroscience 1997, 76, 1159-1171

Muhle R, Trentacoste SV, Rapin I. The genetics of autism. Pediatrics 2004, 113, 472-486

Mulder E. J., Anderson G. M., De Kema I. P. B. A., Van Lang N. D., Den Boer J. A. and Minderaa R. B. Platelet serotonin levels in pervasive developmental disorders and mental retardation. Diagnostic group differences, within-group distribution, behavioral correlates. J Am Acad Child Adolesc Psychiatry 2004, 43, 491–499

Mulligan KA, Törk I. Serotonergic innervation of the cat cerebral cortex. J Comp Neurol 1988, 270, 86-110

Murakami, J. W., E. Courchesne, G. A. Press, R. Yeung-Courchesne, and J. R. Hesselink. Reduced cerebellar hemisphere size and its relationship to vermal hypoplasia in autism. Arch Neurol 1989, 46, 689-694

Nakamura K, Sekine Y, Ouchi Y, Tsujii M, Yoshikawa E, Futatsubashi M, Tsuchiya KJ, Sugihara G, Iwata Y, Suzuki K, Matsuzaki H, Suda S, Sugiyama T, Takei N, Mori N. Brain serotonin and dopamine transporter bindings in adults with high functioning autism. Arch Gen Psychiatry 2010, 67, 59-68

Nanson JL (1992) Autism in fetal alcohol syndrome: a report of six cases. Alcohol Clin Exp Res 1992,16, 558-565

Naranjo CA, Bremner KE. Clinical pharmacology of serotonin altering medications for decreasing alcohol consumption. Alcohol 1993,28, 221-229

Narita N, Kato M, Tazoe M, Miyazaki K, Narita M, Okado N. Increased monoamine concentration in the brain and blood of fetal thalidomide- and valproic acid-exposed rat: putative animal models for autism. Pediatr Res 2002, 52, 576-579

Nelson RJ, Chiavegatto S. Molecular basis of aggression. Trends Neurosci 2001, 24, 713-719

Newschaffer CJ, Fallin D, Lee NL. Heritable and nonheritable risk factors for autism spectrum disorders. Epidemiol. Rev. 2002, 24,137-153

Niitsu Y, Hamada S, Hamaguchi K, Mikuni M, Okado N. Regulation of synapse density by 5-HT_{2A} receptor agonist and antagonist in the spinal cord of chicken embryo. Neurosci Lett 1995, 195, 159-162

Nirenberg MJ, Chan J, Pohorille A, Vaughan RA, Uhl GR, Kuhar MJ, Pickel VM. The dopamine transporter: comparative ultrastructure of dopaminergic axons in limbic and motor compartments of the nucleus accumbens. J Neurosci 1997, 17, 6899-6907

Nishizawa S, Benkelfat C, Young SN, Leyton M, Mzengeza S, P. Blier MC, and Diksic M. Differences between males and females in rates of serotonin synthesis in human brain. Proc Natl Acad Sci USA, 1997, 94, 5308-5313

Nobin A, Björklund A. Topography of monoamine neuron systems in the human brain as revealed in fetuses. Acta Physiol Scand Suppl 1973, 388, 1-40

O'Hearn E, Battaglia G, De Souza EB, Kuhar MJ, and Molliver ME Methylenedioxyamphetamine (MDA) and methylenedioxymetamphetamine (MDMA) cause selective ablation of serotoninergic axon terminals in forebrain: immunocytochemical evidence for neurotoxicity. J Neurosci 1988, 8, 2788-2803

Okado N, Cheng L, Tanatsugu Y, Hamada S, Hamaguchi K. Synaptic loss following removal of serotonergic fibers in newly hatched and adult chickens. J Neurobiol 1993, 24, 687-698

Oliveras JL, Guilbaud G, Besson JM. A map of serotonergic structures involved in stimulation producing analgesia in unrestrained freely moving cats. Brain Res. 1979, 164, 317-322

Olivier B, Mos J, Van der Heyden J, Hartog J. Serotonergic modulation of social interactions in isolated male mice. Psychopharmacol 1989, 97, 154-156

Olivier B, Mos J. Rodent models of aggressive behavior and serotonergic drugs. Prog Neuropsychopharmacol Biol Psychiatry 1992, 16, 847-870

Ollendick TH, King NJ, Chorpita BF. Empirically supported treatments for children and adolescents. In: Kendall PC, editor. Child and adolescent therapy: Cognitive behavioral procedures. 3. NY, NY: Guilford Press 2006, p 492-520

Olson L, Boreus LO, Seiger A. Histochemical demonstration and mapping of 5-hydroxytryptamine- and catecholamine-containing neuron systems in the human fetal brains. Z Anat Entwicklungs Gesch 1973, 139, 259-282

Olszewski J, Baxter D. Cytoarchitecture of the human brain stem. Karger, Basel 1954
Paul SM, Rehavi M, Skolnick P, Goodwin FK. High affinity binding of antidepressants to a biogenic amine tranport site in human brain and platelet; studies in depression. In: Neurobiology of Mood Disorders (Post RM, Bellinger CJ, eds.) Williams and Wilkins, Baltimore, 1984, pp. 845-853
Pena F, Ramires JM. Endogenous activation of serotonin-2A receptors is required for respiratory rhythm generation in vitro. J Neurosci 2002, 22, 11055-11064
Perry R, Cohen I, DeCarlo R. Case study: Deterioration, autism, and recovery in two siblings. J Am Acad Child Adolesc Psych 1995, 34, 232-237
Persico AM et al (2002) Serotonin transporter gene promoter variants do not explain the hyperserotonemia in autistic children. Mol Psychiatry 2002, 7, 795-800
Pickel VM, Joh TH, Reis DJ. Proc Natl Acad Sci USA 1975, 72,659-663
Pickel VM, Sesack SR. Electron microscopy of central dopamine systems. In: Psychopharmacology (Bloom FE, Kupfer DJ, eds). New York, Raven . 1995, 257-268
Pickel VM, Chan J. Ultrastructural localization of the serotonin transporter in limbic and motor compartments of the nucleus accumbens. J Neurosc 1999, 19, 7356-7366
Piven J, Chase GA, Landa R, Wzorek M, Gayle J, Cloud D, Folstein S. Psychiatric disorders in the parents of autistic individuals. J Am Acad Child Adolesc Psychiatryt 1991, 30, 471-478
Poitras D, Parent A 1978. Atlas of distribution of monoamine-containing nerve cell bodies in the brain stem of the cat. J Comp Neurol 1978, 179, 699-718
Qian Y, Melikian HE, Rye DB, Levey AI, Blakely RD. Identification and characterization of antidepressant-sensitive serotonin transporter proteins using site-specific antibodies. J Neurosci 1995, 15, 1261-1274
Ramamoorthy S, Bauman AL, Moore KL, Han H, Yang Feng T, Chang AS, Ganapathy V, Blakely RD, Antidepressant- and cocaine-sensitive human serotonin transporter: molecular cloning, expression, and chromosomal localization. Proc Natn Acad Sci USA 1993, 90, 2542-2546
Rathbun, W. and M. J. Druse. Dopamine, serotonin, and acid metabolites in brain regions from the developing offspring of ethanol-treated rats. J. Neurochem. 1985, 44, 57-62
Redcay, E. Courchesne, E., When is the brain enlarged in autism? A meta-analysis of all brain size reports. Biol Psychiatry 2005, 58, 1-9
Report of the Centers for Disease Control and Prevention (CDC), 2012
Richerson GB. Serotonergic neurons as carbon dioxide sensors that maintain pH homeostasis. Nat Rev Neurosci 2004, 5, 449-461
Rikard-Bell GC, Tork I, Sullivan C, Scheibner T. The distribution of substance P-like immunoreactive fibers and terminals in the medulla oblongata of the human infant. Neuroscience 1990, 34, 133-148
Rind HB, Russo AF, Whittemore SR. Developmental regulation of tryptophan hydroxylase messenger RNA expression and enzyme activity in the raphe and its target fields. Neuroscience 2000, 101, 665-677
Rineer S, Finucane B, Simon EW. Autistic symptoms among children and young adults with isodicentric chromosome 15. Am J Med Genet (Neuropsychiat Genet) 1998, 81, 428-433
Risch SC, Nemeroff CB. Neurochemical alterations of serotonergic neuronal systems in depression. J Clin Psychiatr 1992, 53, Suppl. 3-7.

Ritvo, E. R., B. J. Freeman, A. B. Scheibel, T. Duong, H. Robinson, D. Guthrie, and A. Ritvo. Lower Purkinje cell counts in the cerebella of four autistic subjects: initial findings of the UCLA-NSAC Autopsy Research Report. Am J Psychiatry 1986, 143, 862-866

Robertson RT, Feiner AR. Diencephalic projections from the pontine reticular formation: Autoradiographic studies in the cat. Brain Res 1982, 239, 3-16

Rodier, PM, Ingram JL, Tisdale B, Nelson S, Romano J, Embryological origin for autism: developmental anomalies of the cranial nerve motor nuclei. J Comp Neurol 1996, 370, 491-504

Roth BL. Multiple serotonin receptors: clinical and experimental aspects. Ann Clin Psychiatry 1994, 6, 67-78

Rutter, M., A. Bailey, P. Bolton, and C. A. Le. Autism and known medical conditions: myth and substance. J. Child Psychol. Psychiatry 1994, 35, 311-322

Samanin R, Valzelli L. Increase of morphine-induced analgesia by stimulation of the nucleus raphe dorsalis. Eur J Pharmacol 1971, 16, 298-302

Santos M, Uppal N, Butti C et al. Von Economo neurons in autism: a stereologic study of the frontoinsular cortex in children. Brain Res 2011, 1380, 206-217

Sasayama D, Sugiyama N, Imai J, Hayashida A, Harada Y, Amano N. High dose paroxetine treatment for an adolescent with obsessive-complulsive disorder comorbid with Asperger's disorder. Psychiatry Clin Neurosci 2009, 63, 251

Saudou F, Hen R. 5 Hydroxytryptamine receptor subtypes in vertebrates and invertebrates. Neurochem Int 1994, 25, 503-532

Schain RJ, Freedman DX. Studies on 5-hydroxyindole metabolism in autistic and other mentally retarded children. J Pediatr 1961, 58, 315-320

Scheaffer RL, Mendenhall W, Ott RL, Gerow KG. 2011. Elementary survey sampling. Seventh edition. Pacific Grove, CA: Duxbury Press.

Schloss P, Williams DC. The serotonin transporter: a primary target for antidepressant drugs. J Psychopharmacol 1998, 12, 115-121

Schroer RJ, Phelan MC, Michaelis RC, et al. Autism and maternally derived aberrations of chromosome 15q. Am J Med Genet 1998,76, 327-36

Schumann CM, Hamstra J, Goodlin-Jones BL, Lptspeich LJ, Kwon H, Buonocore MH, Lammers CR, Reiss AL, Amaral DG. The amygdala is enlarged in children but not adolescents with autism; the hippocampus is enlarged at all ages. J Neurosci 2004, 24, 6392-6401

Schumann CM, Amaral DG. 2006. Stereological analysis of amygdala in autistic and other mentally retarded children. J Pediatr 58: 315-320

Séguéla P, Watkins KC, Descarries L. Ultrastructural relationships of serotonin axon terminals in the cerebral cortex of the adult rat. J Comp Neurol 1989, 289, 129-142

Shanahan NA, Velez LP, Masten VL, Dulawa SC. Essential role for orbitofrontal serotonin 1B receptors in obsessive-compulsive disorder-like behavior and serotonin reuptake inhibitor response in mice. Biol Psychiatry 2011,70, 1039-1048

Shankaran M, King C, Lee J, Busch R, Wolff M, Hellerstein MK. Discovery of novel hippocampal neurogenic agents by using an in vivo stable isotope labeling technique. J Pharmacol Exp Ther. 2006, 319, 1172-81

Shopsin B et al. Psychoactive drugs in mania. A controlled comparison of lithium carbonate, chloropromazine, and chaloperidol. Arch Gen Psychiatry 1975, 32, 34-42

Simms ML et al. The anterior cingulate cortex in autism: heterogeneity of qualitative and quantitative cytoarchitectonic features suggests possible subgroups. Acta Neuropathol 2009, 118, 673-684

Smiley JF, Levey AI, Ciliax BJ, Goldman-Rakic PS. D1 dopamine receptor immunoreactivity in human and monkey cerebral cortex: predominant and extrasynaptic localization in dendritic spines. Proc Natl Acad Sci USA 1994, 91, 5720-5724

Sodhi MSK, Sanders-Bush E . Serotonin and brain development. Int Rev Neurobiol 2004,59,111-173

Soghomonian JJ, Descarries L, Watkins KC. Serotonin innervation in adult rat neostriatum. II. Ultrastructural features: A autoradiographic and immunocytochemical study. Brain Res 1989, 481, 67-86

Soubrie P. Reconciling the role of central serotonin neurons in human and animal behavior. Behav Brain Sci 1986, 9, 319-364

Souders MC, Mason TB, Valladares O et al. Sleep behaviors and sleep quality in children with autism spectrum disorders. Sleep 2009, 32, 1566-1578

Spivack B et al. Low platelet-poor plasma levels of serotonin in adult autistic patients. Neuropsychobiology 2004, 50, 157-160

Staley JK, Malison RT, Innis RB. Imaging of the serotonergic system: interactions of Neuroanatomical and functional abnormalities of depression. Biol Psychiatry 1998, 44, 534-549

Stanley M, Virgilio J, Gershon S. Tritiated imipramine binding sites are decreased in the frontal cortex of suicides. Science 1982, 216, 1337-1339

Stanley M, Mann JJ, Gershon S. Alterations in pre- and postsynaptic serotonergic neurons in suicide victims. Psychpharmacol Bull. 1983, 19, 684-687

Steinbusch HWM, Verhofstad AAJ, Joosten HWJ. Localization of serotonin in the central nervous system by immunohistochemistry: Description of a specific and sensitive technique and soma applications. Neuroscience 1978, 3, 811-820

Steinbusch HW. Distribution of serotonin-immunoreactivity in the central nervous system of the rat cell bodies and terminals. Neuroscience 1981, 6, 557-618

Steinbusch HWM, Nieuwenhuys. The raphe nuclei of the rat brainstem: A cytoarchitectonic and immunohistochemical study. In: Chemical Neuroanatomy. P.C. Emerson, ed. Raven Press, New York, 1983, 131-208

Stockmeier C, Shapiro L, Haycock J, Thompson P, Lowy M. Quantitative subregional distribution of serotonin$_{1A}$ receptors and serotonin transporters in the human dorsal raphé. Brain Res 1996, 727, 1-12

Stone J, Dreher B, Törk I. "The Neuroanatomist's Colouring Book". 2nd ed., p123. Maitland, Sydney, Australia 1987

Stromland, K., V. Nordin, M. Miller, B. Akerstrom, and C. Gillberg. Autism in thalidomide embryopathy: a population study. Dev Med Child Neurol 1994, 36, 351-356

Sukhatme PV, Sukhatme BV, Sukhatme S, Asok C. 1984. Sampling theory of surveys with applications. Third edition. Ames, IA: Iowa State University Press.

Sukhodolsky DG, Scahill L, Gadow KD, Arnold LE, Aman MG, McDougle CJ. Parent-rated anxiety symptoms in children with pervasive developmental disorders: Frequency and association with core autism symptoms and cognitive functioning. Journal of Abnormal Child Psychology. 2008, 36, 117-128

Sundstrom, E, Kolare S, Souverbie F, Samuelsson EB, Pschera H, Lunell NO, Seiger A. Neurochemical differentiation of human bulbospinal monoaminergic neurons during the first trimester. Dev Brain Res 1993, 75, 1–12

Sur C, Betz H, Schloss P. Immunocytochemical detection of the serotonin transporter in rat brain. Neuroscience 1996, 73, 217-231

Sutcliffe, J. S., R. J. Delahanty, H. C. Prasad, J. L. McCauley, Q. Han, L. Jiang, C. Li, S. E. Folstein, and R. D. Blakely. Allelic heterogeneity at the serotonin transporter locus (SLC6A4) confers susceptibility to autism and rigid-compulsive behaviors. Am J Hum Genet 2005, 77, 265-279

Symons, FJ. Self injurious behavior in neurodevelopmental disorders: relevance of nociceptive and immune mechanisms. Neurosc Behavioral Reviews 2011, 35, 1266-1274

Takahashi H, Nakashima S, Ohama E, Takeda S, Ikuta F. Distribution of serotonin-containing cell bodies in the brainstem of the human fetus determined with immunohistochemistry using antiserotonin serum. Brain Dev 1986, 8, 355-365

Thomas DP and Vane JR . 5 hydroxytryptamine in the circulation of the dog. Nature 1967, 216, 335-338

Tomchek SD, Dunn w. Sensory processing in children with and without autism: a comparative study using the short sensory profile. Am J Occup Ther 2007,61, 190-200

Törk I, Hornung JP. Serotonergic innervation of the human cerebral cortex. Neuroscience Suppl 1987, 22, S112

Törk I, Hornung JP. Raphé nuclei and the serotonergic system. In: Paxinos G, editor. The human nervous system. San Diego: Academic Press, Inc. 1990 p 1001-1022.

Toth G, Fekete M. 5-hydroxyindole acetic excretion in newborns, infants and children 1986, 27, 221-226

Trottier S, Evrard B, Vignal J-P, Scarabin J-M, Chauvel P. The serotonergic innervation of the cerebral cortex in man and its changes in focal cortical dysplasia. Epilepsy Research 1996, 25, 79-106

Tryba AK, Pena F, Ramirez JM. Gasping activity in vitro: a rhythm dependent on 5-HT_{2A} receptors. J Neurosci 2006, 26, 2623-2634

Tuchman R, Rapin I. Epilepsy in autism. 2002. The Lancet. Neurology 2002, 1, 352-358

Underwood MD, Khaibulina AA, Ellis SP, Moran A, Rice PM, Mann JJ, Arango V. Morphometry of the dorsal raphe nucleus serotonergic neurons in suicide victims. Biol Psychiatry 1999, 46, 473-483

Underwood MD, Mann JJ, Arango V. Serotonergic and noradrenergic neurobiology of alcoholic suicide. Alcohol Clin Exp Res 2004, 28, 57S-69S

Underwood MD, Mann JJ, Arango V. Morphometry of dorsal raphé nucleus serotonergic neurons in alcoholism. Alcohol Clin Exp Res. 2007, 31, 837-45

U.S. Department of Health and Human Services, Centers for Disease Control and Prevention, Morbidity and Mortality Weekly Report. 2007, 56, 1-28

U.S. Department of Health and Human Services, Centers for Disease Control and Prevention Morbidity and Mortality Weekly Report 2012, 61, 1-19

Van Bockstaele E, Pickel V. Ultrastructure of serotonin immunoreactive terminals in the core and shell of the rat nucleus accumbens: cellular substrates for interactions with catecholamine afferents. J Comp Neurol 1993, 334, 603-617

Van den Pol AN, Herbst RS, and Powell JF. Tyrosine hydroxylase-immunoreactive neurons of the hypothalamus: Light and electron microscopic study. Neuroscience 1984, 13, 1117-1156

Van Erp AM and Miczek KA. Aggressive behavior, increased accumbal dopamine, and decreased cortical serotonin in rats. J Neurosci 2000, 20, 9320-9325

Van Kooten, I., S. J. Palmen, P. von Cappeln, H. W. Steinbusch, H. Korr, H. Heinsen, P. R. Hof, H. van Engeland, and C. Schmitz. Neurons in the fusiform gyrus are fewer and smaller in autism. Brain 2008, 131, 987-999

Verney C, Lebrand C and Gaspar P. Changing distribution of monoaminergic markers in the developing human cerebral cortex with special emphasis on the serotonin transporter. Anat. Rec. 2002, 267, 87–93

Vorstman JA, Staal WG, van Daalen E, van Engeland H, Hochstenbach PF, Franke L. Identification of novel autism candidate regions through analysis of reported cytogenetic abnormalities associated with autism. Mol Psychiatry 2006, 11, 18-28.

U.S. Department of Health and Human Services, Centers for Disease Control and Prevention, Morbidity and Mortality Weekly Report, 2012, 61, 1-19

Wardell CF, Bornstein JC, Furness JB. Projections of 5-hydroxytryptamine-immunoreactive neurons in guinea-pig distal colon. Cell Tissue Res 1994, 278, 379-387

Weiss MJ. Differential rates of skill acquisition and outcomes of early intensive behavioral intervention in autism. Behav Interv 1999, 14, 3-22

Wersinger C, Rusnak M, Sidhu A. Modulation of the trafficking of the human serotonin transporter by human alpha-synuclein. Eur J Neurosi 2006, 24, 55-64

Westlund KN, Denney RM, Rose RM, Abell CW. Localization of distinct monoamine oxidase A and monoamine oxidase B cell populations in human brainstem. Neuroscience, 1988, 25, 439-456

Whitaker PM, Vint CK, Morin R. [^{3}H]Imipramine labels sites on brain astroglial cells not related to serotonin uptake. J Neurochem 1983, 41, 1319-1323

Whitaker-Azmitia PM, Azmitia EC. Autoregulation of fetal serotonergic neuronal development: Role of high affinity serotonin receptors. Neurosci Lett 1986, 67, 307-312.

Whitaker-Azmitia PM. Role of serotonin and other neurotransmitter receptors in brain development: basis for developmental pharmacology. Pharmacol Rev 1991, 43, 553-561.

Whitaker-Azmitia PM, Druse M, Walker P, Lauder JM. Serotonin as a developmental signal. Behav Brain Res 1996, 73, 19-29

Whitaker-Azmitia PM. Serotonin and brain development: role in human developmental diseases. Brain Res Bull 2001, 56, 479-485

Whitaker-Azmitia PM. Behavioral and cellular consequences of increasing serotonergic activity during brain development: a role in autism? Int J Dev Neurosci 2005, 23, 75-83

Whitney ER, Kemper TL, Bauman ML et al. Cerebellar Purkinje Cells are reduced in a subpopulation of autistic brains: A stereological experiment using Calbindin-D28k. Cerebellum 2008, **7**, 406–416

Whitney ER, Kemper TL, Rosene DL et al. Density of cerebellar basket and stellate cells in autism: Evidence for a late developmental loss of Purkinje cells. J Neurosci Res 2009, 87, 2245–2254

Wiklund L, Sjolund B, Bjorklund A. A morphological and functional studies on the serotonergic innervation of the inferior olive. J Physiol (Paris) 1981, 77, 183-186

Williams K, Wheeler DM, Silove N, Hazell P. Selective serotonin reuptake inhibitors (SSRIs) for autism spectrum disorders (ASD) Cochrane Database Syst. Rev. 8, CD004677, 2010

Williams EL, Casanova MF. Autism and dyslexia: A spectrum of cognitive styles as defined by minicolumnar morphometry. Med Hypoth 2010,74,59-62

Wisner KL, Zarin DA, Holmboe ES et al Risk-benefit decision making for treatment of depression during pregnancy. Am J Psychiatry 2000, 157, 1933-1940

Wolf HK, Buslei R, Schmidt-Kastner R, Schmidt-Kastner PK, Pietsch T, Wiestler OD, Blümcke I, 1996, 10, 1167-1171

Wong DF, Maini A, Rousset OG. Brasic JR. Positron emission tomography, a tool for identifying the effects of alcohol dependance on the brain. Alcohol Res Healts 2003, 27, 161-173

Yaksh TL, Plant RL, Rudy TA. Studies on the antagonism by raphe lesions of the antinociceptive action of systemic morphine. Eur J Pharmacol. 1977, 41, 399-408

Yonan, A. L., M. Alarcon, R. Cheng, P. K. Magnusson, S. J. Spence, A. A. Palmer, A. Grunn, S. H. Juo, J. D. Terwilliger, J. Liu, R. M. Cantor, D. H. Geschwind, and T. C. Gilliam. A genomewide screen of 345 families for autism-susceptibility loci. Am J Hum Genet 2003, 73, 886-897

Young KA, Bonkale WL, Holcomb LA, Hicks PB, German DC. Major depression, 5HTTLPR genotype, suicide and antidepressant influences on thalamic volume. BJ Psych 2008, 192, 285-289

Zhang, X., Lv, C.C., Tian, J., Miao, R.J., Xi, W., Hertz-Picciotto, I., Qi, L., Prenatal and perinatal risk factors for autism in China. J Autism Dev Disord 2010, 40, 1311-1321

Zhou FC, Xu Y, Bledsoe S, Lin R, Kelley MR. Serotonin transporter antibodies: production, characterization, and localization in the brain. Brain Res Mol Brain Res 1996, 43, 267-278

Zhou FC, Tao-Cheng JH, Segu L, Patel T, Wang Y. Serotonin transporters are located on the axons beyond the synaptic junctions: anatomical and functional evidence. Brain Res 1998, 805, 241-254